RHEOLOGICAL YIELD STRESS MEASUREMENT OF MINE PASTE FILL MATERIAL

BY
Abdolreza Saebimoghaddam

Department of Mining, Metals and Materials Engineering
McGill University
Montreal, Canada

A thesis submitted to McGill University
in partial fulfillment of the requirements for the degree of
Master of Engineering

Your file Votre référence
ISBN: 978-0-494-22668-1
Our file Notre référence
ISBN: 978-0-494-22668-1

This thesis is dedicated to my parents.

ABSTRACT

This thesis addresses rheological characterization of mine tailings and paste materials as saturated solid-liquid or homogenous mixtures. Thickened tailings and paste fill can be classified as viscoplastic or time-independent non-Newtonian fluid material. Viscoplastic fluids deform plastically when the applied shear stress is less than a critical stress, which is known as "yield stress". When the shear stress exceeds the yield stress this type of fluid flows like a viscous material with finite viscosity.

In terms of pipeline design for transportation of mine tailings or paste material, one of the most important rheological parameters that must be measured would be yield stress. There are numerous techniques and equipment that can be used for rheological characterization and specifically for yield stress measurements. Literature review shows that the vane method is one of the best rheometery techniques for determining the yield stress of homogeneous fluids directly.

There is also a method for calculating the yield stress from slump height. Any geometry of slump moulds, cone or cylinder, with different dimensions can be applied in this method. The standard conical slump test is basically used for controlling the workability of fresh concrete. This method was then modified for yield stress and viscosity calculation of cemented mixtures. These slump tests can be categorized as in-situ methods of yield stress measurements.

Several rheometery and in-situ experiments were carried out to measure the yield stress of two mine tailings samples in this study. A rheometer was used in controlled shear rate and controlled shear stress modes for yield stress measurements with the vane method. The results were satisfactory for cemented and non-cemented mixtures. The effect of mixing time on the yield stress of material combined with cement was also assessed using the vane method. No significant difference emerged between increased yield stress of the mixtures after 4 minutes and 12 minutes of mixing.

The accuracy of calculated yield stress values using in-situ methods was also determined by drawing comparisons between these series of data and actual yield stresses measured using a rheometer. Modified conical slump tests overestimated the values of yield stress and did not obtain reliable data for viscosity calculation of the mixtures.

RÉSUMÉ

Cette thèse vise la caractérisation rhéologique des résidus miniers et des matériaux en pâte en tant que matériaux solide liquide saturés ou mélange homogène. Les résidus épaissis ou les remblais en pâte peuvent être classés comme des matériaux viscoplastiques ou fluides non Newtonien stationnaire. Les fluides viscoplastiques se déforment plastiquement lorsque la contrainte de cisaillement est inférieure à une valeur critique, qui est connue comme le seuil de contrainte. Lorsque la contrainte excède ce seuil de contrainte le liquide s'écoule comme un matériau visqueux avec une viscosité déterminée. Pour le design des conduits de transport des résidus miniers ou des matériaux en pâte le paramètre le plus important devant être mesuré serait le seuil de contrainte. Il y a plusieurs techniques et équipements pouvant servir à la caractérisation rhéologique et plus spécifiquement à la mesure du seuil de contrainte. La revue de la littérature montre que la méthode du scissomètre est une des meilleures techniques pour directement déterminer le seuil de contrainte pour un fluide.

Il y a également une technique permettant de calculer le seuil de contrainte à partir d'un essai d'affaissement. Pour cette méthode n'importe quelle géométrie de moule, conique ou cylindrique, de différentes dimensions peut être utilisée. L'essai d'affaissement standard utilisant le moule conique est utilisé couramment pour caractériser le béton frais. Cette méthode a ensuite été modifiée pour calculer le seuil de contrainte et la viscosité des mélanges cimentés. Ces essais d'affaissement peuvent être classés comme des essais in situ de mesure du seuil de contrainte. De nombreux essais rhéologiques et d'essais in situ ont été réalisés dans le cadre de cette étude pour mesurer le seuil de contrainte de deux résidus miniers. Un rhéomètre a été utilisé en mode taux de cisaillement contrôlé et en mode de contrainte de cisaillement contrôlée pour mesurer le seuil de contrainte avec scissomètre.

Les résultats ont été satisfaisants pour les mélanges cimentés et non cimentés. L'effet du temps de mélange sur le seuil de contrainte du matériau combiné au ciment a aussi été évalué avec la méthode du scissomètre. Aucune différence n'a été observée sur la valeur du seuil de fluage pour des temps de mélange de plus de 4 minutes et de 12 minutes.

La précision des valeurs de seuil de contrainte calculées en utilisant les méthodes in situ a aussi été déterminée en comparant les données avec des seuils de contraintes mesurées en utilisant un rhéomètre. L'essai d'affaissement conique modifié a surestimé le seuil de contrainte et n'a pas fourni de données fiables pour le calcul de la viscosité des mélanges.

ACKNOLDGEMENTS

I would like to express my sincere gratitude to my supervisor professor Ferri Hassani for his guidance, patience, support and encouragement and for giving me the opportunity to study at McGill University.

I am appreciative to professor Jacques Ouellet and Dr Momayez for their supports over last two years in Mining Engineering Department. I am also grateful to Mr. Michel Li from Noranda Inc./Falconbridge Ltd. and Mr. Martin Malservisi from Noranda Technology for providing me with the R/S-CPS Rheometer and technical information.

I would like to extend my appreciation to my fellow graduate students; Mehdi Razavi, Bassam El Husseini, Afshin Mantegh, Shahe Shnorhokian, James Powell and Afsaneh Hosseini for their helps and persistent friendships. As well, I am thankful to my best friend, Patricia Deek, and Nikki Middlemiss for their unconditional helps.

I wish to deeply thank my family for their unceasing love, support and encouragement.

Some part of the financial support received through the National Sciences and Engineering Research Council of Canada (NSERC) is gratefully appreciated. The cooperation of mining companies, LaRonde and Louvicourt, is appreciated.

TABLE OF CONTENTS

ABSTRACT........ i
RESUME........ ii
ACKNOWLEDGEMENTS........ iii
TABLE OF CONTENTS........ iv
LIST OF FIGURES........ viii
LIST OF TABLES........ xiii

CHAPTER 1
INTRODUCTION

1.1. Research Description........ 1
1.2. Research Background........ 2
1.3. Goals and Objectives........ 6
1.4. Research Plan and Methodology........ 6

CHAPTER 2
PASTE TECHNOLOGY

2.1. Definition of Paste........ 8
2.2. Advantages and Disadvantages........ 10
2.3. Mechanical Properties........ 12
2.3.1. Macroscopic Parameters........ 12
2.3.2. Intrinsic Parameters........ 12
2.4. Paste Preparation and Dewatering 14
2.4.1. Conventional Thickening 15
2.4.2 Deep Tank Thickeners........ 16
1. Paste Production Storage Mechanism........ 17
2. Baker Process Deep Tank........ 17
3. Fluidization........ 18
4. Deep Cone Paste Thickener........ 19
5. Outokumpu High Compression and Paste Thickener........ 20

2.4.3. Filter Methods of Dewatering... 21
1. Pressure Filtration... 21
2. Vacuum Filtration... 22
2.4.4. Centrifuge Dewatering... 24
2.5. Paste Plant Design... 25

CHAPTER 3
RHEOLOGY

3.1. Basic Rheological Concepts... 27
3.2. Rheological Models and Parameters... 30
3.2.1. Yield Stress... 32
3.2.2. Viscosity... 32
3.3. Yield Stress Measurements... 34
3.3.1. Indirect Methods... 35
1. Direct Data Extrapolation... 35
2. Extrapolation Employing Flow Models... 35
3.3.2. Direct Methods... 36
1. Stress Relaxation... 36
2. Strain Recovery... 36
3. Stress Growth Experiment... 37
4. Cone Penetration... 38
3.4. Vane Method... 40
3.4.1 Principles of Vane Measurements... 40
3.4.2 Calculation of Yield Stress with Vane Method... 41
3.4.3 Vane Dimensions... 43
3.4.4 Rotational Speed of Vane... 44
3.5. Rheometery/ Viscometery... 44
3.5.1 Tube Viscometery... 45
3.5.2 Concentric Cylinder Rheometery... 47
3.5.3 Cone and Plate Viscometery... 49
3.6. Slump... 50

3.6.1. Standard Slump Test Method 50
3.6.2. Yield Stress Measurement Using Conical Geometry 52
3.6.3. Cylindrical Slump Test Method 55
3.6.4. Yield Stress Measurement Using Cylinder Geometry 55
3.6.5. Modified Conical Slump Test 56

CHAPTER 4
MINE TAILINGS CHARACTRIZATION &
EXPERMENTAL PROCEDURE

4.1. Mine Tailings Samples 60
4.1.1. LaRonde Mine 60
4.1.2. Louvicourt Mine 61
4.2. Basic Characterizations of Mine Tailings 62
4.2.1. Chemical Composition 63
4.2.2. Mineralogy of Mine Tailings 64
4.2.3. Particle Size Characterization 65
4.2.4. Specific Gravity and pH 67
4.3. Sample Preparation for Rheological Measurements 68
4.3.1. Mixing 68
4.3.2. Binders 69
4.4. Slump Test Procedures 69
4.4.1. Standard Slump Test Procedure 69
4.4.2. Cylindrical Slump Test Procedure 70
4.4.3. Modified Conical Slump Test Procedure 70
4.5. Vane Method 71
4.5.1. Equipment 72
1. R/S.CPS Brookfield Rheometer 72
2. Vane Dimension and Adjustment 74
3. Computer System and Software 75
4.5.2. Rheometery Test Procedure 76
4.5.3. Controlled Shear Rate Mode 76

1. Yield Stress Calculation.. 76

2. Software Programming.. 78

3. Rotational Speed.. 78

4.5.4. Controlled Shear Stress Mode.. 79

CHAPTER 5
RESULTS AND DATA ANALYSIS

5.1. Classification of Results.. 82

5.2. The Results of Non-cemented Mixtures.. 82

5.2.1. Vane Rheometery Results of Non-cemented Mixtures.. 82

5.2.2. The Comparison Between CSR and CSS Results.. 86

5.2.3. Standard and Cylindrical Slump Test Results.. 86

5.2.4. Modified Conical Slump Test Results.. 92

5.3. The Results of Cemented Mixtures.. 95

5.3.1. Vane Rheometery Results of Cemented Mixtures.. 95

5.3.2. Slump Test Results of Cemented Mixtures.. 98

5.4. Comparison Between LaRonde and Louvicourt Results.. 101

5.5. Discussion.. 102

CHAPTER 6
CONCLUSION AND RECOMENDATIONS

6.1. Conclusion.. 106

6.2. Recommendations.. 108

REFERENCES 109

LIST OF FIGURES

CHAPTER 2

Figure 2.1. Status of science for flow of bulk particulate material at various moisture contents........ 10

Figure 2.2. Paste technology........ 13

Figure 2.3. Conventional thickeners with diverse configurations........ 15

Figure 2.4. Deep tank thickener operating curve........ 16

Figure 2.5. Paste production storage system........ 17

Figure 2.6. PPSM in a mine paste backfill production system........ 18

Figure 2.7. Paste fill preparation plant using the Mag Engineering fluidization process........ 19

Figure 2.8. Schematic of paste disposal production using Eimco deep cone thickener........ 20

Figure 2.9. A schematic of a high compression thickener........ 21

Figure 2.10. A flow-scheme horizontal belt filter........ 22

Figure 2.11. Side view of disk filter........ 23

Figure 2.12. Operational cycle of drum filter........ 24

Figure 2.13. Continual paste preparation plant........ 25

Figure 2.14. Batch paste preparation plant........ 26

CHAPTER 3

Figure 3.1. Non-Newtonian fluid classification based on the yield power-law model........ 28

Figure 3.2. Rheogram of different types of time-independent fluids and Newtonian fluid........ 29

Figure 3.3. Rheological behaviour of time dependent fluids........ 29

Figure 3.4. Behaviour of apparent viscosity of time independent fluids....... 34

Figure 3.5. Cross model viscosity curve... 35

Figure 3.6. Typical strain (creep)-time curves at different shear stresses...... 37

Figure 3.7. Typical stress-time curve with applying constant shear rate...... 38

Figure 3.8. Cone geometry and the equilibrium state in cone penetration method... 39

Figure 3.9. Schematic of a four-bladed vane installed in a sample............ 41

Figure 3.10. Typical torque-time curve obtained with a vane method.......... 42

Figure 3.11. Maximum stress vs. rotational speed for titanium suspension..... 45

Figure 3.12. Schematic of tube viscometer.. 46

Figure 3.13. Schematic of tube cross-section and plug zone..................... 47

Figure 3.14. Simplified diagram of a concentric cylinder rheometer........... 47

Figure 3.15. Diagram of a cone and plate viscometer........................... 49

Figure 3.16. Mould for standard slump test method............................ 50

Figure 3.17. Standard slump test method... 51

Figure 3.18. Initial and final state of the material shape and stress distributions in a conical slump model............................ 52

Figure 3.19. Deformation of an element of thickness dz to thickness dz_1...... 54

Figure 3.20. Initial and final state of the material shape and stress distributions in a cylindrical slump model.......................... 56

Figure 3.21. Experimental set up for the modified slump test and top plate dimensions.. 58

Figure 3.22. Dimensionless yield stress versus dimensionless slump for the cylindrical and modified slump models............................ 59

CHAPTER 4

Figure 4.1. Location of LaRonde Mine... 61

Figure 4.2. LaRonde XRD graph........ 64

Figure 4.3. Louvicourt XRD graph........ 65

Figure 4.4. Particle size distribution of fine portion of LaRonde mine tailings........ 66

Figure 4.5. Particle size distribution of fine portion of Louvicourt mine tailings........ 66

Figure 4.6. Particle size distribution of LaRonde and Louvicourt total tailings........ 67

Figure 4.7. Hobart Mixer........ 68

Figure 4.8. 150 cm diameter cylindrical mould (left) 200 cm diameter cylindrical mould (right)........ 70

Figure 4.9. Modified conical slump test equipment........ 71

Figure 4.10. Modified conical slump test procedure and the final shape of mixture........ 72

Figure 4.11. The R/S.CPS Brookfield Rheometer and Peltier thermo regulator........ 73

Figure 4.12. Custom made six-bladed stainless steel vane........ 74

Figure 4.13. Start up menu of the software Rheo 2000........ 75

Figure 4.14. Test procedure for rheometery experiments using data acquisition software........ 77

Figure 4.15. Creating a block file........ 78

Figure 4.16. Measure/Analysis box........ 79

Figure 4.17. The effect of rotational speed on the maximum torque........ 80

Figure 4.18. Creating a block file in the CSS mode........ 81

CHAPTER 5

Figure 5.1. LaRonde torque-time graph for non-cemented mixtures with different water contents........ 83

Figure 5.2. Louvicourt torque-time graph for non-cemented mixtures with different water contents.. 83

Figure 5.3. LaRonde non-cemented mixtures rheogarm........................ 85

Figure 5.4. Louvicourt non-cemented mixtures rheogarm...................... 85

Figure 5.5. The yield stress values in CSR and CSS modes for LaRonde mine tailings... 87

Figure 5.6. The yield stress values in CSR and CSS modes for Louvicourt mine tailings... 87

Figure 5.7. Calculated yield stress from slump height for LaRonde non-cemented mixtures.. 90

Figure 5.8. Calculated yield stress from slump height for Louvicourt non-cemented mixtures.. 90

Figure 5.9. The relationship between dimensionless slump and water content of non-cemented mixtures.................................. 91

Figure 5.10. The height of modified slump and standard slump................. 93

Figure 5.11. The yield stress calculated from slump of modified conical test for LaRonde mixtures.. 94

Figure 5.12. The yield stress calculated from slump of modified conical test for Louvicourt mixtures... 94

Figure 5.13. The relationship between slump and time in the modified conical slump test.. 95

Figure 5.14. The yield stress values of LaRonde cemented mixtures after 4 minutes and 12 minutes of mixing time............................ 97

Figure 5.15. The yield stress values of Louvicourt cemented mixtures after 4 minutes and 12 minutes of mixing time............................ 97

Figure 5.16. The correlation between the yield stress values measured after 4 minutes and 12 minutes for both LaRonde and Louvicourt cemented mixtures.. 98

Figure 5.17. Dimensionless slump height of cemented mixtures in comparison with non-cemented mixtures for LaRonde and Louvicourt materials.. 99

Figure 5.18. Yield stress of cemented and non-cemented mixtures calculated from slump tests and vane rheometery for LaRonde mine mixtures... 100

Figure 5.19. Yield stress of cemented and non-cemented mixtures calculated from slump tests and vane rheometery for Louvicourt mine mixtures... 100

Figure 5.20. Dimensionless slump changes for cylindrical and conical moulds... 104

Figure 5.21. Actual slump changes for cylindrical and conical moulds......... 104

LIST OF TABLES

CHAPTER 3

Table 3.1. Shear thinning and shear thickening behaviour.................... 30

Table 3.2. Rheological parameters of different types of non-Newtonian fluids.. 31

Table 3.3. Estimation of errors involved in employing Equation 3.15 compared with P=0.. 43

Table 3.4. The advantages and disadvantages of the tube and rotational viscometers... 48

CHAPTER 4

Table 4.1. Statistics of production of gold, silver, copper and zinc in LaRonde Mine (1998-2004)... 61

Table 4.2. Proven-probable mineral reserves and possible mineral resources of LaRonde Mine as of February 2004..................... 61

Table 4.3. Breakdown of Louvicourt's reserves and resources............... 62

Table 4.4. The chemical composition of LaRonde and Louvicourt Mine tailings.. 63

Table 4.5. The value of the base metals in LaRonde and Louvicourt Mine tailings.. 63

Table 4.6. The size distribution characteristics.................................. 67

Table 4.7. Technical features of R/S.CPS Brookfield Rheometer............ 74

CHAPTER 5

Table 5.1. Maximum torque and yield stress values of LaRonde and Louvicourt mixtures.. 84

Table 5.2. Yield stress values in controlled shear stress mode................ 84

Table 5.3. Curve-fitting parameters and the average relative error........... 86

Table 5.4. The results of cylindrical slump tests with 150mm diameter cylinders 88

Table 5.5. The results of cylindrical slump tests with 200mm diameter cylinders 89

Table 5.6. The results of standard slump tests.................................... 89

Table 5.7. The average percent error and the correlation coefficient for slump tests.. 92

Table 5.8. The results of modified conical slump test.......................... 92

Table 5.9. Maximum torque and yield stress values of LaRonde and Louvicourt cemented mixtures...................................... 96

Table 5.10. The result of slump height and yield stress for non-cemented mixtures.. 99

CHAPTER 1
INTRODUCTION

1.1. Research Description

This research addresses the methods of measuring yield stress of paste as a fluid material. The key issues, therefore, are:

a. Definition of "yield stress" as one of the rheological parameters of fluids.
b. Description and characterization of "paste" material as one of the solid-liquid mixture types.
c. Identification of the "methods for measuring" the yield stress of paste material.

Paste technology has been accepted in the mining industry for many years. Two of its main applications are:

- underground backfilling; and
- disposal of tailings and mineral wastes.

One of the latest surveys of mine-fill practices in Canada indicates that developments in the production, transportation and placement aspects of backfill operations are necessary to establish more efficient, safer and less-costly mine-fill practices (De Souza et al., 2001). Recent surveys indicate that the mining industry is increasing employment and research funding in these areas and is developing new methods and techniques to address total tailings and use of paste backfill in Canadian mines.

Although paste technology has been used for more than 20 years, the 'science' of granular-viscous flow for analysing paste mixtures and designing paste reticulation systems is poorly understood (Cooke, 2001 and Li et al, 2002). Therefore, the transportation of paste through pipelines, one of the main stages of backfill operations or waste deposition, is of utmost importance. In this regard, the rheological behaviour of paste as fluid should be understood to design an efficient pipeline system in any specific mine. There are several existing methods of measuring the yield stress of fluid mixtures. All these techniques, as well as the background of their usage will be described in this text.

1.2. Research Background

There are numerous techniques for determining the rheological behaviour of solid-liquid mixtures. Some of the mixtures, such as concentrated suspensions, thickened tailings and paste fill, behave as viscoplastic fluids (Bird et al 1983, Utracki 1988, Nguyen et al 1992). By applying shear stress, these fluids begin deforming plastically like solids. When the applied shear stress is more than a certain critical stress, these fluids flow as viscous material with finite "viscosity". This critical stress, which depends on the characterization of the mixture, is called "yield stress". The transitional behaviour of paste between soil and slurry resulted in the study of paste as a unique science, which is called the science of granular-viscous flow (Li et al 2002).

Nguyen and Boger (1992) described several methods for measuring the yield stress of fluids. According to them, there are two main methods of measurements; indirect and direct methods. With indirect methods, yield stress will be obtained by the extrapolation of the shear stress-shear rate data (rheogram) at the point where the shear rate is zero and is known as "extrapolated" or "apparent" yield stress. Nguyen and Boger also explained seven techniques for the direct measurement of yield stress. As the value of yield stress measured by direct methods is usually done under static situations, it is named the "static" or "true" yield stress.

The main characteristics of several types of rheometers/viscometers such as "capillary rheometery", "concentric cylinder viscometery" and "cone and plate viscometery" were also described by Nguyen et al (1992). These instruments are used for obtaining yield stress by direct methods. Cooke and Paterson (1996) also compared capillary rheometery and concentric cylinder viscometery, concluding that using the "tube viscometer" is better than using the "rotational viscometer" for mine slurries. In addition, it has been noted that the rotational viscometers are not suitable for characterizing solid-liquid mixtures (Lazarus and Slatter 1986, Cooke 2001).

Nguyen et al (1983) adopted the vane method for measuring rheological properties of concentrated suspensions. The vane method is basically a technique in soil mechanics used for in situ measurements of the shear strength of cohesive soils. The American Society for Testing and Materials has devised standard procedures for miniature vane tests in saturated fine-grained clayey soils (ASTM D 4648- 87).

Nguyen et al (1985) developed their studies on this subject by assuming a uniform stress distribution along a cylindrical yield surface using a four-bladed vane. They concluded that the results achieved from this method were reasonable, and comparable to the conventional method employed in soil mechanics for yield stress calculation. The vane method has for many years been established as a simple and accurate technique for direct yield stress measurement. Many researchers have confirmed the accuracy of this method and noted that the vane method is most suitable for determining the yield stress of greater than 10 Pa. (James et al 1987, Yoshimura et al 1987, Nguyen et al 1992).

Liddell et al (1996) employed the vane method in a stress-controlled and a rate-controlled mode for yield stress measurements of a 65 wt.% suspension. In addition, they described the advantages of using the "Bohlin" rheometer for the stress-controlled mode, as well as the differences between the "Haake" rheometer and a modified "Weissenberg" rheogoniometer employed for rate-controlled measurements. They also investigated the effect of rotational speed, vane dimensions and stiffness of the system on the measured yield stress.

A very unsophisticated method that has been used for measuring the yield stress in situ or in the laboratory is the slump test; this method is known as "a fifty cent rheometer" when using a cylinder (Pashias et al 1996). The standard cone slump test was initially developed to determine the "workability" or consistency of fresh concrete (ASTM C 143-95). Pashias et al (1996) adopted this method for cylindrical geometry, and developed a relationship between slump height and yield stress. It should be mentioned that Murata

(1984) was the first person to offer a model relating the slump height to yield stress for conical geometry in concrete industry.

A series of experiments have been conducted to assess whether the slump test is appropriate for yield stress measurements. The effect of aspect ratio of cylinder, lift rate, mixture structure, type of material and measurement time on slump height were investigated by Pashias et al (1996). They concluded that the measurement time and the surface material have no effect on the slump height. It was also reported that the cylinder should be lifted at the speed of between 1 m/s (approximate to manual lifting) and 10 m/s. The aspect ratios of frustum were suggested to be around one. It is good to mention that with a large aspect ratio (larger than one), the material collapses rather than flowing and with a small aspect ratio (less than one) the degree of slumping would be very small.

Paterson (2002) debated on the validity of slump as a suitable measurement of rheological properties in mining industry. He compared two models of yield stress prediction; the model of Pashias et al (1996) that uses cylindrical slump, and the model employing the Bingham yield stress measurement in the concrete industry, as suggested by Ferraris et al (1998).

Ferraris and de Larrard (1998) modified Hu's equation for estimating yield stress of plastic concrete from slump height (Hu et al 1995). This equation was based on finite element analysis of the slump test as well as on the empirical method of measurement. Ferraris and Larrard improved Hu's model in conducting several experiments, and also in evaluating the plastic viscosity of concrete by measuring the time when the slump height is 100 mm after lifting the mould.

According to Paterson (2002), both Pashias' and Ferraris' equations are most accurate for those mixtures with dimensionless slump greater than 0.333. However, there is a huge difference between the yield stresses predicted by these two methods at the given slump. On the other hand, the equation employed in the concrete industry overestimates the yield stress when used for slurries (Paterson 2002).

It has been reported that although the analysis for a conical slump is different for a cylinder, the results of slump are similar if the bottom diameter of both the cylinder and cone are the same (Paterson 2002). Of course, the validity of this statement has been postponed as the author is investigating this further. In addition, Paterson (2002) reported that there are no timed slump data for evaluating Ferraris'method of viscosity measurement.

The slump test has found wide industrial application, particularly in mine tailings disposal and mine paste-fill operations, as a simple method for controlling consistency of materials (Pashias et al 1999, Kuganathan 2001, Crowder et al 2002, Brackebusch 2002). In this regard, Clayton et al (2003) reviewed the theory and applicability of the slump test using a cone and a cylinder. He demonstrated that the cylinder has greater advantages over the cone due to its geometry, it is less mathematically challenging for modeling, and it has increased reliability for measuring the yield stress of materials. He also conducted several experiments to assess the effect of cylinder height on measured slump, and he mentioned that the slump is not an independent value while the yield stress is a unique property of the material. However, according to Gawu et al (2004), some researchers believe that true yield stress is not a reliable value of material property. It seems that this topic is still open for discussion.

Gawu et al (2004) conducted several experiments to assess the cylindrical slump test as a measure of yield stress for qualifying transportation and deposition of thickened tailings. Three methods, the rotational rheometer in controlled-stress mode, the circular cylindrical slump test, and the vane method were applied to the materials and the results were compared to each other. Gawu et al concluded that the yield stresses of different tailings measured by rheometer and slump method have shown a good correlation to the yield stresses obtained by the vane method. It was also emphasized that the yield stress is an important parameter in characterizing the rheological behaviour of thickened tailings (Gawu et al 2004).

The relationship between yield stress and solid concentration has been considered by many engineers (Boger 1998, Clayton et al 2003, Gawu et al 2004). It was usually found that high solid concentration of material results in an increased yield stress. It should be mentioned that although there is a relationship between yield stress and slump, slump is not dependent on solid concentration. Slump is related to particle size distribution and water content of paste or thickened tailings (Brackebusch 2002, Crowder et al 2002) as well as chemical composition, mineral shape and specific gravity of particles (Brackebusch 2002, Clayton et al 2003).

1.3. Goals and Objectives

According to the literature review and the existing background on this subject, which was previously detailed, the goals and objectives of this research can be articulated as follows:

- Assessment of the modified slump test as a measure of the yield stress of paste mixtures by using cylinders.
- Consideration of diameter and aspect ratio of cylinders on the value of slump, and consequently on the estimated yield stress of paste mixtures.
- Comparison of yield stresses measured by direct methods (such as the vane method) and of those determined by slump tests using cylinders (standard cone and modified conical slump).
- Estimation of plastic viscosity of paste mixtures by adopting the modified cone slump technique employed in concrete testing technology.
- Evaluation of the influence of water content, particle size distribution, additives and binders on the rheological properties of paste mixtures.

1.4. Research Plan and Methodology

Mineralogy and size distribution of tailings, process history and final application of the paste mixtures are the three main factors that control the properties of each paste and its application. This means that every paste mixtures is unique and its application should be subject to detailed evaluation and testing to properly assess local conditions. Therefore, the method of research is based on experimental applications for a specific type of mine tailings and paste fill. In addition, the applicability of the empirical models for measuring the properties of paste fill and the accuracy of theoretical methods will be considered in this research.

In order to ensure that all goals and objectives are achieved, several experiments will be completed for each paste backfill type, including:

- vane method rheometery;
- standard slump test;
- modified slump test using cylinders with different diameters and aspect ratios; and

- modified cone slump for measuring the viscosity of paste.

This thesis includes 6 chapters. The definition of mine paste material, its advantages and disadvantages, and the methods of preparation of paste backfill will be described in Chapter 2. The science of rheology including rheological measurements of material is the topic of Chapter 3. Chapters 4 and 5 address two types of mine tailings used to measure the basic and rheological properties of the samples and to interpret the results. Lastly, the conclusion and recommendation for further study appear in Chapter 6.

CHAPTER 2
PASTE TECHNOLOGY

2.1. Definition of Paste

Paste can be defined through different approaches. Paste is basically a uniform fluid mixture composed of fill materials, which can be divided into three groups: inert material (solid-water), binding agents and chemical additives (Hassani and Archibald, 1998).
The inert materials commonly used are total tailings or alluvial sand and silt with a relatively solid concentration between 70-75% and 85%, or water content between 15% and 25-30% (Hassani and Archibald, 1998; Brackebusch, 1998).
The density of paste depends on both the particle size distribution and the specific gravity of solids. A wide range of size distributions has been employed to produce paste. However, paste should have a minimum weight of 15% of the particles that are smaller than 20 microns. (Cincilla et al., 1997; Tenbergen, 2000). The role of fine particles (<20 microns) is to preserve the water to obtain a non-segregated mixture. Also, the surface area of aggregate particles affects paste properties. The finer the particle size distribution, the more water exists surrounding the particle surface area. This is due to an increase in aggregate particle surface area. The density of paste decreases with an increase in fines of the particle size distribution. The specific gravity of minerals, which makes up the solid parts of the mixture, controls the density of paste at a given water content (Brackebusch, 1998).

Binder agents such as Portland cement, slag and fly ash are employed to increase the mechanical properties, strength and durability of the paste. Cement (usually Type 10) should be added at the time of preparation. Variations of cement percent used in paste and its effect on paste properties have been reported by many engineers. For example, Ouellet et al. (1998) have reported the cement ratio of paste backfills of some Canadian mines between 3 and 6.5 percent of the dry weight. Also, Brackebusch (2000) mentioned that small amounts of Portland cement (0.5%) would increase the shear strength of tailings, up to 20 KPa, which is acceptable in terms of safety and stability for the purpose of tailings disposal. The combinations of cement-slag and cement-fly ash have different effects on the strength and mechanical behaviour of paste (Benzaazoua et al 2004).

Chemical additives such as flocculants, accelerators and retarders may be employed to improve the permeability or consolidation of fill or to increase the flowability of the mixture.

As mentioned previously, paste requires sufficient fine particles to retain the water within the mix matrix, resulting in a no segregating mixture even if paste is not in motion. A small percent of water bleeds to the surface of the paste when it remains without movement. This bleeding causes shrinkage in the paste volume, which has been reported to be about five percent of total volume in many cases (Brackebusch, 1998).

Within the context of rheology, paste is a non-Newtonian fluid material. It is a saturated and homogenous mixture that may show time-independent or time-dependent behaviour. For example, most paste materials from base metal mines have time-independent characterizations while pastes from kimberlite mines demonstrate time-dependent behavior (Brackebusch, 2002; Li et al, 2002, Crowder et al, 2002). Paste as a fluid has its own consistency and shear strength and it can be transported at varing velocity or with shear rate through the pipes.

Consideration of paste as a material, which is fitted between moist soil and slurry, is another approach used to define the characteristics of paste. Figure 2.1. illustrates a variety of particulate materials, from dry powder to pure water, when the water content has been changed from zero to one hundred percent.

Arrangement of particles in paste resembles soil in the way that they must be essentially in contact, while in a slurry they are separated. This transitional state of paste can be shown in the status of saturation. While soils are unsaturated and slurries are over saturated, paste is a saturated mixture. However, to describe the behaviour of paste it can be applied to either slurry rheology or to soil mechanics (Li et al 2002).

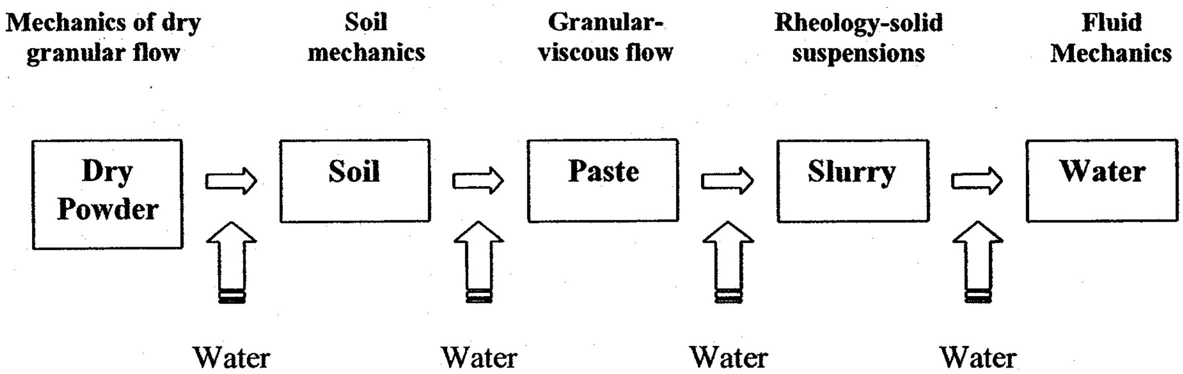

Figure 2.1. Status of science for flow of bulk particulate material at various moisture contents (After Li et al 2002).

As discussed above, it is concluded that each paste application is unique (Tenbergen, 2000) or the paste is not an engineered product (Li et al, 2002) because of the following reasons:

- Changes in tailings mineralogy
- Variation of size distribution
- History of mineral processing
- Final application of the paste

These reasons are valid not only for different mines but also for a single mine over time. Each application should be subject to a precise review in order to properly assess local conditions so that a practical and cost-effective paste application may be designed. Figure 2.2. shows the relative science and application of paste technology.

2.2. Advantages and Disadvantages

The most important benefit of paste according to the definition is that paste is a low water content material with low permeability. The other advantages and disadvantages of using paste as a filling material in the mining industry can be classified as follows (Hassani and Archibald, 1998):

Advantages:

- Reduction of mining cycle due to reaching a high compressive strength within a short period of time;
- Decrease of binder usage such as cement;
- Increase of total tailings consumption as inert material;
- Elimination of slimes draining from the stope in a backfill process;
- Decrease of adjacent ore dilution due to low water content, and consequently high early strength;

Disadvantages:

- The need for dewatering technology, and consequently increase of technical consideration;
- Increase of pressure in pipelines while transporting.

The concept of thickened tailings disposal and its advantages have been recognized for more than a decade. In terms of solid concentration, paste is situated between thickened tailings and filter cake. Paste technology has been suggested as a suitable material for surface tailings disposal due to its environmental and economic advantages (Brackebusch and Shillabeer, 1998). These are some of the advantages:

- Less water inventory and increased safety of impoundment failure;
- Less acid mine generation due to low permeability and capillary action;
- Limitation of ground water pollution resulting from decrease of land usage as well as the reasons mentioned above;
- Constructional cost saving due to elimination of impoundment dikes;
- No need for liners, and capability of using paste with rock waste.

The disadvantages of paste for tailings disposal could be described as the disadvantages for backfilling, which include increased dewatering costs and higher pressure needs for pumping.

2.3. Mechanical Properties

Paste used for backfill purposes usually necessitates a certain strength after its placement underground. Depending on the type of mining method, early and long-term paste strength are required (Tenbergen 2000). Generally, there are several parameters that may affect the mechanical properties of paste fill materials. As described by Benzaazoua et al (2004), these parameters can be articulated as follows:

2.3.1. Macroscopic Parameters

In this category, all phenomena occurring are involved in interaction between paste and adjacent rock at the scale of a stope filled with paste material. For instance, the effects of the following phenomena are more pronounced:

- Interface of the paste fill–rock wall,
- Consolidation due to the pressure change,
- Drainage and cracks in the rock, which may have an effect on the amount of water within the paste fill.

2.3.2. Intrinsic Parameters

In this category, all the parameters depend on the inert material (solids and water), binder agent and the changes occurring during the curing process.

These two groups of parameters, macroscopic and intrinsic, influence one another. Among all parameters, the physical and mineralogical characteristics of tailings as a solid part of the paste material have a significant effect on the mechanical strength of the paste. Mineralogy of tailings determines the chemistry of them. The minerals with sulphides and the portion of the sulphides in mine tailings are very important. The amount of sulphides changes the density of the tailings and the amount of binder requirements. It has been mentioned that the strength of paste fill depends on the sulphides proportion. For sulphide contents less than 12%, there is an adverse effect on the strength of the paste (Benzaazoua et al 2004).

Particle size distribution of tailings is another factor that controls the strength of paste.

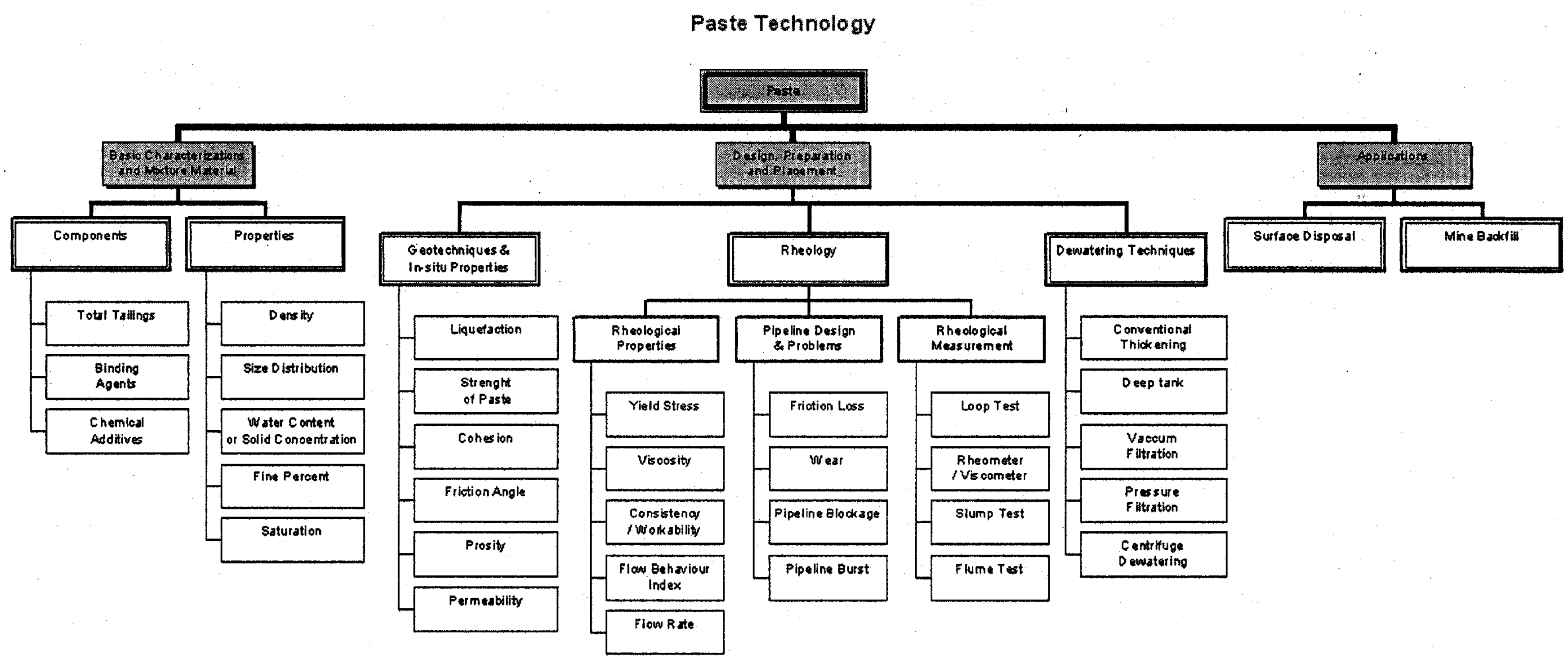

Figure 2.2. Paste technology.

It has been shown that the paste fill reaches higher strength for a uniformity coefficient ($C_u=D_{60}/D_{10}$) value of 12 if the other variables such as the type of binder and the curing time remain constant (Benzaazoua et al 2004).

The type of binder and the proportion of binder are two other factors that affect the strength of paste. It is clear that an increase in the percent of binder in a mixture results in an increase in the strength of the paste material. As discussed before, Portland cement (usually Type 10) is a popular binder agent used for paste fill. Benzaazoua et al (2004) have shown that a combination of cement and slag (20/80) results in a very good strength (higher than cement by itself) while the binders containing fly ash (e.g. cement/fly ash, 50/50) have a weak strength performance for certain types of fill. It is important to note that the mixture with slag-cement binder has shown a very high strength in medium term curing time (28 days), while the long-term paste strengths for all binders vary significantly.

Water content of the mixture is another parameter that controls the paste strength. The higher the water content the lower the strength of paste fill. The uniaxial compression test may be employed for measuring the strength of the paste.

All the parameters described above which affect the strength of paste backfill material are the subject of paste strength determination for the purpose of tailings surface disposal. The difference between these two applications is that only minimal strength is required for stability of paste as stacks or mounds in tailing disposal techniques. It has been mentioned that a drained triaxial compression test is useful for measuring the internal angle of friction (Brackebusch, 2002).

2.4. Paste Preparation and Dewatering

Paste preparation systems have been developed both underground and on surface. While paste technology needs some high fines content and high solid concentration, dewatering systems become increasingly important as an essential part of paste preparation. It has been mentioned that the preparation stage involves expensive dewatering costs when conventional dewatering is followed by filtration techniques (Newman 1992, Hassani et al 1998). However, economical dewatering methods and innovative solutions are required for this purpose. Some of the dewatering systems are described in this chapter.

2.4.1. Conventional Thickening

Thickeners are often employed in the first step of the dewatering stage, although paste as a backfill material will necessitate more dewatering processes such as vacuum filtration, after being passed through a thickener. Thickeners are able to condense large volumes of tailings slurry quickly, and the operation is very simple.

Dorr patented the first commercial thickener in 1907, which utilized revolving rakes. It was a sedimentary machine that worked on the basis of settling particles using gravity. According to sedimentation theory, the rate of settling is directly proportional to the difference in density between the particle and the surrounding liquid (Newman 1992).

Slurry enters through a feed-well to the thickener tanks. The purpose of using a feed-well is to dampen the turbulence of the incoming feed in order to produce a laminar flow and reduce interference with solids that are already inside the tank. The settled solids are raked from the periphery to the central outlet in the tank, and are then pumped away. There are two types of rake driving mechanisms:

- centrally driven; and
- peripherally driven.

Figure 2.3. shows the two main thickener groups and their various configurations. A large number of thickeners are available with different capacities and materials of construction. The capacities of thickener have developed from 0.45 ton/m^2 of thickener area per hour to 2.7 ton/m^2/hr over recent decades (Tenbergen, 2000).

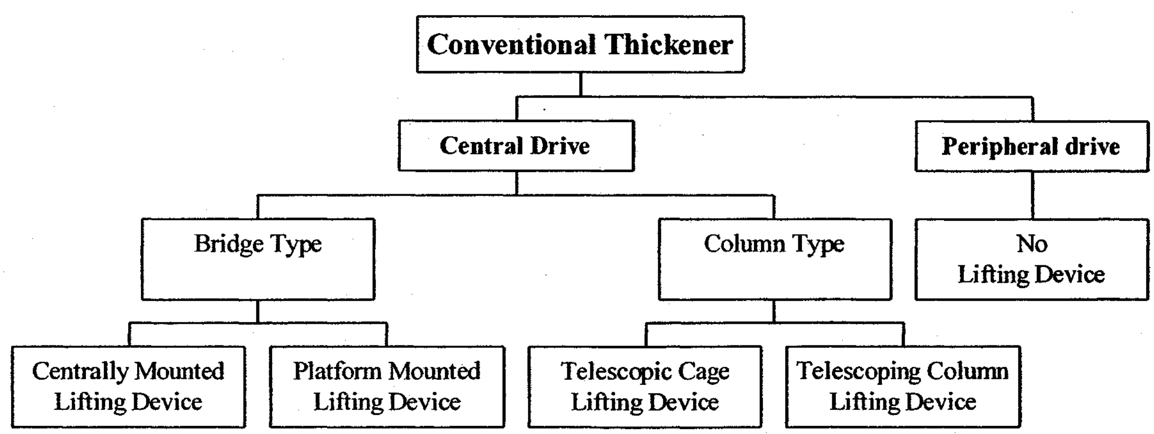

Figure 2.3. Conventional thickeners with diverse configurations (www.solidliquid-separation.com).

Thickener tanks may be constructed from either concrete or steel. Some parameters such as mineralogical properties of tailings and process of production to dewater the tailings should be considered when choosing a suitable construction material. In order to improve thickening efficiencies, flocculent may be added in the process. The purpose of flocculent is to aid agglomeration of the solids and speed settling.

2.4.2. Deep Tank Thickeners

Deep tank thickeners have a significant function in surface paste disposal and in underground paste fill manufacture. They may be employed to produce a fluid material with a higher slump for surface disposal purposes. The underflow produced by a deep tank thickener can be mixed with aggregate to obtain the required structural strength for underground backfill. It can also be used without aggregate when paste strength is not very important (Tenbergen, 2000).

As described by Tenbergen (2000), on the basis of plant design systems, continuous or batch, there are two common types of deep tank thickeners. The following deep tank dewatering systems have been accepted in both the paste backfill and the paste disposal industry. These dewatering units produce a solid-liquid mixture with a yield stress near the part of the curve in Figure 2.4. where it begins to increase rapidly.

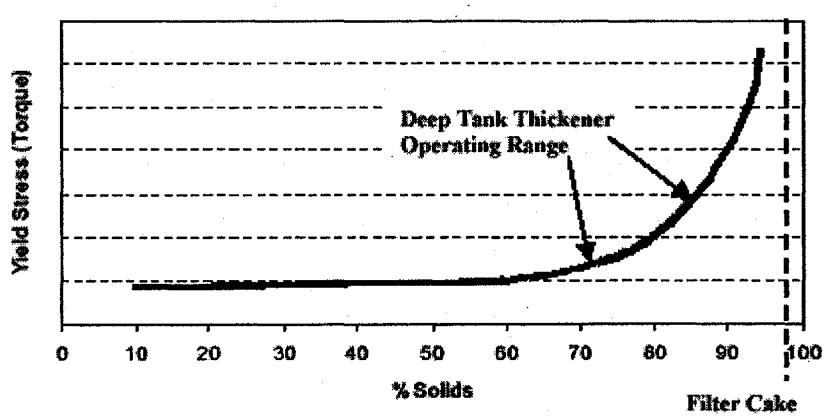

Figure 2.4. Deep tank thickener operating curve (Jewell et al 2002).

1. Paste Production Storage Mechanism

One of the continuous paste production systems is called PPSM (Naylor 1997, Hassani et al 1998). This type of deep tank thickener was designed by GL&V and INCO Ltd. and was developed for backfill purposes. This system includes a tall tank with a typical height of 13 meters and a diameter of 10 meters (Tenbergen, 2000). A shaft helix and raking mechanism inside the tank control paste consistency solids. Tailings are initiated with a flocculent into a feed-well and the paste is removed from the discharge pod that is at the base of the hemispherical bottom of the tank (Figure 2.5.).

The circulation of tailings paste in the tank keeps them sheared and fluid while the reorganization of particle distribution to provide high concentration mixture is attempted (Landriault et al 1996). Indeed, the material has been maintained in storage for up to 2 weeks. Besides, the circulation mechanism of the PPSM results in an increased material strength and prevents the formation of rat-holes when paste is discharged, unlike conventional thickeners. There is anticipated potential of the PPSM for use in mineral processing flow sheets for high thickening and storage in a mine backfill preparation system. Figure 2.6. shows the application of the PPSM for mine paste backfill purposes.

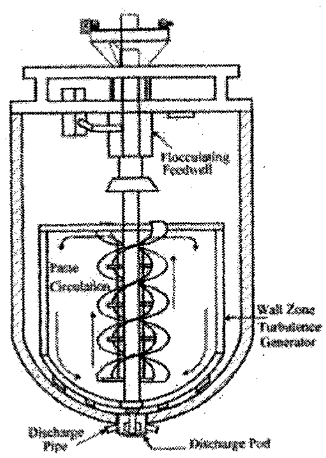

Figure 2.5. Paste production Storage System (GL&V, Process Equipment Group INC.).

2. Baker Process Deep Tank

Baker Process of Salt Lake City (Utah) has marketed another continuous paste production system that has considerable experience with red mud disposal (Tenbergen 2000). The typical height and diameter of the unit are 15 and 10 meters respectively. There is a specialized raking system to keep the settled material mobile in the discharge pod at the bottom of the tank. This system, as with the PPSM, uses flocculent to speed settling, and consequently increases the capacity of the tank.

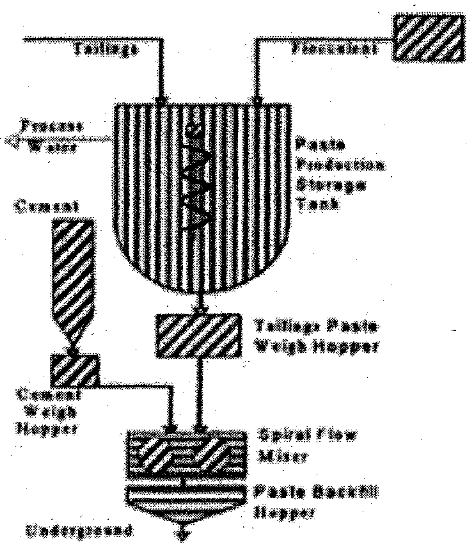

Figure 2.6. PPSM in a mine paste backfill production system (GL&V, Process Equipment Group INC.).

3. **Fluidization**

This type of deep tank batch system has been designed and marketed by Mag Engineering International (Sudbury, Ontario). As described by Hassani et al (1998), fluidization should be considered as an alternative to filtration and PPSM in dewatered tailings preparation to produce high-density material for paste backfill and surface disposal of mine tailings.

The number of tanks or silos that are used in the system depends on the tonnage and turnover requirements. These tanks will be fitted with specialized equipment including dewatering devices and fluidization nozzles. Each tank may be in different modes. For example, in a three-tank system where the first tank is filling and settling the material, another would be in the compaction and decantation mode, and the third in the fluidization mode.

The tailings are added to the top of the silos using a feed-well device after milling. The aspect ratio of the silos varies approximately from 2 to 1 and depends on the type of material. Tailings at the first stage are allowed to settle and densify while the water is removed at the same time. The specific gravity of dry solids and the percent of fine particles are two effective factors in this stage. This process typically takes between 3 to 6 hours. No flocculent or other agents are required and there is no raking aspect in this system.

The next stage in the fluidization of dewatered tailings involves employing nozzles. It depends on the physical properties of the materials and normally takes 30 to 90 minutes to complete. The nozzles, which are placed in the silos, mix the material and keep it agitated to prevent fluctuations in discharge density. In addition, due to the use of these nozzles there is no rat holing or hang-ups required at the time of discharge of tailings material from silos to the binder mixer. Figure 2.7. shows a schematic of paste preparation using the fluidization process.

4. **Deep Cone Paste Thickener**

A deep cone thickener has been produced and marketed by Eimco Process Equipment for paste disposal of mine tailings (Brackebusch, 2002). The discharged underflow from this thickener has workability near the limit of flow ability.

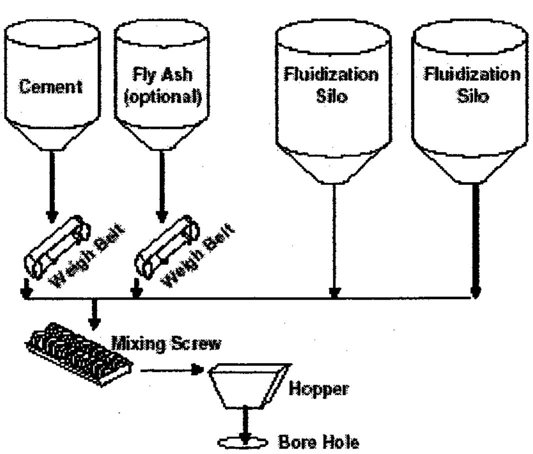

Figure 2.7. Paste fill preparation plant using the Mag Engineering fluidization process (Hassani et al 1998).

The capacity for containing high-density flow is up to 20 times greater than for conventional thickeners, while the capability of hydraulic loading is ten times greater (Figure 2.8.).

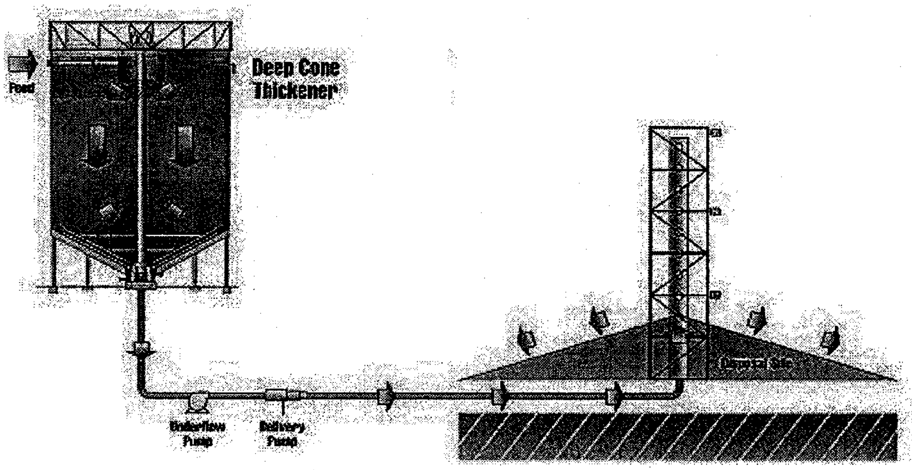

Figure 2.8. Schematic of paste disposal production using Eimco deep cone thickener (www.mining-technology.com).

5. Outokumpu High Compression and Paste Thickener

The Outokumpu high compression and paste thickeners provide constantly higher underflow density. The principle of paste thickeners is that the compression zone is much deeper (more than 3 metres) than on high compression units (Figure 2.9.). Longer bed settling time and higher compressive force on settling flocs are two reasons for increasing underflow density at a given flux rate (tph/m^2) while the compression zone becomes deeper. The advantages of these types of thickeners can be articulated as increasing tailings dam capacity, filter capacity as well as recovery of process water.

These types of thickeners can be employed in a paste backfill preparation system. Some other features of these thickeners are as follows:

- Floc-Miser feed-well
- De-aeration chamber
- Controlled bed level
- Free standing or in-ground tanks
- High rake torque capacity

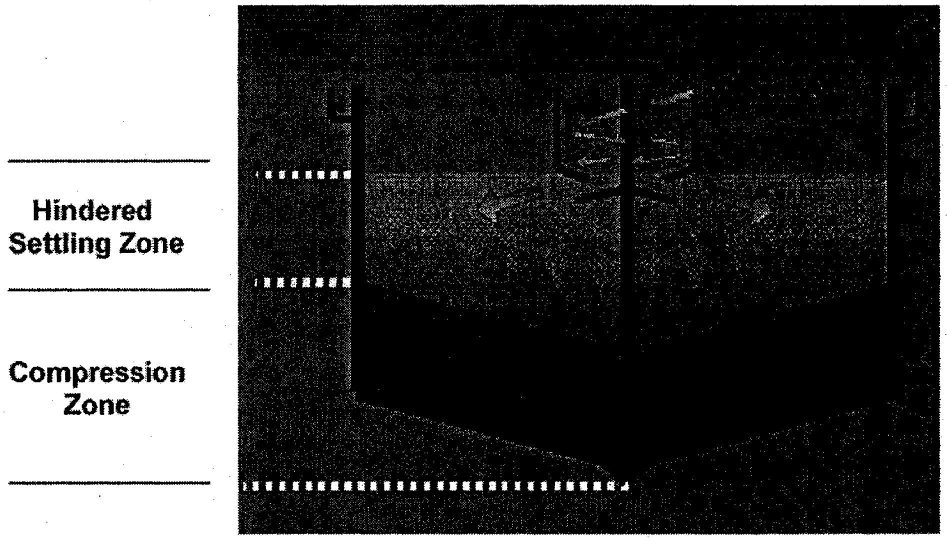

Figure 2.9. A schematic of a high compression thickener (www.outokumpu.com).

2.4.3. Filter Methods of Dewatering

Filtration is an expensive and relatively complicated method of dewatering. Filters are usually employed in the final process of dewatering. There are two common types of filtration techniques, vacuum and pressure filtration.

1. **Pressure Filtration**

The most common types of pressure filtration equipment are the vertical chamber filter press, the continuous belt horizontal chamber and the pressure filter type with an enclosed disk or ceramic disk filter. Some vertical chamber filters have been used for dewatering of tailings in surface disposal industry (Tenbergen 2000). While pressure filters are able to dewater the slurries up to 90 per cent (wt%) of solids concentration, it seems that they are an overkill, and not suitable for paste fill preparation.
The basic operation in all types of pressure filters involves squeezing the mixture against the filter cloth, employing either mechanical or hydraulic pressure. The four processing steps can be defined as feeding into the chamber, pressing, cake washing and filter cloth cleaning. This cycle depending on a situation that takes between 8 to 30 minutes.

2. Vacuum Filtration

Various types of vacuum filtration equipment are available. Disk, drum and belt filters are common types, while belt presses and ceramic media disk filters are more sophisticated.

Belt Filters: The first belt filter was the Landskrona filter built in the 1920's and installed at SUPRA, Sweden (Hassani et al 1998). A variation of cake formation and dewatering zone size are accepted by belt filters. One of the most important features of this system is to separate the filtration zones and multiple cake washings by separating mother and wash filtrates. A typical flow scheme of this filter is shown in Figure 2.10. The operational sequence on a belt filter at the maximum configuration consists of the cake formation and pre-drying, two washing and pre-drying stages, and final washing and drying.

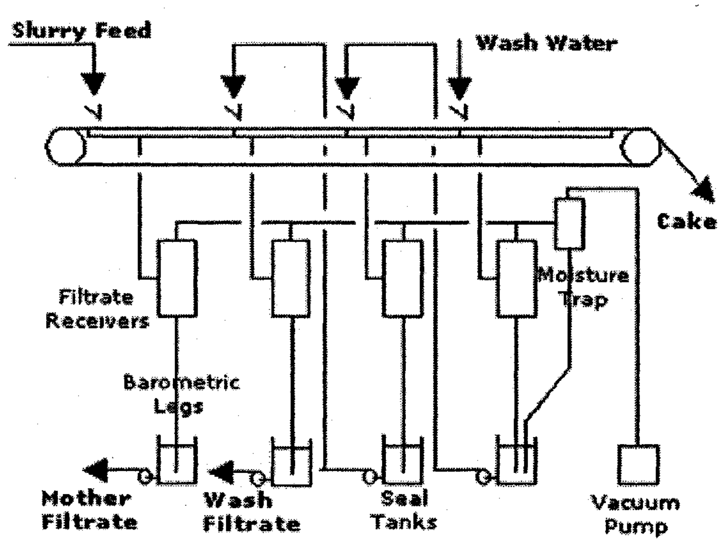

Figure 2.10. A flow-scheme horizontal belt filter (www.solidliquid-separation.com).

Disk Filters: As described by Hassani et al (1998), the original prototype for all continuous vacuum disk filters was developed in 1906. In the late 1980's a disk filter specifically for the production of "high density backfill" was developed. The filter includes several disks (up to 15 disks at the maximum condition), which are made up of pie-shaped sectors covered by a suitable filtering medium. A side view of this filter is shown in Figure 2.11.

During operation, each sector is covered by solids while the disk revolves through the slurry. Consequently, a cake is formed on the face of the disk. It then passes into the drying zone. At this stage the liquid drains into the vacuum receiver via a central barrel. In the discharge zone the vacuum is shut off and a snap or low-pressure blow is applied to fall the cake. Scraper blades on the sides of the disk guide the cake to discharge chutes.

This system requires minimal maintenance. The sectors are easily removed and replaced and the only consumable parts of the machine are the filter cloths. It has been mentioned that the capacity of the machine for tailings dewatering to produce paste backfill is very good (Hassani et al 1998).

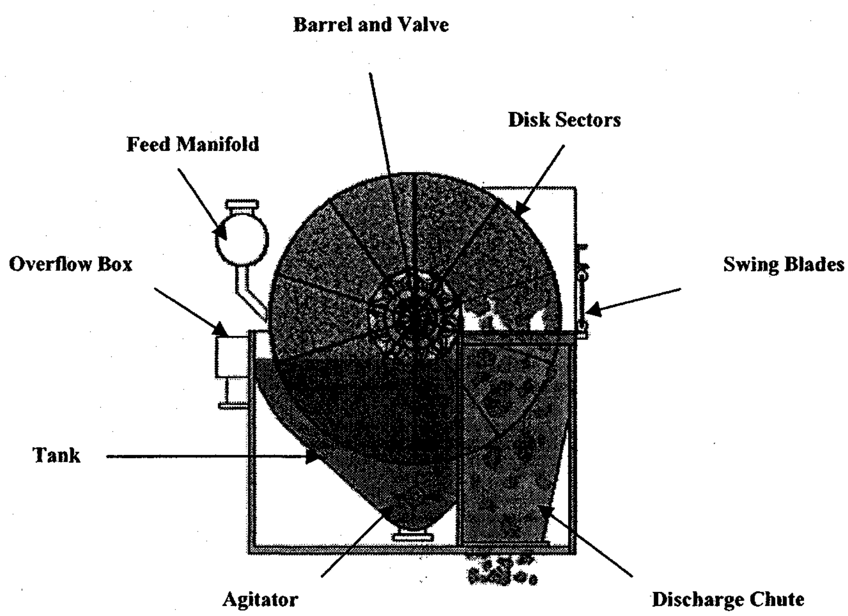

Figure 2.11. Side view of disk filter (www.solidliquid-separation.com).

Drum Filter: The vacuum based rotary drum filter is the most common type of drum filter, and offers a wide variety of solid-liquid separation options. Although this machine is an older filtration system, it has been reported that a vacuum drum filter was used at the Lucky Friday Mine during the paste preparation process.

The operational sequence on a drum filter can be described as cake formation, cake washing and drying, and cake discharge (Figure 2.12.). Once a sector enters submergence, the vacuum is applied and a cake starts to form up to a point where the sector emerges from the slurry. The drying stage of the cycle begins right after making a cake.

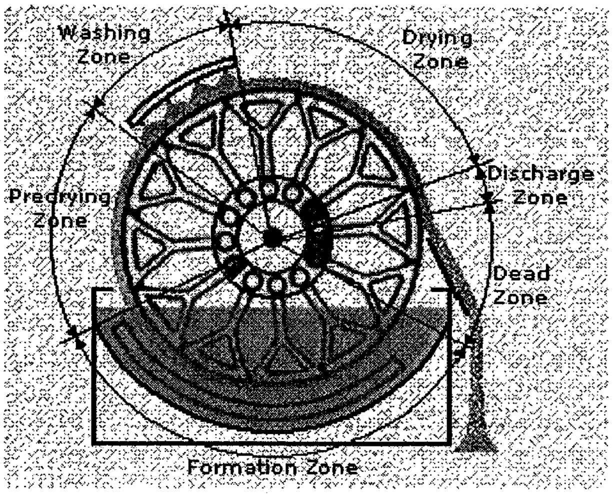

Figure 2.12. Operational cycle of drum filter (www.solidliquid-separation.com).

For some applications there is no wash portion and therefore the drying continues up to vacuum shut off. After the vacuum is shut off, a low-pressure blow is applied to assist cake discharge. After discharging, and in order to prevent vacuum loss on the entire drum surface, there are bridges to block the air. This area is called the dead zone.

2.4.4. Centrifuge Dewatering

According to Tenbergen (2000), the centrifuge technique of dewatering would not be considered for base metal mine tailings. If the mine tailings are very fine with a low specific gravity in a brine solution, centrifuge dewatering may be employed.

There is a special centrifugal dewatering equipment, called Tailspinner (Hassani et al 1992). This equipment was designed by Joy Manufacturing in the 1970's for use underground. It is able to produce a high-density mixture with a solid concentration of 76 to 84 percent (wt%) by dewatering hydraulic fill (60%) at the entrance of the stope. The advantages of this system consist of mobility and design sturdiness. Low capacity, low solids recovery and a poor maintenance record are its disadvantages.

2.5. Paste Plant Design

The design of a paste fill system is related to the characteristics of the material used, the transportation method and the engineering end-use of the paste (Jewell 2002). Two of the most important characteristics of material that may affect design are the mineralogy and the size distribution of tailings (Slottee 2004). In addition, other factors that may control the design of a plant process are expected final paste strength, cost of binders and paste quality control requirements (Tenbergen 2000).

As discussed by many authors (Landriault et al 1996, Hassani et al 1998, Tenbergen 2000, and Jewell 2002), continuous and batch systems are two common plant arrangements for paste preparation. Two key processes in both systems can be classified as dewatering and mixing. Figures 2.13. and 2.14. show the flow sheets of these two systems.

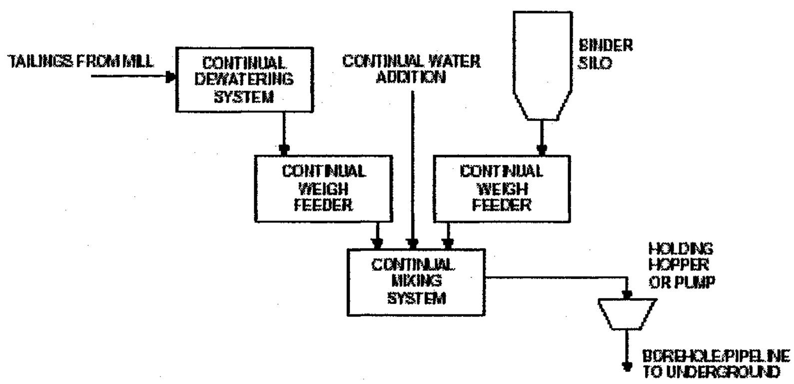

Figure 2.13. Continual paste preparation plant (After Landriault et al 1996 and Hassani et al 1998).

Continual mixers are not self-calibrating and it is not possible to recognize the quality of fluid material properties quickly when a mixture is passing through them. It is unlikely that batch mixers have the capability to readjust incorrect mixture properties by water addition and before discharge into the underground distribution system. It is obvious that a continual system requires a high level of maintenance for calibrating equipment in order to provide acceptable quality production on an ongoing basis.

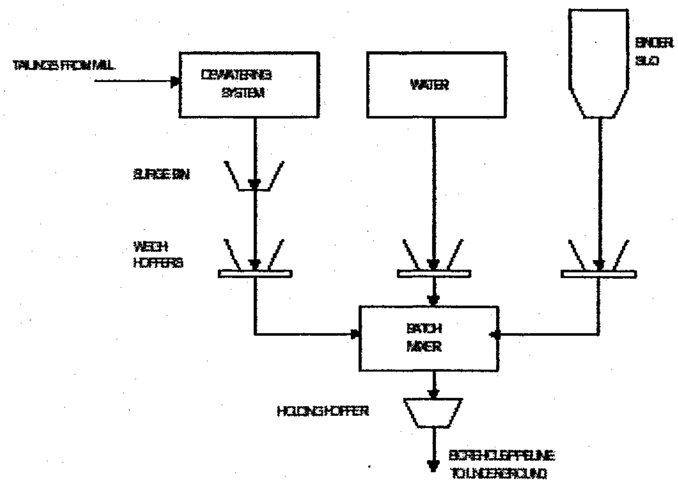

Figure 2.14. Batch paste preparation plant (After Landriault et al 1996, Hassani et al 1998).

CHAPTER 3
RHEOLOGY

3.1. Basic Rheological Concepts

According to the Concise Oxford dictionary, rheology is the science of flow and deformation of matter. Rheology, in the context of paste pipeline flow, is determined as either the viscous characteristics of a fluid that indicates laminar flow phenomenon or as a homogenous solid-liquid mixture that refers to the uniformity of distribution of solid particles across the pipe section. (Slatter 1994, Cooke 2001). As mentioned previously, paste can be such a homogenous mixture.

Generally, fluid materials may be classified as Newtonian or non-Newtonian fluids. The relationship between shear stress (τ) and shear rate (γ) can determine the type of flow or rheological behaviour of a fluid.

Inelastic Newtonian fluids present a linear relationship between shear stress and shear rate. The coefficient of this relationship can be described as constant viscosity (η), as shown in Equation 3.1.

$$\eta = \frac{\tau}{\dot{\gamma}} \qquad \text{(Equation 3.1)}$$

where τ = shear stress (Pa)

$\dot{\gamma}$ = shear rate (s^{-1}).

While shear stress demonstrates a frictional force due to applied force to the fluid, shear rate can be defined as a gradient of velocity (du/dy) across the fluid layers.

A fluid can be identified as non-Newtonian when only one of the following characterizations is valid:

- no linear relationship exists between shear stress and shear rate;
- a linear relationship between shear stress and shear rate exists, but the line does not pass through the origin;
- the relationship between shear stress and shear rate demonstrates time dependency.

Two common types of non-Newtonian fluids are classified as time-independent and time-dependent. There are many models that describe non-Newtonian fluids or solid-liquid mixture behaviour. For example, the Casson (1959) model describes the laminar flow of time independent fluids in a number of instances; Herschel-Bulkley or the yield power law model (1926) shows many different types of fluid for laminar flow, the Govier and Aziz (1972) model classifies non-Newtonian flow as time-dependent and viscoelastic (Cooke and Paterson 1996). The Ostwald-De Waele model (Power law) is used for classification of time-dependent material (Boger 2002). Figure 3.1 shows the classification of non-Newtonian fluids. Figure 3.2 indicates the rheogram of all time-independent fluids as well as the linear behavior of Newtonian fluid based on the yield power law model.

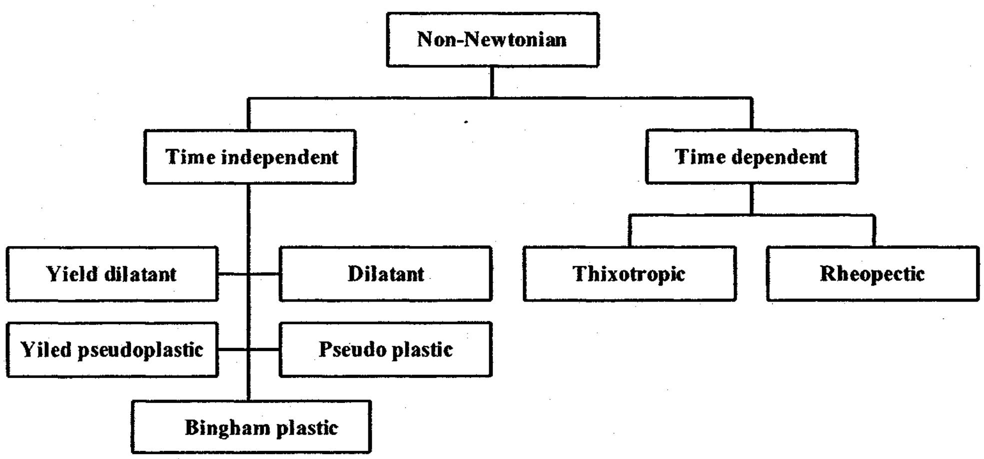

Figure 3.1. Non-Newtonian fluid classification based on the yield power law model.

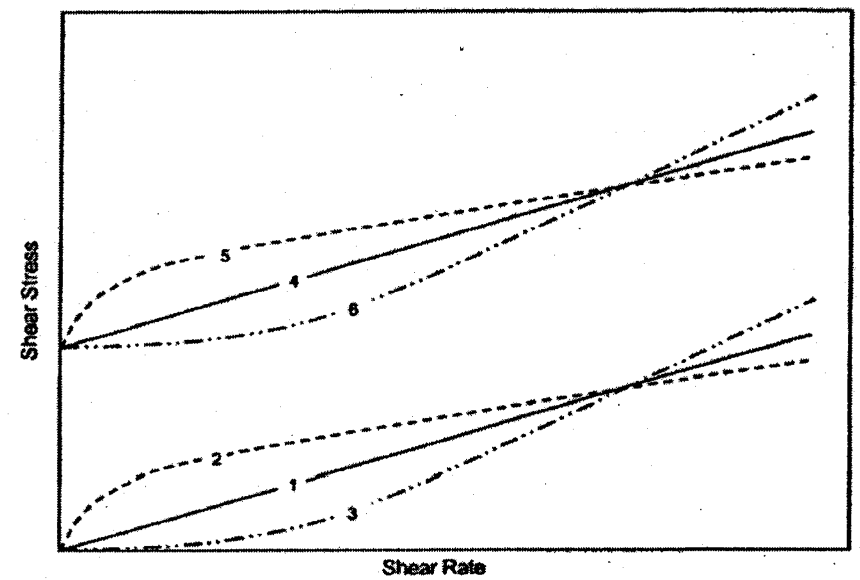

Figure 3.2. Rheogram of different types of time-independent fluids and Newtonian fluid.

There are two types of time-dependent fluids, thixotropic and rheopectic. The viscosity of rheopectic fluid increases with time, while that of thixotropic fluids decreases (Figure 3.3). Generally, the following reasons cause the time dependency of fluid rheology:

- mixing and shearing energy input;
- temperature and pressure changes;
- progression of chemical, electrochemical and surface reactions (Li et al, 2002).

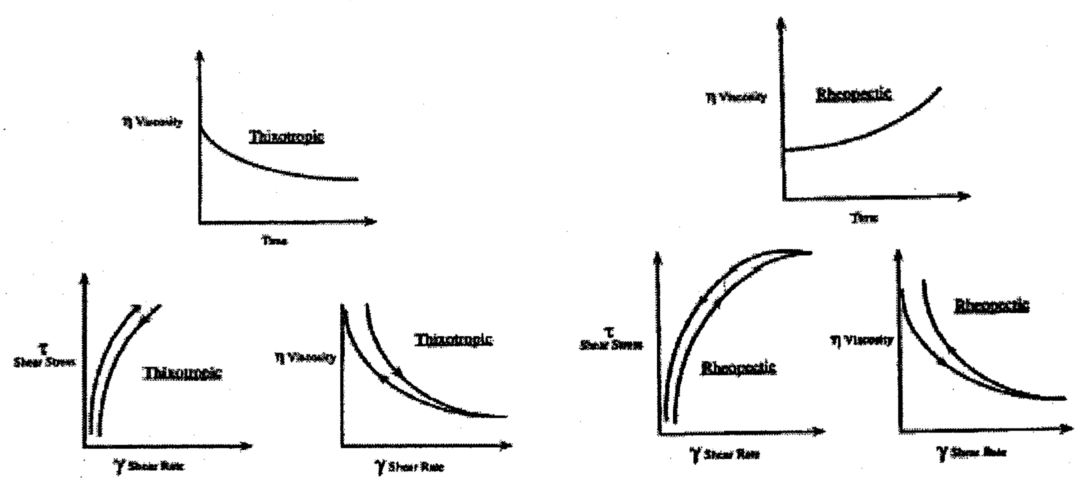

Figure 3.3. Rheological behaviour of time dependent fluids (Li et al 2002).

The terms shear thinning and shear thickening have been used for both time-independent and time-dependent fluid materials. Table 3.1 explains this terminology.

Table 3.1. Shear thinning and shear thickening behaviour.

Behaviour	Shear-thinning (Decreased viscosity)	Shear-thickening (Increased viscosity)
Time-independent	Pseudoplastic &Yield-pseudoplastic (with increasing shear rate)	Dilatant and Yield-dilatant (with increasing shear rate)
Time-dependent	Thixotropic (with increasing time)	Rheopectic (with increasing time)

3.2. Rheological Models and Parameters

There are several empirical flow models for different fluids. The most common equations can be categorized as follows:

- **Herschel-Bulkley or Yield Power Law Model:**

$$\tau = \tau_y + K\dot{\gamma}^n \quad \text{(Equation 3.2)}$$

where τ_y = yield stress

K= fluid consistency

n= flow behaviour index.

For a Newtonian fluid (n=1 and $\tau_y = 0$ substituted in Equation 3.2), the viscosity (K= η) is represented by the slope of the rheogram, and is constant, as function 3-2 demonstrates a linear relationship between shear stress and shear rate.

The yield power law model is usually employed for non-Newtonian (time independent) materials. The rheological parameters of time independent fluids are presented in Table 3.2 and the relevant curves are shown in Figure 3.2.

- **Ostwald-De Waele or Power Law Model:**

$$\tau = K\dot{\gamma}^n \quad \text{(Equation 3.3)}$$

This model is used for shear thinning and shear thickening materials. For $\tau_y = 0$ in Equation 3.2, the yield power law model is reduced to the power law model.

Table 3.2. Rheological parameters of different types of non-Newtonian fluids.

Behaviour	τ_y	n
Pseudo-plastic	0	<1
Dilatant	0	>1
Bingham plastic	>0	=1
Yield pseudo-plastic	>0	<1
Yield dilatant	>0	<1

- **Bingham Plastic Model:**

$$\tau = \tau_{yB} + K_B . \dot{\gamma} \qquad \text{(Equation 3.4)}$$

where τ_B = Bingham yield stress

K_B = Bingham plastic viscosity.

This model presents a linear equation and is very suitable for use when measuring the yield stress of material.

- **Casson Model:**

$$\tau^{1/2} = \tau_y^{\ 1/2} + \mathrm{K}(\dot{\gamma})^{1/2} \qquad \text{(Equation 3.5)}$$

It has been mentioned that $K = (\eta_P)^{1/2}$ where η_P is the plastic viscosity (Yan et al 1997). The first three models are more generally used in paste technology and in the mining industry.

Generally, factors that may affect rheology of solid-liquid mixtures are (Cooke 2001):

- Solids characteristics: particle size and shape, density, chemical composition, surface charge and concentration;
- Liquid properties: density, viscosity, temperature and chemistry;
- pH, binder type and dosage.

Two main rheological properties of fluid can be described in the following subtitles.

3.2.1. Yield Stress

The concept of yield stress in fluid material was recognized and introduced by Bingham and Green in 1920. The yield stress of a fluid is usually defined as the minimum shear stress required to initiate significant flow (Uhlherr et al 2002). This stress is related to the strength of the bond network structure (Nguyen & Boger 1983 and Bhattacharya 1999). Generally, the mechanical behaviour of a non-Newtonian fluid, such as paste, is elastic at shear stresses less than yield stress. The fluid is supposed to flow like a viscous material with a finite viscosity when the shear stress exceeds the yield stress (Pashias & Boger 1996). The "shear yield stress" may be a better term, but for reasons of economy it is called yield stress (Gawu et al 2004).

According to Liddell et al (1994), the value of yield stress depends on pH for the suspension fluid or thickened tailings. The yield stress of mixtures usually changes with percentage of solid, and the correlation between the two has been used by many designers for surface disposal of mine tailings and prediction of pumping energy requirements in a pipeline transportation system (Sofra and Boger 2000, Sofra and Boger 2001, van Dijk 2001, Gawu et al 2004). If paste is considered a mixture, it is preferable to use water content due to the definition of paste as a saturated mixture and its dependency on size distribution. However, the yield stress of paste or thickened tailings is one of the important parameters that must be determined prior to applying them to paste fill or tailings disposal.

According to the yield power law model, the yield stress of fluid material (if $\tau_y > 0$) is presented as the intercept of the shear stress-shear rate curve, and can be measured by different techniques. The Herschel-Bulkley model, which is a combination of power law and Bingham plastic models, is usually used for indirect determination of yield stress.

3.2.2. Viscosity

For non-Newtonian fluids, the viscosity is not constant and is referred to as apparent viscosity (Cooke 2001, Slatter 2004). Based on the rheological models discussed earlier, the following equations have been introduced to describe the viscosity of fluid materials (Steffe 1996, Yan et al 1997, Slatter 2004).

- **Herschel-Bulkley Model:**

$$\tau = (\frac{\tau_y}{\dot{\gamma}} + K\dot{\gamma}^{n-1})\dot{\gamma} \qquad \text{if } \tau > \tau_y,$$

$$\eta = \frac{\tau_y}{\dot{\gamma}} + K\dot{\gamma}^{n-1} \qquad \text{(Equation 3.6)}$$

For the Bingham model (n=1, K= K_B) and the power law model ($\tau_y = 0$), the viscosity relationships can be derived from equation 3-6, as follows:

$$\eta = \frac{\tau_{yB}}{\dot{\gamma}} + K_B \qquad \text{(Equation 3.7)}$$

$$\eta = K\dot{\gamma}^{n-1} \qquad \text{(Equation 3.8)}$$

These equations show the apparent viscosity as a function of shear rate for non-Newtonian fluids. Figure 3.4 presents the viscosity-shear rate curves for different time independent fluids. These three models offer a suitable calculation of viscosity for paste pipeline designers but they are not satisfactory at high and low shear rates (Saltter 2004). There are other models for calculating viscosity of time independent fluids, such as the following (Steffe 1996):

- **Van Wazer Model (1963):**

$$\eta = \eta_\infty + \frac{\eta_0 - \eta_\infty}{1 + K_1 + \dot{\gamma}K_2(\dot{\gamma})^{n_1}}, \qquad \text{(Equation 3.9)}$$

- **Cross Model (1965):**

$$\eta = \eta_\infty + \frac{\eta_0 - \eta_\infty}{1 + K_1(\dot{\gamma})^{n}}, \text{ and} \qquad \text{(Equation 3.10)}$$

- **Carreau Model (1968):**

$$\eta = \eta_\infty + (\eta_0 - \eta_\infty)\left[1 + (K_1\dot{\gamma})^2\right]^{(n-1)/2} \qquad \text{(Equation 3.11)}$$

where K_1 and K_2 are arbitrary constants and n is a power indicate determined from experimental data.

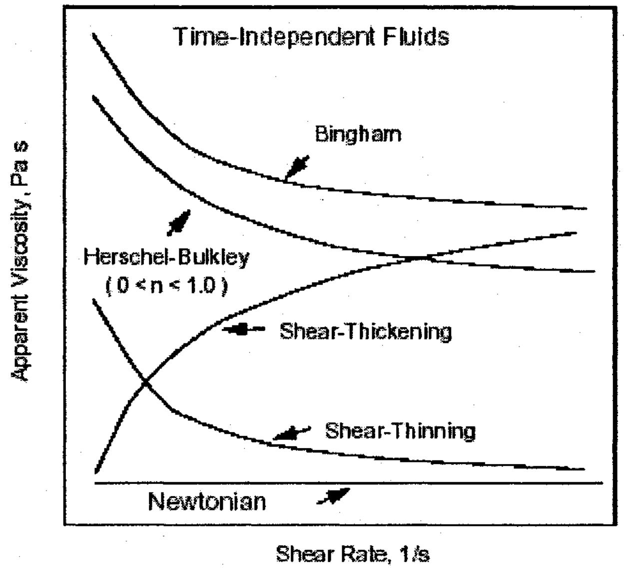

Figure 3.4. Behaviour of apparent viscosity of time independent fluids (Steffe 1996).

Slatter (2004) has described the Cross model as a replacement equation that can improve the fundamental shortcomings of the other models at high and low shear rate (Figure 3.5).

3.3. Yield Stress Measurements

A number of techniques have been developed for measuring the yield stress of fluid material. These techniques can be classified as direct and indirect methods. Generally, indirect methods refer to the measurement of yield stress with extrapolation of shear stress- shear rate data. The yield stress value is obtained in the limit of zero shear rate. A rheological model can be considered for the measurement, and the related value can be named as "apparent" or "extrapolated" shear stress (Nguyen and Boger 1992). Direct methods are involved in the independent assessment of yield stress, and the measured value can be referred to as "true" yield stress , describing the critical shear stress when the fluid begins to flow.

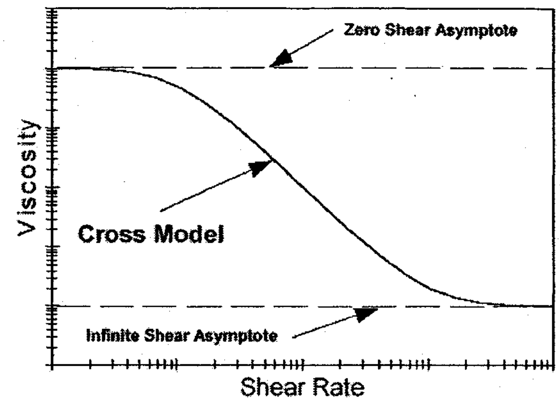

Figure 3.5. Cross model viscosity curve.

3.3.1. Indirect Methods

Two common types of indirect methods are described below:

1. **Direct Data Extrapolation**

The procedure for this fast method involves obtaining a rheogram of fluid and taking the shear stress intercept (γ=0) as the yield stress. The data may show a linear or non-linear curve. Obtaining the yield stress from a linear curve is very straightforward, and the behaviour of the flow is called the Bingham plastic fluid behaviour. With non-linear behaviour, obtaining the yield stress becomes more sophisticated due to the dependence of yield stress on the lowest shear rate data. Therefore, it is vary important to assess the reliability of the low shear rate data before extrapolation can be made. Wildemuth & Williams (1985) presented a simple method for this assessment (Nguyen et al 1992).

2. **Extrapolation Employing Flow Models**

One of the visco-plastic flow models can be employed to extrapolate the data. This method of extrapolation is very straightforward, particularly when the Bingham plastic model has been selected as a fitting curve. In most cases, such as suspension fluids, this model can approximate an over-prediction of the yield stress value. It has been mentioned that the yield stress of a fluid can be determined by different models, and consequently more than one yield stress value can be measured for a specific fluid. Therefore, such assumptions are not recommended for extrapolation of fluid data.

3.3.2. Direct Methods

As described by Nguyen and Boger (1992), a number of techniques have been developed for measuring the yield stress directly. The criteria used for determining the yield stress differ for each technique, although the basic principle of considering yield stress between flow and non-flow is usually applied.

1. **Stress Relaxation**

The yield stress is measured when an applied constant shear rate or shear stress is suddenly or gradually brought to rest. Therefore, the residual stress remaining in the fluid upon termination of flow is representative of the yield stress. In this method, a rotational viscometer can be used for shearing the fluid. It has been mentioned that the stress relaxation method is appropriate for the yield stress measurement of fluids that have previous shear history independency due to pre-shearing action.

While the yield stress is interpreted as the residual stress that remains at equilibrium on the stationary body, the characteristics of the rotating body, such as wall slip, inertia and damping, may affect the measured residual stress. These characteristics, which reproduce poorly, are limitions of this technique (Bantoft 1959, Cokelet et al 1963, Nguyen and Boger 1983, Magnin and Piau 1990 and Nguyen and Boger 1992).

2. **Strain Recovery**

In this method, yield stress is measured when a constant shear stress is applied to the fluid. A shear strain (creep)-time curve can show the behaviour of fluid during the test. In the elastic zone, the strain increases with time up to a constant value, and it is obviously possible to have a strain recovery after removing the shear stress. The shear stress in this zone is less than the yield stress. For stresses that exceed the yield point, the strain also increases with time and the fluid behaves like a viscous flow with a finite shear rate. Figure 3.6 shows a number of typical strain-time curves for yield stress measurement of fluids using this method. The yield stress can be determined from sharp changes in the curve slope. However, in some systems such as suspensions it is somewhat difficult to recognize yield stress of material from shear strain- time curves.

This method can be applied using a rotational viscometer and is very sensitive in terms of assessing the characteristics of flow and deformation. One of the drawbacks of this technique as well as other techniques using a rotational viscometer is the effect of wall slip under slow flow state on the estimation of yield stress. The effects of two other characteristics of this instrument, damping and inertia, on the measurements have also been reported for this method (Davis 1971, Komatsu et al 1973, Krieger 1990 and Nguyen and Boger 1992).

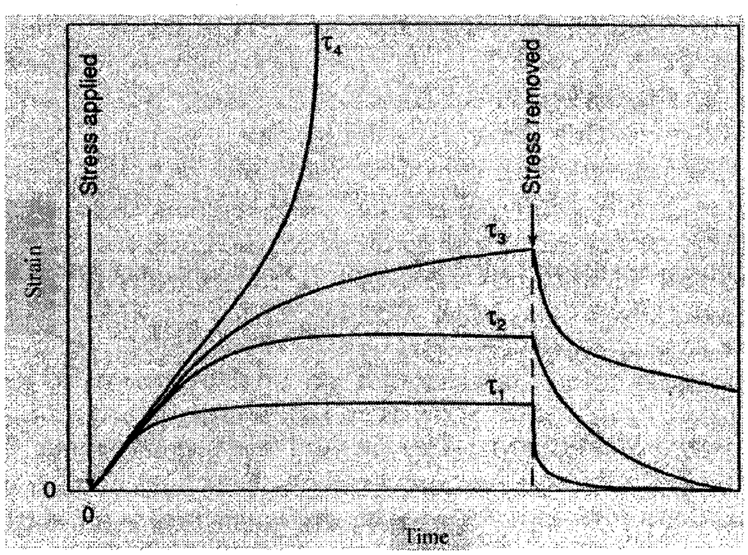

Figure 3.6. Typical strain (creep)-time curves at different shear stresses (Nguyen and Boger 1992).

3. Stress Growth Experiment

A constant low shear rate is applied to the fluid, and shear stress is measured as a function of time in this method. A typical shear stress-time curve presents three regions; the linear region, the non-linear region and the stress decay portion (Figure 3.7). The peak (point A) of the curve, which shows the maximum shear stress and corresponds to a complete breakdown of the fluid structure, has been suggested by Pryce-Jones (1952), Van den Temple (1971) and Papenhuijzen (1972) as a value of the yield stress (Nguyen and Boger 1992). According to several other researchers, such as Lin & Brodkey (1985) and Nagase & Okada (1986), the stress overshoot depends on applied shear rate and the value of yield stress can be considered at the end of the elastic region (point B) where fluid begins yielding. Hence, upper and lower yield stress values should be considered with these two points of view (Nguyen and Boger 1992).

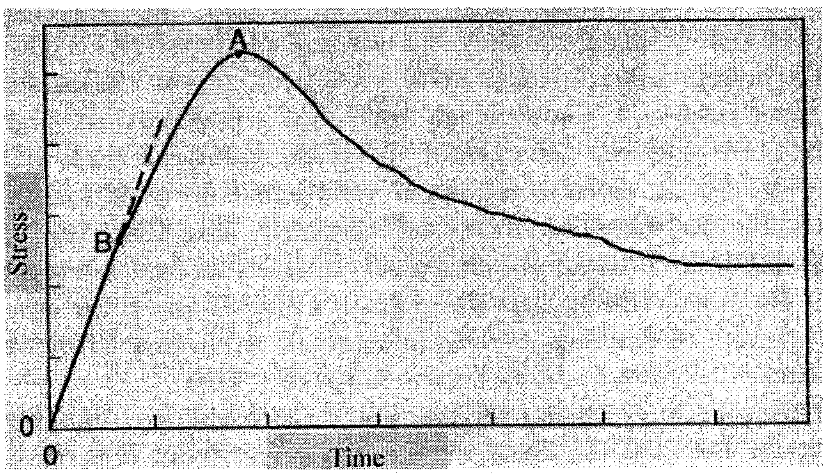

Figure 3.7. Typical stress-time curve with applying constant shear rate (Nguyen and Boger 1992).

A rotational viscometer can also be employed for this method, and some limitations and difficulties can be expected when using such rotational devices for measuring yield stress. In this method, the poor reducibility of the result has been identified due to wall slip, instrument inertia, sensitivity to external distribution, and fluid fracture after yielding.

4. Cone Penetration

The cone penetration technique has been employed in many fields of engineering and in other industries. In this method, a cone penetrates under a constant force into a fluid horizontal surface. While the cone is entering the fluid, the surface area of shear between the cone and the fluid increases, and consequently the shear stress decreases. The yield stress can be considered at the equilibrium state of the shear stress and the yield stress of the fluid where the cone stops penetrating. Figure 3.8 shows the geometry of the cone, and the yield stress can be determined as follows (Equation 3.12):

$$\tau_y = \frac{K.F}{Z^2} \qquad \text{(Equation 3.12)}$$

where: F is the force (including the weight of cone)

Z is the indentation depth

K is a geometrical factor and may be determined from the following equation.

$$K = (\cot\psi)^2 / \pi, \qquad \text{(Equation 3.13)}$$

where 2ψ is the cone angle.

It has been mentioned that this method is most suitable for a fluid material with a high yield stress or low viscosity due to minimal effect of viscous resistance to penetration of the cone. On the other hand, the lesser the penetration time the more reliable the yield stress value (Nguyen and Boger 1992).

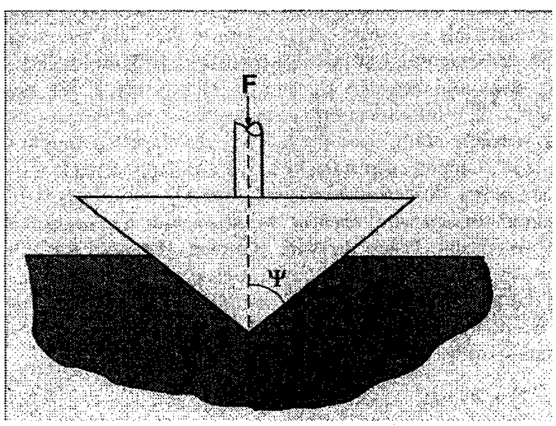

Figure 3.8. Cone geometry and the equilibrium state in cone penetration method (Nguyen and Boger 1992).

The vane method is another method of direct measurement of yield stress. As the vane method has been chosen for this study due to its applicability and advantages, details of the principles and theory of the method are discussed in this chapter.

3.4. Vane Method

Basically, the vane method has been used for measuring the shear strength of cohesive soils. A standard test method for a laboratory miniature vane shear test for saturated clayey soil ($\varphi=0$) has been devised and published by ASTM (ASTM D 4648-87). Nguyen and Boger (1983) adopted this method to determine the yield stress of concentrated suspensions. Although Russell (1936) and Hobson (1940) had used this method for measuring the yield value, they did not obtain a direct relationship between the true rheological yield stress and the value measured by them (Nguyen & Boger 1983).

As described above, the effect of wall slip on the yield stress was the major problem for many methods using a rotating cylinder. The idea of using the vane method was to eliminate this problem, which is due to the geometry of the vane, as well as to minimize any disturbance caused by immersing the vane in the fluid.

This method is used in the mining industry for measuring the yield stress of thickened tailings and paste material (Crowder et al 2002, Gawu et al 2004) as well as concentrated suspensions.

3.4.1. Principles of Vane Measurements

In this method, a vane spindle, including 2-8 small blades, is inserted into the sample held in a beaker. In order to prevent the effect of rigid boundaries, the depth and diameter of the beaker should, as a rule of thumb, be twice as large as the length and the diameter of the vane (Nguyen and Boger 1983). Figure 3.9 presents the installation of a vane in a sample as well as the dimensions of the vane and beaker. Nguyen and Boger (1985) suggested the following criteria for vane and container dimensions:

$H/D_v < 3.5$; $D_T/D_v > 2.0$; $Z_1/D_v > 1.0$; and $Z_2/D_v > 0.5$.

After the vane is fully immersed it is rotated at a very low constant rotational speed, and the torsion required to maintain the constant motion of the vane is measured as a function of the time. A typical torque-time curve is shown in Figure 3.10. The first region of the curve shows linear behaviour, which is responding to the elastic deformation of the fluid close to the edges of the vane blades.

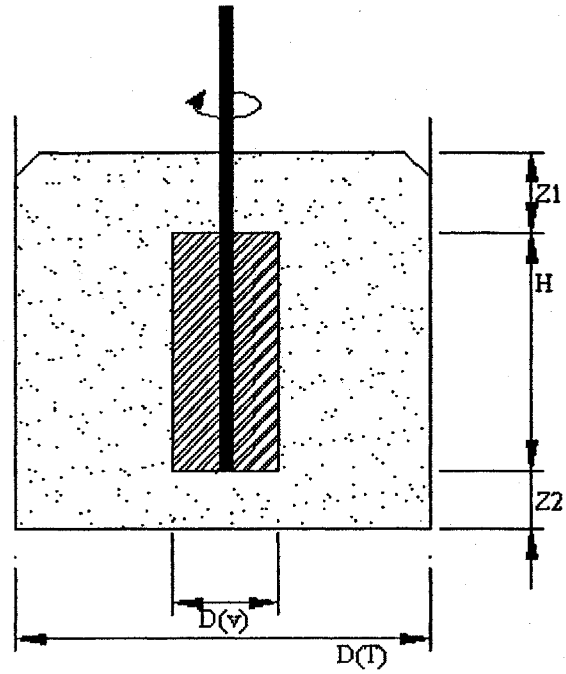

Figure 3.9. Schematic of a four-bladed vane installed in a sample (After Nguyen et al 1985).

It has been mentioned that the stretching of the "network bonds", which are connecting the structural elements of the fluids, may manifest the same deformation behaviour. This means that the resistance of the network increases due to the involvement of more bonds, and consequently, more torque would be required to maintain a constant rotational speed. The network bonds start breaking at the maximum torque, and after collapsing all of the network bonds the fluid may manifest viscoplastic behaviour. It has been mentioned that the appearance of maximum torque in the torque-time curve is a true characteristic of fluid materials with a yield stress, and that this value can be related to the yield stress (Nguyen and Boger 1983).

3.4.2. Calculation of Yield Stress with Vane Method

In order to calculate the yield stress of material from maximum torque, Nguyen and Boger (1983 and 1985) cited two main assumptions as follows:

- yield surface is considered to be a cylinder whose dimension is equal to the vane;

- shear stress is uniformly distributed on the cylinder.

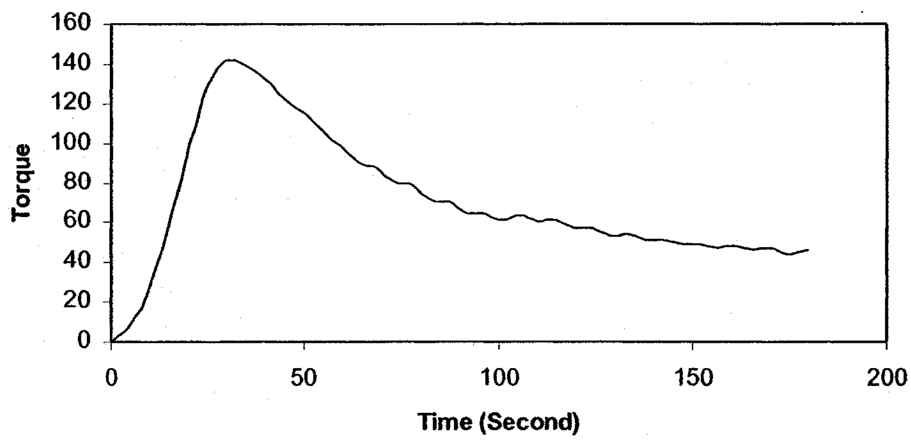

Figure 3.10. Typical torque-time curve obtained with a vane method.

The third assumption, made by Barens et al (1990), is that:

- There is no secondary flow between the blades.

The reliability of these assumptions has been investigated for Herschel-Bulkley and Casson plastic fluid using a numerical method (Yan et al 1997). Based on these assumptions, the total torque measured is equal to the two components created on the cylindrical wall and the two end surfaces due to shearing of material. The force balance is given as follows:

$$T = (2\pi R_v H)\tau_w R_v + 2\left[2\pi \int_0^{R_v} \tau_e(r).r.dr.r\right], \qquad \text{(Equation 3.14)}$$

where T = torque;

R_v = radius of the vane;

H = length of the vane;

τ_w = shear stress at the cylindrical wall;

τ_e (r) = shear stress at the end surface.

For the small diameter vane, τ_e is equal to τ_w (second assumption) and at the maximum torque (T_m) the shear stress τ_w is equal to the material yield stress τ_y. Therefore, the Equation 3.14 can be re-written as Equation 3.15.

$$T_m = \frac{\pi D_v^3}{2}\left(\frac{H}{D_v} + \frac{1}{3}\right)\tau_y \qquad \text{(Equation 3.15)}$$

It is obvious that the yield stress of material in this method depends on the maximum torque and the vane dimensions.

As described by Nguyen and Boger (1983), the error of the second assumption can be estimated by either empirical techniques or analytical methods. The analytical technique, which has been developed for this estimation, can be explained as follows.

If: $\tau_e(r) = (\frac{r}{R_v})^P \tau_w$, $0 \leq r \leq R_v$, (which satisfies the boundary conditions)

where P (≥ 0) is a constant describing the radial distribution function of τ_e.

With substituting τ_e in Equation 3.14 at maximum torque, then:

$$T_m = \frac{\pi D_v^3}{2}\left(\frac{H}{D_v} + \frac{1}{P+3}\right)\tau_y . \qquad \text{(Equation 3.16)}$$

It is obvious that with a P = 0, Equation 3.16 is the same as Equation 3.15. Table 3.3 shows the error involved in employing Equation 3.15 as a function of H/D_v and P.

Yoshimura et al (1987) suggested placing the vane in the fluid (emulsion) such that there is no space between the top edges of the blades and the surface of the fluid. This positioning causes the elimination of one of the end surfaces of the assumed cylinder, and consequently, the following equation has been used for yield stress calculation:

$$T_m = \frac{\pi D_v^3}{2}\left(\frac{H}{D_v} + \frac{1}{6}\right)\tau_y \qquad \text{(Equation 3.17)}$$

Table 3.3. Estimation of errors involved in employing Equation 3.15 compared with P=0.

H/D_v	P = 1	P = 2	P = 3
1	6.67%	11.11%	14.29%
2	3.7%	6.06%	7.69%
4	1.96%	3.17%	4.00%

3.4.3. Vane Dimensions

As discussed above, a vane spindle consists of several small blades joined around a cylindrical shaft. There should be between 2-8 blades. The common type of vane has four blades. The number of blades has no effect on the measurement. For example Yoshimura et al (1987) have not detected any difference between four-bladed and eight-bladed vanes. The aspect ratio of the vane ranges between 1-3.5, as suggested by Nguyen and Boger (1983), or between 1.5-4, as suggested by Steffe (1992). These criteria, which are very similar, have been used by several researchers (e.g. Liddell et al 1996, Gawu et al 2004). There are numbers of commercial vanes for different applications and for different ranges.

3.4.4. Rotational Speed of Vane

As described in the principle section, for detecting the maximum torque in the shear rate controlled mode, the vane spindle should be rotated at very low speeds. Due to viscous resistance associated with instrument inertia and insufficient damping at very high rotational speeds, significant errors may occur when measuring the maximum torque and calculating the yield stress (Nguyen and Boger 1983). It has therefore been suggested that the stress-controlled mode should be used rather than constant shear rate due to independence of the maximum stress on rotational speed (Yoshimura et al 1987).

However, to discover the suitable range for rotational speed whereby the maximum torque is independent of the shear rate, several experiments should be conducted on the fluid (Nguyen and Boger 1983, Liddell et al 1996, Barnes et al 2001). For example, Figure 3.11 presents the maximum torque measured for a 70 % titanium suspension at different rotational speeds. It is obvious that the suitable rotational speed for the Haake rheometer is between 0.003-0.007 (rad/sec), and for the Weissenberg Rheogoniometer is between 0.01-0.03 (rad/sec). In another instance, the rotational speed of 0.3 (rpm) has been used for yield stress measurements of thickened tailings and paste with the vane method (Crowder et al 2002 and Gawu et al 2004).

3.5 Rheometery/ Viscometery

The following rheometers and viscometers are more commonly used for measuring rheological properties of slurry and paste materials.

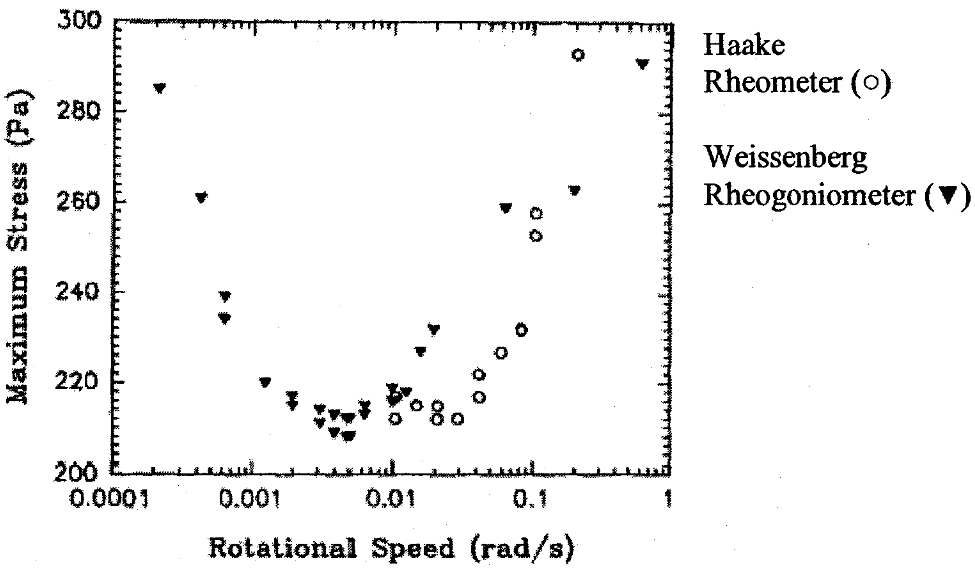

Figure 3.11. Maximum stress vs. rotational speed for titanium suspension (Liddell et al 1996).

3.5.1. Tube viscometery

This type of viscometer, which is also called the capillary viscometer, has been used and recommended by several engineers in the mining industry (Cooke & Paterson 1996, Cooke 2001 and Slatter 2004).

In this rheometer, a fluid flows at a constant velocity V through a tube with a length L and an inside diameter D. This demonstrates exactly what may happen in a pipeline fluid transportation system. Figure 3.12 shows a schematic of a tube viscometer. If ΔP considered as pressure drops within the rheometer tube, for a laminar of inelastic fluid, the shear stress and shear rate are given as:

$$\tau_{rz} = \frac{r\Delta P}{2L} \qquad \text{(Equation 3.18)}$$

$$\dot{\gamma} = f(\tau_{rz}) = -\frac{dv_z}{dr} \qquad \text{(Equation 3.19)}$$

These rheological parameters at the wall of the tube can be determined as:

$$\tau_w = \frac{D\Delta P}{4L} \qquad \text{(Equation 3.20)}$$

$$\dot{\gamma} = f(\tau_w) = \left(\frac{3n'+1}{4n'}\right)\left(\frac{8V}{D}\right), \qquad \text{(Equation 3.21)}$$

where $\left(\frac{8V}{D}\right)$ is called apparent shear rate and is defined as:

$$\frac{8V}{D} = \frac{32Q}{\pi D^3} = \frac{4}{\tau_w^3}\int_0^{\tau_w} \tau_{rz}^2 \dot{\gamma}(\tau_{rz}) d\tau_{rz}, \qquad \text{(Equation 3.22)}$$

and $n' = \dfrac{d(\log(\tau_w))}{d(\log(8V/D))}$.

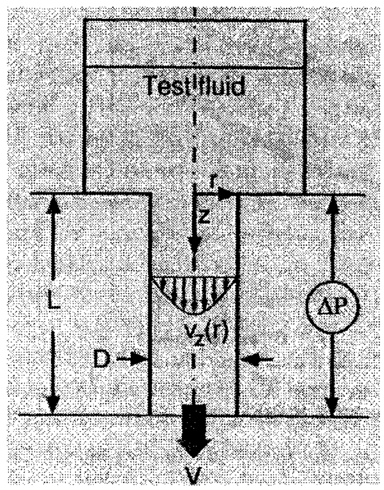

Figure 3.12: Schematic of tube viscometer (Nguyen and Boger 1992).

The Equations 3.21 and 3.22 are known as the Rabinowitsch-Mooney and the Rabinowitsch-Weissenberg equations, respectively (Slatter 2004). As mentioned by Nguyen and Boger 1992, if fluids have yield stress, they will not be sheared uniformly across the tube cross-section. Fluid flows as a plug zone in the centre of the tube and is sheared between $r_y \leq r \leq (D/2)$, where $\tau_{rz} \geq \tau_y$ (Figure 3.13). In this condition, the lower limit of the integral in Equation 3.22 is replaced by τ_y.

The steady and fully developed flow is assumed to be a principle of the rheometery. End effects and wall effects are two major sources of errors that may occur in this equipment. End effects are caused by losing pressure when the flow enters and leaves the rheometer, and wall effects may be caused from an apparent reduction in viscosity when suspensions flow through small tubes.

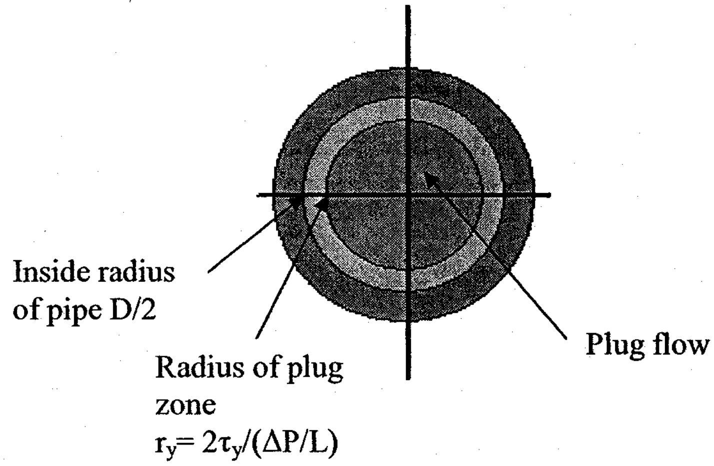

Figure 3.13. Schematic of tube cross-section and plug zone.

3.5.2. Concentric Cylinder Rheometery

This type of rheometer appears to be very popular in most research laboratories (Nguyen and Boger 1992, Slatter 1997, Slatter 2004). This rheometer consists of a rotating inner cylinder (bob) and a stationary hollow cylinder (cup). Torque is required for rotating the bob at a constant rotational speed (Ω) when fluid is located between the cup and the bob (Figure 3.14).

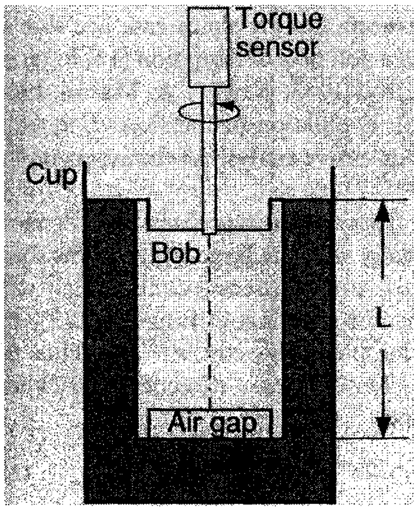

Figure 3.14. Simplified diagram of a concentric cylinder rheometer (Nguyen et al 1992).

The torque (T) is related to shear stress, and the rotational speed is related to shear rate. For time-independent fluids with some assumptions such as steady laminar flow, no slip at the surface and no end effect, the rheological parameters at the surface can be described as follows:

$$\Omega = \frac{1}{2}\int_{cup}^{bob} \dot{\gamma}(\tau)\frac{d\tau}{\tau}\ , \qquad \text{(Equation 3.23)}$$

$$\tau_{bob} = \frac{T}{2\pi L r_{bob}^2} \quad \text{and} \quad \tau_{cup} = \frac{T}{2\pi L r_{cup}^2} \qquad \text{(Equation 3.24)}$$

This type of rheometer is very simple to operate and is not very expensive. The shear rate usually ranges up to $1000s^{-1}$ and the rheometer has no sensitivity at below 1 s^{-1}. The main disadvantage of this equipment is the tedious procedure for data reduction with non-Newtonian fluids. The ends effects and the apparent wall slip are two main sources of errors (Nguyen et al 1992). Paterson and Cooke (1996) compared the advantages and disadvantages of tube viscometers and rotational viscometers for measuring the rheology of slurries (Table 3.4).

Table 3.4. The advantages and disadvantages of the tube and rotational viscometers (After Paterson and Cooke 1996).

Rotational viscometer	
Advantages	Disadvantages
• Time dependency can be measured • Widely accepted, commercially available instruments • Compact, and can be installed as a "bench top" instrument • Small slurry samples are required • Rheograms can be obtained directly when linked to a PC	• The annular gap must be much larger than the largest particles • Fluid type must be assumed to account for non-Newtonian end effects • No indication of laminar/turbulent transition • The centrifuge action causes a size distribution and a concentration gradient in the annulus
Tube viscometer	
Advantages	Disadvantages
• Mechanically simple • Geometric similarity • Can attain high shear rates • Can measure the laminar/turbulent transition • Can measure diameter dependent effects	• Sample is subject to a varying shear rate over the tube cross-section • The same sample of fluid cannot be subjected to sustained flow for measuring time-dependent fluids • Larger sample volumes are required • The apparatus is large

3.5.3. Cone and Plate Viscometery

This type of rheometer basically consists of a cone and a plate, whereby both can act as the rotation body. The fluid is sheared within the gap, as shown in Figure 3.15. A torque (T) is required to rotate the cone or plate at the constant angular velocity (Ω), and the rheological parameters are given as follows:

$$\dot{\gamma}(r) = f(\tau) = \frac{\Omega}{\tan\theta}, \qquad \text{(Equation 3.25)}$$

$$\tau = \frac{3T}{2\pi R^3}, \qquad \text{(Equation 3.26)}$$

where θ is the cone angle and R is cone radius.

In this rheometer, both shear stress and shear rate are constant and can be calculated directly from torque and cone angle, which is its advantage. There are several commercial types of this equipment with a different range of shear rate, usually from 10^{-3} to $10^{3}s^{-1}$. The cone and plate device is not very suitable for all types of fluids due to a small gap requirement.

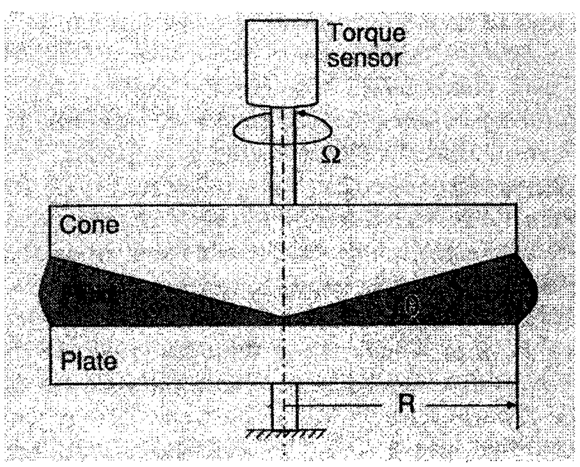

Figure 3.15. Diagram of a cone and plate viscometer.

The alternative case for the cone is a truncated cone, and can be used for suspensions where the minimum gap is at least ten times greater than the largest particle size (Nguyen and Boger 1992).

3.6. Slump

The slump test has been used recently as a very simple method of measuring the yield stress of solid-liquid fluid materials. For many years this method has typically been employed to estimate the workability or consistency of fresh concrete. "Workability is a qualitative term used to describe a combination of effects due to varying yield stress and viscosity" (Pashias et al 1996). The flow ability and the strength of the final hardened concrete are of the greatest importance. The higher the water content, the lesser the strength of the concrete. However, the slump test is a good measurement for controlling the quality and the balance of flow ability and strength.

A similar concept can be adopted for other types of solid –liquid mixtures. For example, the flow properties of mine tailings should be optimized for the assessment of slope deposition in surface disposal of waste material (Ritcey 1989, Pashias et al 1996), or for the assessment of final paste fill strength in an underground mine.

3.6.1. Standard Slump Test Method

The standard test method for evaluating the consistency of concrete has been developed by using the frustum of a cone-shaped mould (ASTM C143-90a 1998). The mould should be made of metal that is cement paste-resistant with the geometry shown in Figure 3.16.

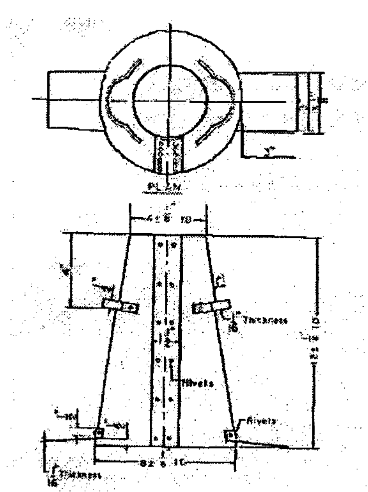

Figure 3.16. Mould for standard slump test method (ASTM 1998).

The test method involves three stages: first, the sample is placed and compacted in the mould; second, the mould is removed vertically and the mixture is allowed to subside, and finally, the distance between the original and final position of the centre of the top surface of the sample is measured. This distance is called the slump height. Figure 3.17 shows the test method schematically.

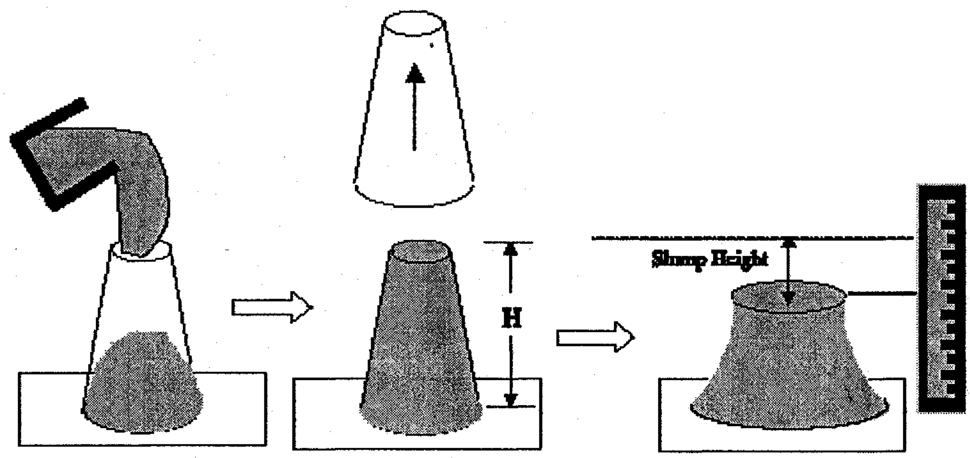

Figure 3.17. Standard slump test method (Clayton et al 2003).

As described by Clayton et al (2003), the slump height is related to both the density of material as well as the yield stress. In other words, the slump depends on chemical composition, particle size and specific gravity of particles. Among these variables, the yield stress is preferred as an indicator of material consistency due to its unique material properties.

The idea of relating the slump height to the yield stress was innovated by Murata (1984) for a conical geometry. The materials used in his experiments were limited to concrete. A simple integration error was observed and corrected in the original Murata theory by Christensen (1991). The results of both values calculated by the models were compared with the yield stress of material measured directly by rotational devices (Pashias et al 1996). Further investigations on conical slump models have been made by Rajani and Morgenstern (1991), Schowalter and Christensen (1998) Ferraris et al (1998), and Clayton et al (2003).

3.6.2. Yield Stress Measurement Using Conical Geometry

The generalized cone slump model for measuring the yield stress has been developed for a cone regardless of base and top diameter of the cone (Clayton et al 2003). Several assumptions should be made for this model:

- Initial material shape is considered as a perfect truncated cone
- No effects on material form while removing the cone
- Perfect slip at the inner surface of the slump cone
- Material weight causes the only (vertical) stress on the material.

Figure 3.18 presents the initial and final state of the material shape and stress distributions. On the basis of these assumptions, the pressure (P) in the material at a certain height (z) below the top surface can be expressed as follows:

$$P|_z = \frac{\rho g H}{3}\left(\frac{R_0}{R_H - R_0}\right) \times \left(1 + \frac{z}{H}\left(\frac{R_H - R_0}{R_0}\right) - \frac{1}{\left(1 + \frac{z}{H}\left(\frac{R_H - R_0}{R_0}\right)\right)^2}\right), \text{ (Equation 3.27)}$$

where H is the initial height of the material, ρ is the density of the material and the other variables are shown in Figure 3.18.

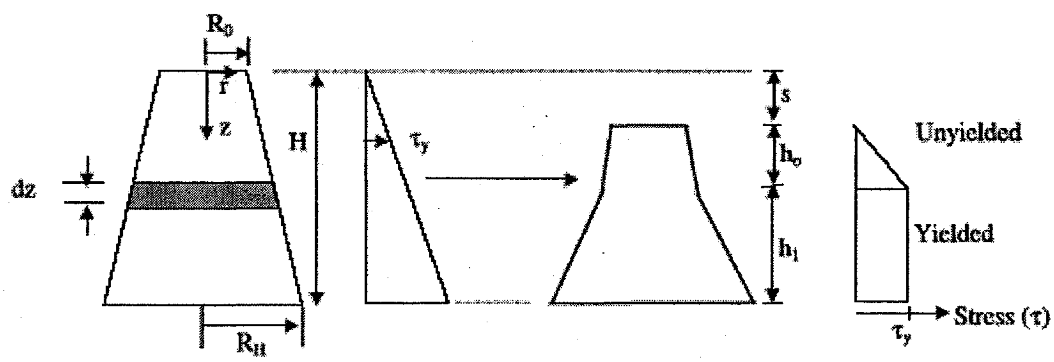

Figure 3.18. Initial and final state of the material shape and stress distributions in a conical slump model (Schowalter and Christensen 1998 and Clayton et al 2003).

Another assumption is to have an elastic solid material for which $\tau_{maximum}=1/2\ P|_z$ (Hibbeler 1997 and Clayton et al 2003). For the dimensionless form, the variables are defined using the following form:

$\tau_{z'} = \tau_z / \rho gH$ and $z'=z/H$. and also:

$\tau'_y = \tau_y / \rho gH$ = dimensionless yield stress,

$s' = s / H$ = dimensionless slump height,

$h'_0 = h_0 / H$ = dimensionless height of undeformed region,

$h'_1 = h_1 / H$ = dimensionless height of deformed region.

$$\tau\big|_{z'} = \frac{\tau\big|_{Z}}{\rho gH} = \frac{1}{2}\times\frac{1}{3}\left(\frac{R_0}{R_H - R_0}\right)\times\left(1 + z'(\frac{R_H - R_0}{R_0}) - \frac{1}{\left(1 + z'(\frac{R_H - R_0}{R_0})\right)^2}\right),$$

If $\alpha = \dfrac{R_0}{R_H - R_0}$, which is a dimensionless quantity, the equation is then given:

$$\tau\big|_{z'} = \frac{\alpha}{6}\left(\left(1 + \frac{z'}{\alpha}\right) - \frac{1}{\left(1 + \frac{z'}{\alpha}\right)^2}\right), \qquad \text{(Equation 3.28)}$$

The material subsides along the yielded zone until the stress is reduced to the yield stress (τ'_y). The stress does not exceed the yield stress for the material above the yielded zone, and it remains unyielded. The interface layer between the yielded (below) and unyielded (above) material is assumed to be a horizontal surface. This surface descends as the material flows in the slumping process. Therefore, the final height of material consists of an unyielded zone (h_0) and a yielded zone (h_1). The height of the dimensionless unyielded zone (h'_0) can be obtained by substituting (τ'_y) for $\tau|_z'$ in Equation 3.28.

$$\tau'_y = \frac{\alpha}{6}\left(\left(1 + \frac{h'_0}{\alpha}\right) - \frac{1}{\left(1 + \frac{h'_0}{\alpha}\right)^2}\right) \qquad \text{(Equation 3.29)}$$

For the yielded section of material, the height can be divided into two elements, thickness (dz) and radius (r_z). These elements change to dz_1 and r_{z1} at their final position.

Figure 3.19 shows the deformation of elements. It is assumed that the volume of each element remains constant. Thus:

$$(r|_{Z_1})^2 dz_1 = (r|_Z)^2 dz \quad \text{(Equation 3.30)}$$

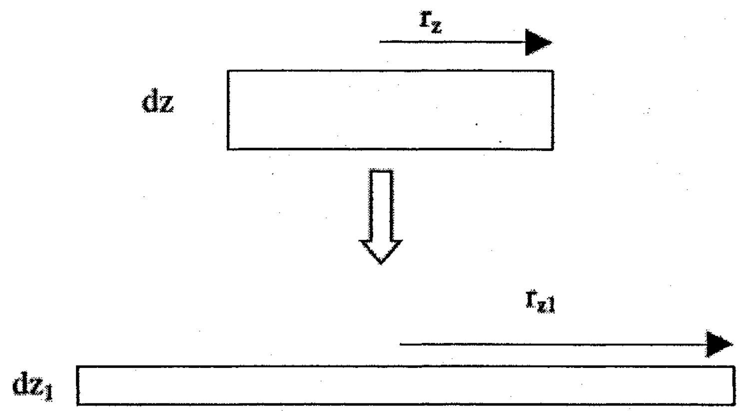

Figure 3.19. Deformation of an element of thickness dz to thickness dz_1 (Clayton et al 2003).

Slump occurs until the cross-section area increases such that the yield stress needed to support the weight of material above any given plane is reduced to the yield stress. Therefore, the product of stress and cross-section area is proportional to the weight of material above the plane:

$$(r|_{Z_1})^2 \tau_y = (r|_Z)^2 \tau|_z, \quad \text{(Equation 3.31)}$$

then the height h_1 can be calculated as:

$$h_1 = \int_{h_0}^{H} dz_1 \quad \text{(Equation 3.32)}$$

When substituting Equations 3.28, 3.30 and 3.31 into Equation 3.32 the relationship between h'_1 and τ'_y is given as:

$$h'_1 = 2\tau'_y \ln\left(\frac{\left(1+\frac{1}{\alpha}\right)^3 - 1}{\left(1+\frac{h'_0}{\alpha}\right)^3 - 1}\right) \quad \text{(Equation 3.33)}$$

As $s' = 1 - h'_0 - h'_1$ (Equation 3.34), the final expression relating dimensionless slump and dimensionless yield stress can be defined by substituting Equation 3.33 into 3.34.

$$s' = 1 - h_0' - 2\tau_y' \ln\left(\frac{\left(1+\frac{1}{\alpha}\right)^3 - 1}{\left(1+\frac{h_0'}{\alpha}\right)^3 - 1}\right) \qquad (3.35)$$

To calculate the actual yield stress, it is obvious that the dimensionless yield stress obtained from Equation 3.35 should be multiplied by ρgH.

3.6.3. Cylindrical Slump Test Method

The conical mould was first changed to a cylindrical geometry by Chandler (1986). The cylindrical slump method was used for controlling the flow behaviour of bauxite residue. Pashias et al (1996) developed a model relating the slump height and the yield stress of material for a cylindrical mould. The test procedure is the same as the one used for the conical geometry (shown in Figure 3.17), and the procedure of calculating the yield stress is more suitable than for the conical mould due to the simple geometry of the cylinder. According to Pashias et al (1996), the slump height does not depend on factors such as sample structure, cylinder material, aspect ratio of the cylinder (H/D), lift rate, and measurement time. Meanwhile, they have used a cylinder made from PVC or stainless steel with an aspect ratio between 0.78 and 1.28. It has been mentioned that the surface on which the materials are tested has no effect on the slump height. There are several surfaces that have been chosen for testing, such as stainless steel, rubber, smooth wood, and rough wood (Pashias et al 1996).

3.6.4. Yield Stress Measurement Using Cylinder Geometry

When developing a relationship between the yield stress and the slump height of a cylinder, the same assumptions should be considered for that of a conical mould. Figure 3.20 presents both initial and final situations of material structure using a cylinder. The pressure (P) at any given height below the top surface can be expressed as:

$$P|_z = z\rho g\,. \qquad \text{(Equation 3.36)}$$

For the elastic model, ($\tau_{maximum}$=1/2 $P|_z$), the stress in a dimensionless mode can be expressed as

$$\tau\big|_{z'} = \frac{1}{2}z' \qquad \text{(Equation 3.37)}$$

The height of dimensionless unyielded region (h'_0) can be determined by substituting τ'_y for $\tau|'_z$ in Equation 3.37.

$$\tau'_y = \frac{1}{2}h'_0 \qquad \text{(Equation 3.38)}$$

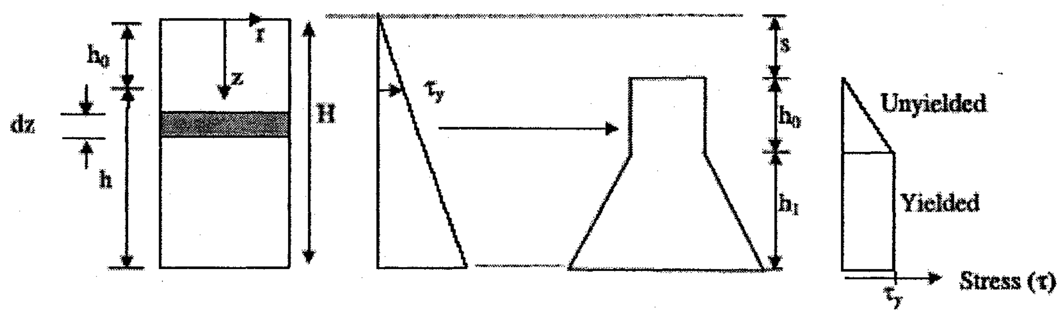

Figure 3.20. Initial and final state of the material shape and stress distributions in a cylindrical slump model (Pashias et al 1996 and Clayton et al 2003).

When considering the Equations 3.30, 3.31, and 3.37, and substituting them into Equation 3.32, the dimensionless height of the yielded region is calculated as:

$$h'_1 = -2\tau'_y \ln(h'_0) \qquad \text{(Equation 3.39)}$$

As $s' = 1 - h'_0 - h'_1$, the expression which relates the dimensionless yield stress to the dimensionless slump height can be presented as:

$$s' = 1 - 2\tau'_y\left[1 - \ln(2\tau'_y)\right] \qquad \text{(Equation 3.40)}$$

The actual yield stress is then calculated by multiplying the dimensionless yield stress by ρgH.

3.6.5. Modified Conical Slump Test

A survey by Ferraris (1996) concluded that none of the methods employed for measuring the rheological parameters of fresh concrete are able to estimate the plastic viscosity. This parameter appears to be more important in modern concretes. Ferraris and De Larrard

(1998) then empirically modified the standard slump test apparatus, test procedure and calculation for determining both the yield stress and the plastic viscosity of fresh concrete based on the works produced by Tanigawa et al (1989 and 1991) and Hu et al (1995). Tanigawa et al (1989 and 1991) considered the slump to be a function of time, and suggested simulating the slump-time curve by finite element analysis for fresh concrete, which was considered as a Bingham Plastic material. Hu et al (1995) then developed the relationship between slump height and yield stress based on finite element analysis as

$$\tau_y = \frac{\rho}{270}(300 - s), \qquad \text{(Equation 3.41)}$$

where ρ (kg/m^3) is density, τ_y (Pa) is yield stress and s (mm) is slump. According to Hu et al, if the plastic viscosity of concrete is more than 300 Pa.s the correlation is poor for Equation 3.41. There is an average error and underestimation for yield stress in this model. Its accuracy was improved empirically by some modification and addition in Equation 3.41 (Ferraris & De Larrard 1998). The modified equation is given as:

$$\tau_y = \frac{\rho}{347}(300 - s) + 212\ . \qquad \text{(Equation 3.42)}$$

The comparison between direct measurements and predictions from Equation 3.42 indicates a 162 (Pa) average deviation for yield stress measurement.

In addition, a semi-empirical model has offered the following equations when estimating the plastic viscosity of fresh concrete (Ferraris and De Larrard 1998):

$$\eta_P = \rho T \times 1.08 \times 10^{-3}(s - 175) \qquad \text{for } 200 < s < 260 \text{ mm}$$

$$\eta_P = 25 \times 10^{-3} \rho T \qquad \text{for } s < 200 \text{ mm} \qquad \text{(Equation 3.43)}$$

where T is the time of 100mm-slump and ρ is the density of fresh concrete. For slumps less than 200 mm, the plastic viscosity is independent of slump height. These equations have been generalized and derived from the correlation between final slump (s) and the factor $\eta/\rho gT$, where η is the plastic viscosity measured directly with a rheometer.

In this method, the procedure for measuring the slump and time can be described as follows:

A small plate which can slide on a centrally located rod has been designed to measure the time (T) when the top surface of a sample falls 100 mm after the mould is lifted. Figure 3.21 presents the details of top plate dimensions, base and attached rod. The mould is located on the base where its axis coincides with the rod. The mould is then filled with the sample, as is done for standard slump test. Finally, the plate is placed on the top of the sample. A stopwatch is started as soon as the slump cone is lifted, and is stopped when the sliding plate reaches the stop on the rod.

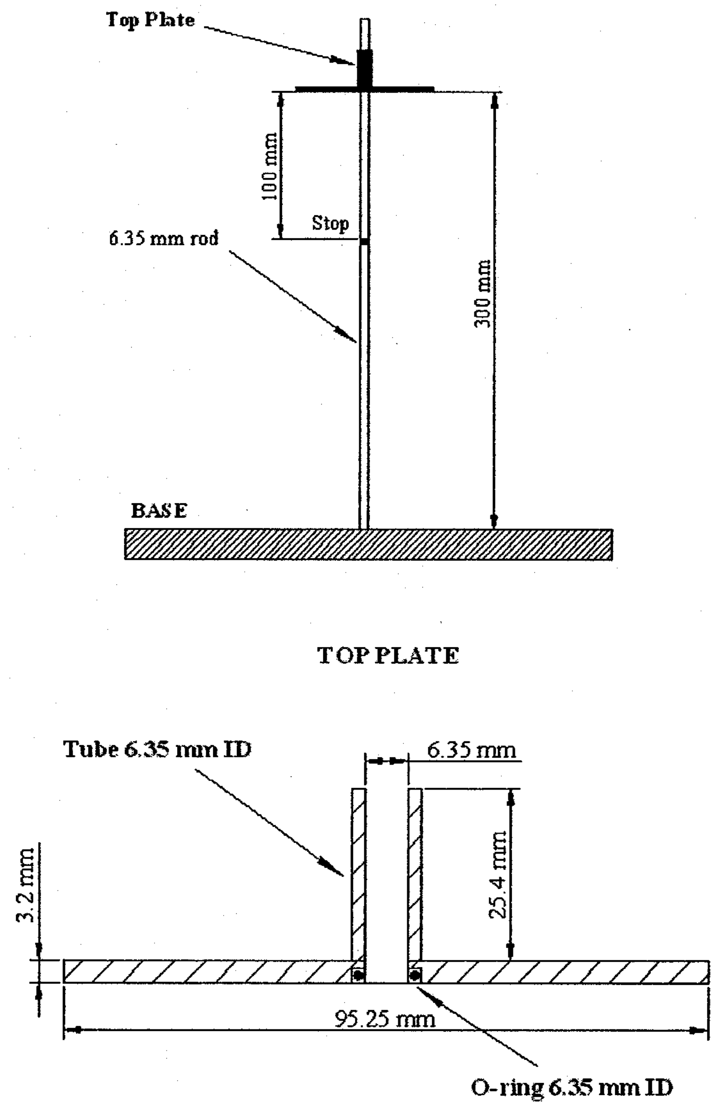

Figure 3.21. Experimental set-up for the modified slump test and top plate dimensions (after Ferraris and De Larrard 1998).

The measured time is used for calculating the plastic viscosity, and the final slump is measured for calculating the yield stress. Some other considerations regarding equipment can be articulated as follows:

- The weight of the top plate must be 212 g.

- The rod, top plate and base should be made of stainless steel.
- The purpose of the rubber O-ring seal is to prevent fine materials from interfering with the fall of the disks.

The rod should be coated with petroleum jelly. Figure 3.22 presents the relationship between dimensionless yield stress and dimensionless slump for both Ferraris'and Pashias' models. The most accurate part of the curve for Pashias' model (equation 3-40) corresponds to dimensionless yield stresses less than 0.15, which shows dimensionless slump values of 0.333 or greater. Interestingly, Ferraris' equation (Equation 3.42) is also more accurate for concretes (ρ=2400 kg/m^3) with a slump greater than 0.333 (Paterson 2002).

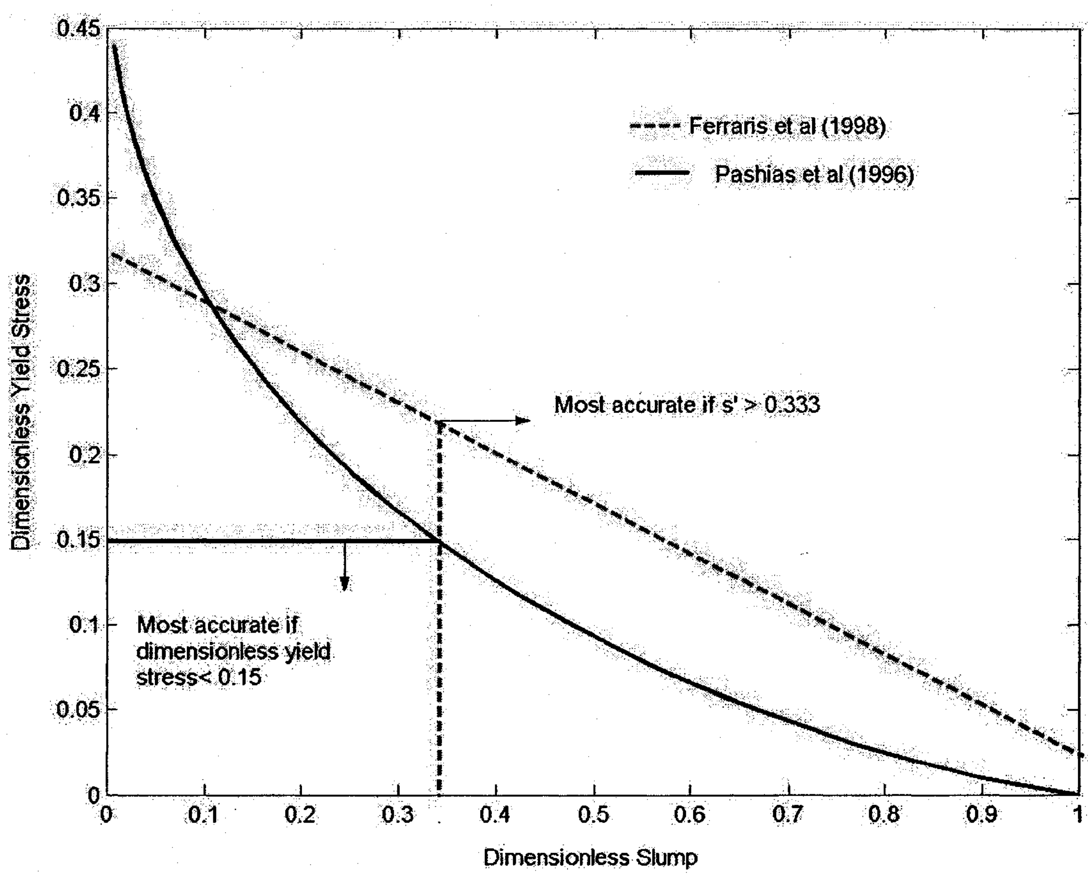

Figure 3.22: Dimensionless yield stress versus dimensionless slump for the cylindrical and modified slump models (after Paterson 2002).

It is obvious that there is a significant difference between these two models at the given slump. The accuracy of each model will be assessed by experimental investigation for paste and thickened tailings.

CHAPTER 4
MINE TAILINGS CHARACTRIZATION & EXPERMENTAL PROCEDURE

4.1. Mine Tailings Samples

To achieve the goals and objectives of the thesis, two different samples of tailings were obtained from two mines, LaRonde and Louvicourt. The general information about the mines can be articulated as follows:

4.1.1. LaRonde Mine

The LaRonde Mine is located in northwestern Quebec between the cities of Rouyn-Noranda and Val d'Or, which can be reached by highway 117. LaRonde is a polymetallic mine that contains gold, silver, copper and most recently zinc. Geologically, LaRonde is situated in the southern portion of Archean-age Abitibi volcanic belt within the Bousquet Formation of the Blake River volcanic group (see Figure 4.1).

Agnico-Eagle Mines Limited Company, which is a leader among mid-sized gold producers, is operating this mine. Table 4.1 represents the total production of metals from 1988 to 2004. The combined proven and probable mineral resources of LaRonde are estimated to include 45.3 million tons of ore with 3.4 grams per ton gold (Table 4.2). In addition, the LaRonde Mine hosts a possible mineral resource of 15.9 million tons of ore with 5.4 grams per ton gold. It is noteworthy that LaRonde is Canada's largest gold deposit.

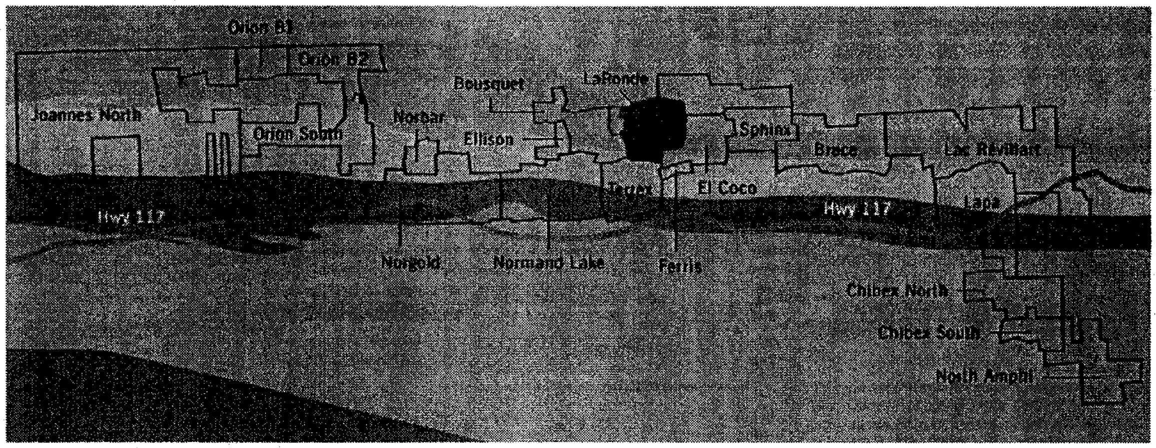

Figure 4.1. Location of LaRonde Mine (www.agnico-eagle.com).

Gold-copper and zinc-silver mineralzation occur in the form of massive and disseminated sulphide lenses throughout the southern felsic unit of Black River Group. This unit is characterized by the dominance of quartz and feldspar porphyritic rhyodacite to rhyolitic flows and pyroclastic rocks.

Table 4.1. Statistics of production of gold, silver, copper and zinc in LaRonde Mine (1998-2004) (www.agnico-eagle.com).

Gold (ton)	Silver (ton)	Copper (kiloton)	Zinc (kiloton)
67.9	382.3	51.4	182

Table 4.2. Proven-probable mineral reserves and possible mineral resource of LaRonde Mine as of February 2004 (www.agnico-eagle.com).

Production	Scale	Proven and Probable	Possible
Gold	Grade of ore (g/ton)	3.4	5.4
	Tonnage (ton)	154	85.8
Silver	Grade of ore (g/ton)	44.17	32.56
	Tonnage (ton)	2001	518
Copper	Grade of ore (%)	0.32	0.35
	Tonnage (million ton)	14.496	5.565
Zinc	Grade of ore (%)	2.51	0.94
	Tonnage (million ton)	113.703	14.946

4.1.2. Louvicourt Mine

The Louvicourt Mine is located 25km east of Val D'Or in the SE part of the Archean Abitibi Sub-Province. The Louvicourt deposit is a Cu-Zn-Au-Ag volcanic hosted massive sulphide. In the Val D'Or area, the volcanic rocks form an east-west striking, steeply dipping, overturned and south-facing sequence comprised of thick mafic and ultramafic flows of the Lower Malartic group.

The Louvicourt property consists of 170 claims and covers 8277 acres of land. It is operated by Aur Resources but is owned by three partners, Novicourt (45%), Aur Resources (30%) and Teck Cominco (25%). Aur Resources has become a major Canadian-based mining company with 95% of its revenues from the production of copper at the Quebrada Blanca, Andacollo and Louvicourt Mines in 2002. The mineral reserves and resources as of December 2002 are 2,629, 000 tonnes and 3,143,000 tonnes, respectively. A breakdown of the current metal grades of reserves and resources is found in Table 4.3.

Table 4.3. Breakdown of Louvicourt's reserves and resources.

Variables	Unit	Mineral Reserves	Mineral Resources
Tonnage	Tons	2,629	3,143
Gold	Grade of ore (g/ton)	0.81	0.83
Silver	Grade of ore (g/ton)	25.4	25.6
Copper	Grade of ore (%)	2.97	2.91
Zinc	Grade of ore (%)	1.93	2.01

Louvicourt has sufficient reserves to sustain production until approximately mid-2005 at which time it is expected to close. In 2004, production from Louvicourt is expected to be 29000 tons of copper, 19000 tons of zinc as well as silver and gold. A detailed mine closure plan has been prepared and submitted to the Quebec Ministry of Natural Resources. This closure plan will ensure that environmental reclamation at the highest standards will be carried out in this region (www.aurresources.com).

4.2. Basic Characterizations of Mine Tailings

The following experiments were carried out to characterize the physical and chemical properties of LaRonde and Louvicourt mine tailings.

4.2.1. Chemical Composition

A series of XRF analyses were performed to determine the chemical compositions of the mine tailings samples. Table 4.4 presents the weight percent of 10 major oxides of LaRonde and Louvicourt mine tailings and their detection limits. The detection limits are based on three times the background sigma values.

Total iron present has been recalculated as Fe_2O_3. In cases where most of the iron was originally in the ferrous state (usually the case with unaltered rocks) a higher total is the result. According to Table 4.4, more than 78% of LaRonde and 74% of Louvicourt samples include SiO_2, Fe_2O_3 and Al_2O_3.

Table 4.4. The chemical composition of LaRonde and Louvicourt mine tailings.

Variable	LaRonde (%)	Louvicourt (%)	Detection Limits (ppm)
SiO_2	37.71	35.12	60
TiO_2	0.464	0.418	35
Al_2O_3	8.66	8.2	120
Fe_2O_3	33.35	30.93	30
MnO	0.03	0.279	30
MgO	0.19	3.49	95
CaO	0.67	2.23	15
Na_2O	1.26	0.62	75
K_2O	0.75	0.77	25
P_2O_5	0.054	0.161	35
LOI	17.43	17.65	100
Total	100.57	0	---

Another analysis was conducted on the mine tailings for 5 base metals, Cu, Zn, Ni, Pb and Cr. The results are shown in Table 4.5. Although during the mineral processing all the Cu and Zn must be extracted, there are still some small amounts of these two metals in the mine tailings.

Table 4.5. The value of the base metals in LaRonde and Louvicourt mine tailings.

Variables	Cr	Cu	Ni	Zn	Pb
LaRonde (ppm)	42	1108	44	3403	942.9
Louvicourt (ppm)	43	944	31	2426	600.5
Detection Limit (ppm)	15	2	3	2	1

The amounts of sulphur (S) are as much as the percents of LOI for both samples. According to these tables, there is no significant difference between the chemical compositions of LaRonde and Louvicourt mine tailings.

4.2.2. Mineralogy of Mine Tailings

To determine the mineralogy of the samples, the x-ray diffraction method was employed for both LaRonde and Louvicourt. The results indicate the two major minerals are quartz (SiO_2) and pyrite (FeS_2) for both types of mine tailings (Figure 4.2 and Figure 4.3). Pyrite is the source of sulphur in the mine tailings which can potentially generate acid mine drainage after deposition. There are also some minor minerals such as Ca (Mg_2Al) ($Al_{2.8}$ $Si_{1.2}$) $O_{10}(OH)_2$ and $K_{0.27}$ Mn O2 (H_2O) $_{0.54}$ for both sorts of mine tailings and NaN_3 for Louvicourt samples only.

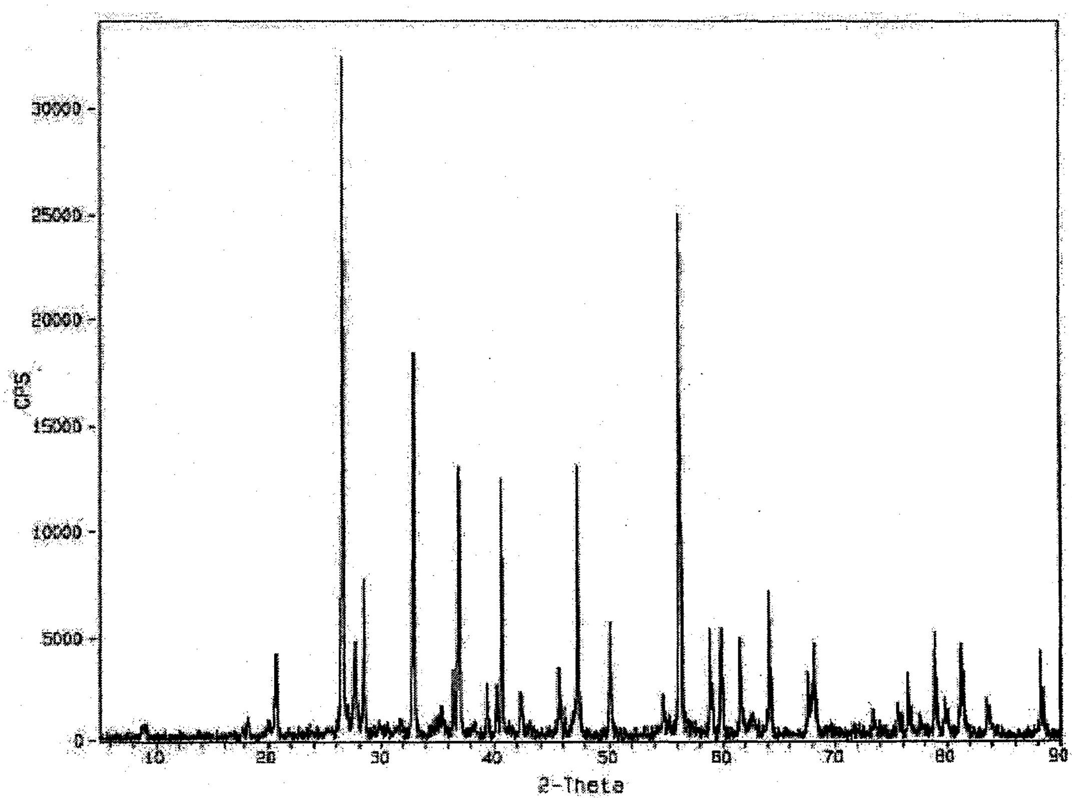

Figure 4.2. LaRonde XRD graph.

4-2-3 Particle Size Characterization

Two test methods were employed to determine the particle size distribution of coarse and fine aggregates of mine tailings. The standard sieve analysis method (ASTM C 136–93) was used to determine the size of particles which are more than 150 microns.

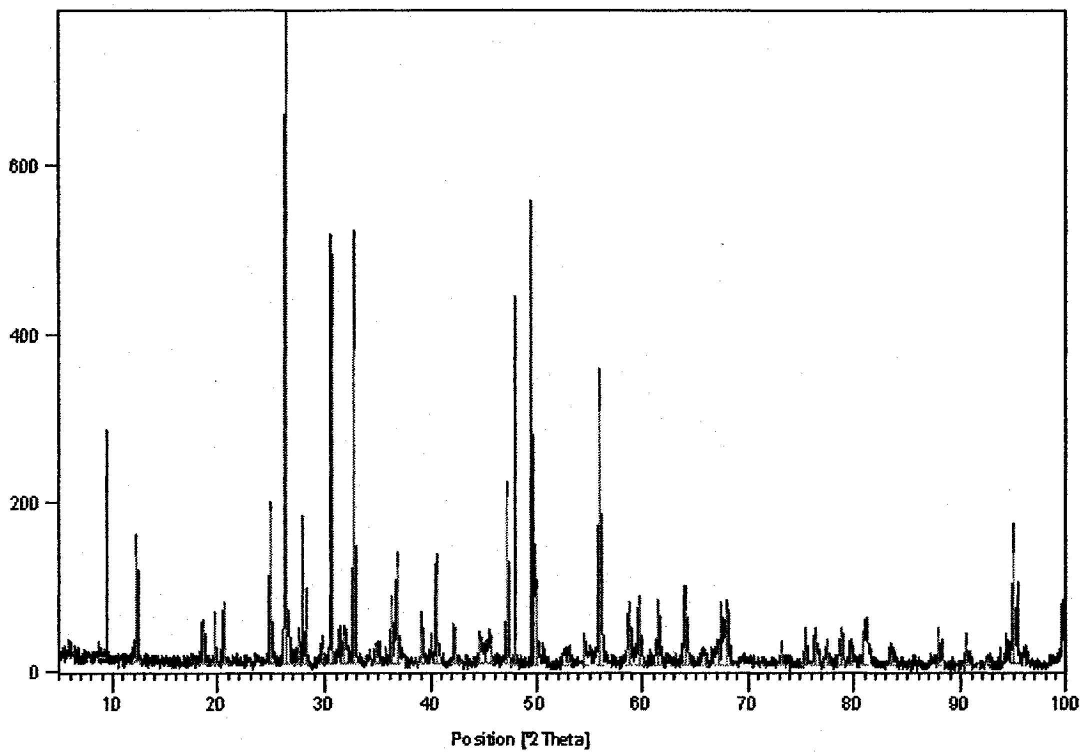

Figure 4.3. Louvicourt XRD graph.

The tailings were sampled in accordance with the Standard Practice for Sampling (ASTM D 75-87) and the sample was dried to constant weight at a temperature of 110±5° C. As the aggregates passed sieve number 8, the total weight of each sample sieved was 250 grams. Seven sieves, numbers 30, 35, 40, 50, 60, 80, 100, were employed for this purpose. The amount of each sample, which was passing sieve number 100, was collected to be characterized by the Laser Light Diffraction Techniques (Jillavenkatesa et al). This technique showed an error of less than 3% for the particles passing sieve No. 100 when using standard sieve analysis. Figures 4.4 and 4.5 represent the distribution of particle size of LaRonde and Louvicourt mine tailings finer than 150 microns respectively.

After merging the data derived from these two techniques, the final size distribution curves were achieved as shown in Figure 4.6. According to this figure, the size of particles varies from medium clay to medium sand for LaRonde and from fine clay to medium sand for Louvicourt. The distribution curves also show that more than 40 percent of particles are less than 20 microns, this ratio makes an ideal paste mixture.

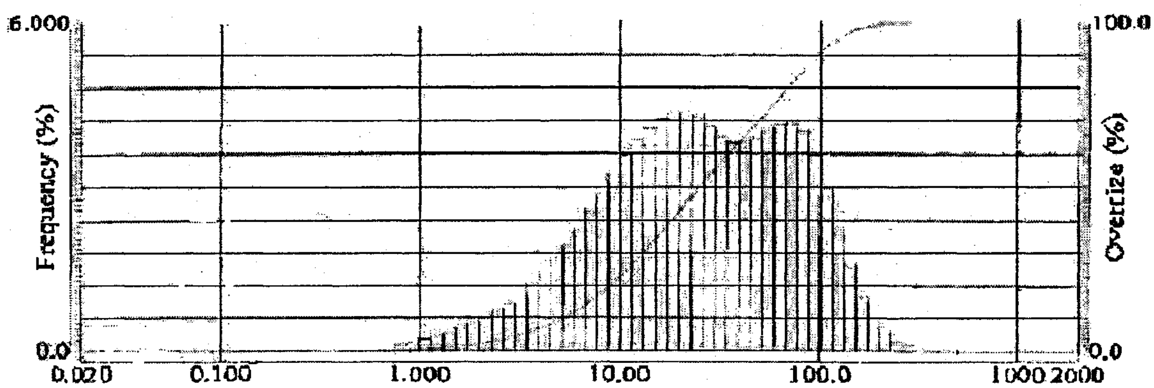

Figure 4.4. Particle size distribution of fine portion of LaRonde mine tailings.

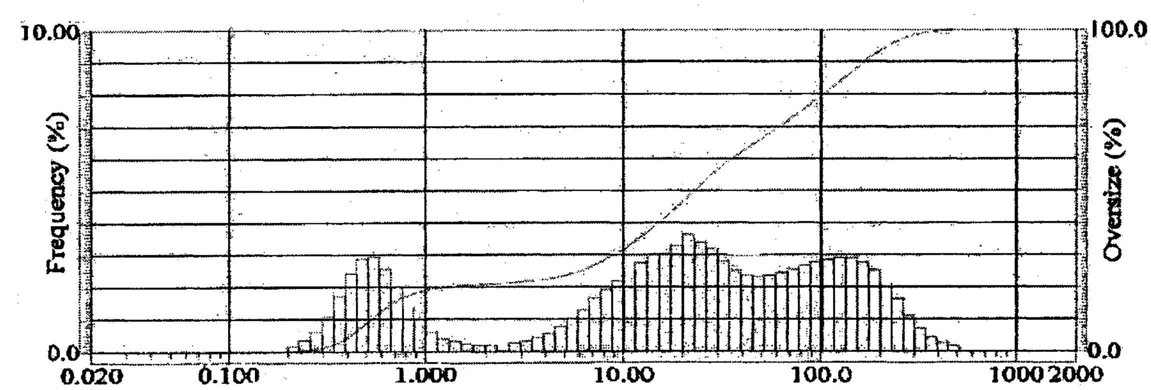

Figure 4.5. Particle size distribution of fine portion of Louvicourt mine tailings.

The other characteristics such as the uniformity coefficient, C_u, and the coefficient of gradation, C_c, are presented in Table 4.6. There is a significant difference between the percent of clay (< 2 microns) particles of LaRonde and Louvicourt mine tailings.

Table 4.6. The size distribution characteristics.

Mine Tailings	C_u	C_c	Clay (<2μm)	Fines (<20 μm)	Fines (<75μm)
LaRonde	7.25	1.04	3%	42%	80.21%
Louvicourt	72	4.5	20%	47%	74.24%

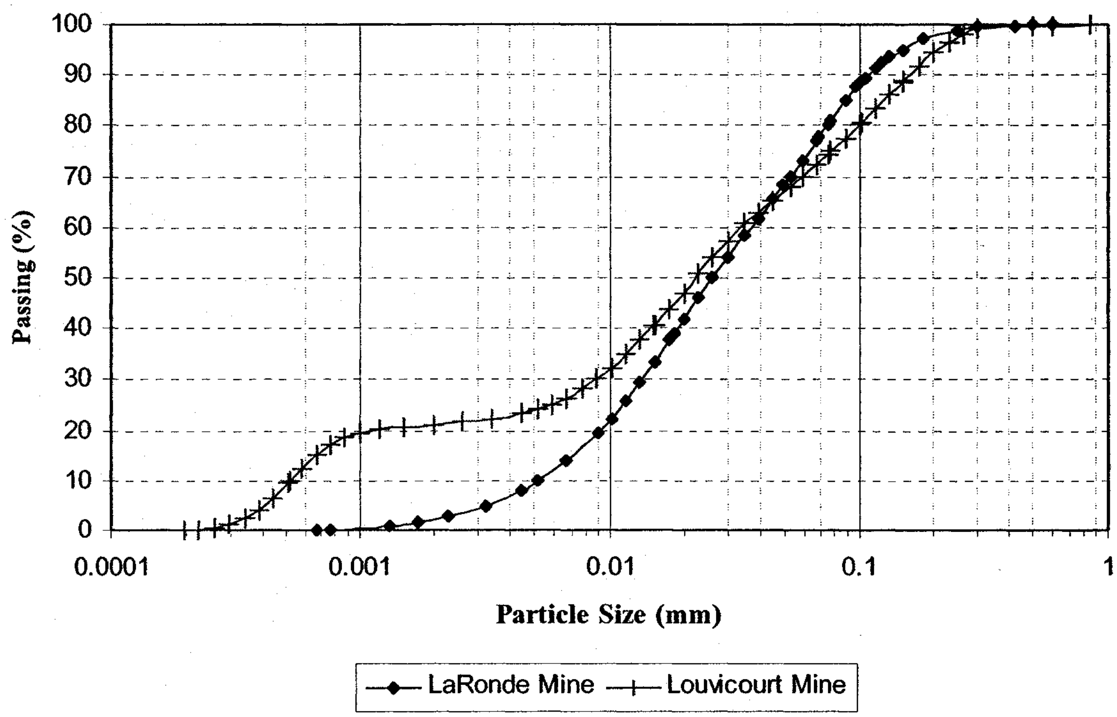

Figure 4.6. Particle size distribution of LaRonde and Louvicourt total tailings.

4.2.4. Specific Gravity and pH

The specific gravity of two mine tailings samples were determined in accordance with the ASTM Test Method (D 854-83). LaRonde and Louvicourt mine tailings had specific gravities of 3.228 and 3.213 at the temperature of 20°C respectively.

An electronic pH meter was used to determine the pH of the tailings. The test procedure employed for pH measurement is ASTM D 4972-89. The Laronde mine tailings sample had an average pH of 7.2 at the temperature of 20°C. The average pH of Louvicourt tailings was 6.7 at 20°C.

4.3. Sample Preparation for Rheological Measurements

The tailings received from mines had been sealed in barrels and covered by approximately 10 cm of water. The initial water content was about 21% for LaRonde and 17% for Louvicourt tailings. In this study, for each mine tailings two different types of mixtures were prepared, the mixture without binder and the mixture with binder.

4.3.1. Mixing

The mixtures without additives were prepared by adding some tap water to the mine tailings to create suitable water content for testing. The material was then mixed for a minimum of 15 minutes at two different rotational speeds to ensure the materials were well blended by using a Hobart mixer shown in Figure 4.7.

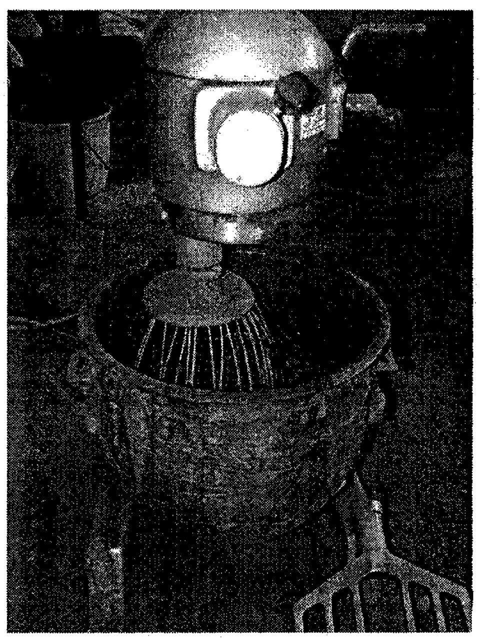

Figure 4.7. Hobart Mixer.

For the mixture with binder, the same procedure was carried out, but the procedure differed by adding the binder after 15 minutes and mixing the paste for 3 more minutes. For slump tests and vane rheometery experiments a maximum of 1 minute mixing was needed to adjust or replace the sample for testing. In some rheometery experiments in this study, two different mixing-times were considered to evaluate their effects on the rheological properties of material.

4.3.2. Binders

Portland cement type 10 was utilized as a binder in this study. The percent of cement added to the mixture was 5 wt% of solid particles.

4.4. Slump Test Procedures

In this study, three test methods for measuring the slump of paste materials were used:

- Standard slump
- Cylindrical slump
- Modified-conical slump.

After preparation of mixtures in accordance with the mentioned procedures, the slump heights of the mixtures were measured and consequently the relevant yield stresses were calculated.

4.4.1. Standard Slump Test Procedure

In this method a standard cone was used. The upper ($2R_O$) and the lower ($2R_H$) diameter of the cone are 10 cm and 200 cm respectively. Therefore:

$\alpha = \dfrac{R_0}{R_H - R_0} = 1$ and with substituting this value in Equations 3.29 and 3.35, the dimensionless slump and yield stress are given as:

$$s' = 1 - h'_0 - 2\tau'_y \ln\left(\frac{7}{(1+h'_0)^3 - 1}\right) \quad \text{(Equation 4.1)}$$

$$\tau'_y = \frac{1}{6}\left((1+h'_0) - \frac{1}{(1+h'_0)^2}\right) \quad \text{(Equation 4.2)}$$

After recording the slump height for each mixture and calculating the s' by dividing the slump height by H (300 mm), the variables h_0' and τ'_y are calculated by using the trial and error method from Equations 4.1 and 4.2. The yield stress is then estimated by multiplying τ'_y by ρgH.

4.4.2. Cylindrical Slump Test Procedure

Two PVS cylinders with diameters of 150 mm and 200 mm and aspect ratios of 1.17 were employed to evaluate the effect of diameter on the slump height and consequently yield stress (Figure 4.8). The test procedure was similar to the test procedure for the standard method but filling the moulds and calculating the yield stress in this method were less challenging. After recording the height of slump and dividing the slump value by the height of cylinder H, which is 175.5 mm for the small size and 234 mm for the large cylinder, the dimensionless yield stress is calculated for each mixture by using the trial and error method from Equation 3.40. The yield stress was then calculated by multiplying τ'_y by ρgH.

Figure 4.8. 150 mm diameter cylindrical mould (left) 200 mm diameter cylindrical mould (right).

4.4.3. Modified Conical Slump Test Procedure

As was mentioned in Chapter 3, this method has been designed for measuring the yield stress and the plastic viscosity in the cement industry. The additional equipment that must be used in this method includes a base-rod and a top plate shown in Figure 4.9.

Figure 4.9. Modified conical slump test equipments.

Several experiments were conducted to measure the height of slump and to record the time. Unfortunately, it was observed that at the time of lifting out the mould and slumping of the material, the adjusted plate on the top of the material did not slide by gravity along the rod. It led us to increase the inside diameter of the top plate to 1 cm and to decrease the height of the edge to 0.5 cm without any changes in the total weight (212 g) of the plate. This plate must be placed in the centre of the rod on the upper diameter of the mould so it will distribute a uniform load to the entire material. As the material slumps concentrically, the adjusted plate on the top of the material follows the speed of the mixture. The final shapes of the mixtures confirm that these changes have no effect on the slump when the top plate can drop freely (Figure 4.10).

After recording the final slump height and the time of slump when it drops 10 cm, the yield stress of the mixture is calculated from Equation 3.42 and the plastic viscosity is estimated from Equation 3.43. This test method of slump is challenging in terms of test procedure. The results derived from all these test methods and their accuracy and practicability will be discussed in Chapter 5.

4.5. Vane method

After sample preparation in accordance with the mentioned procedure, the yield stress of each mixture was determined by using the R/S-CPS Brookfield Rheometer in two modes, controlled-shear-rate (CSR) and controlled-shear-stress (CSS). Before explaining the test procedure, it is useful to discuss the features and characteristics of the rheometer and the other equipments.

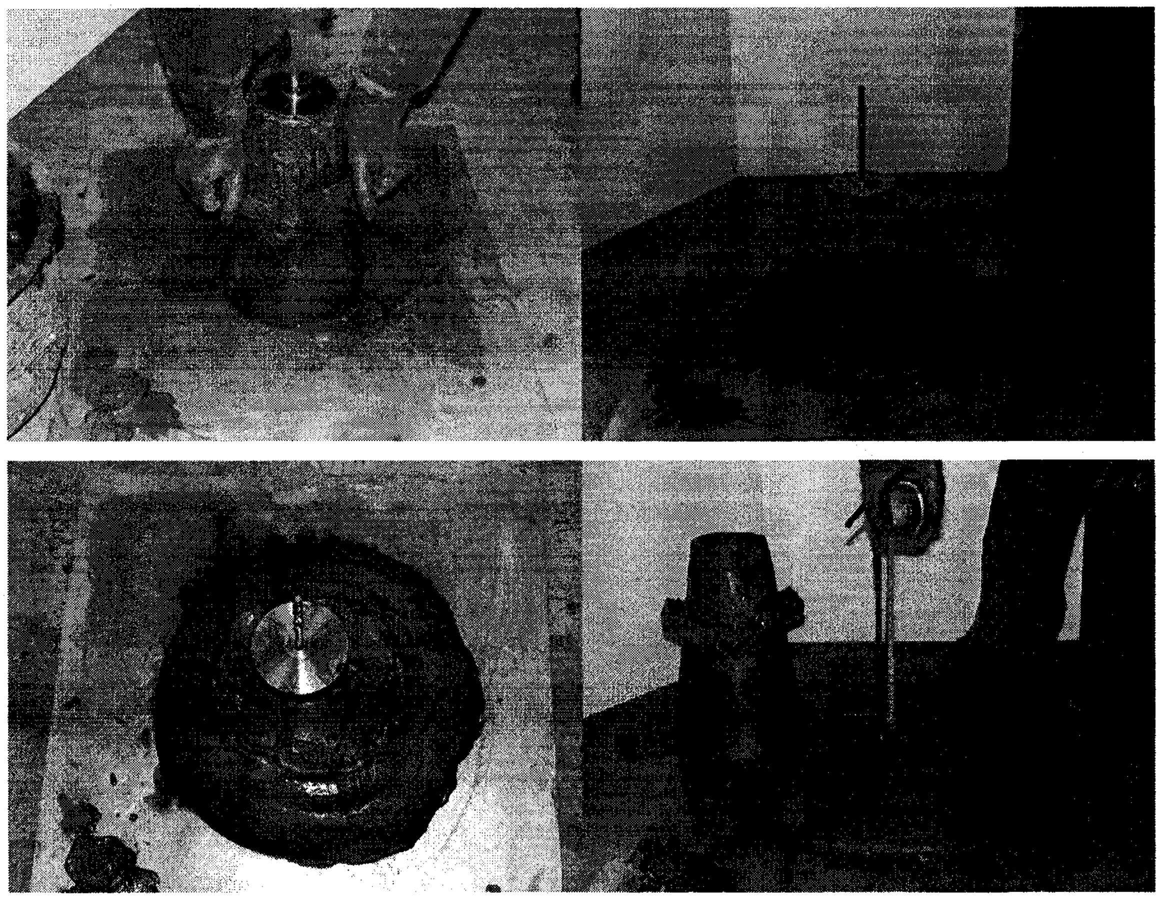

Figure 4.10. Modified conical slump test procedure and the final shape of mixture.

4.5.1. Equipments

1. R/S-CPS Brookfield Rheometer

This rheometer provides the possibility to measure the viscosity of Newtonian fluids, to record the flow curves as well as to determine the viscosity functions of non-Newtonian fluids in steady shear flows.

The measuring system of the R/S-CPS Rheometer is basically designed for cone and plate rheometery measurements according to DIN 53018. It is also possible to employ it as a rotational rheometer with a vane spindle. The measuring drive developed for this instrument is characterized by a highly dynamic system of integrating motor and shaft encoder without mechanical force transducers, by torque measurement without deflection and by an optical shaft encoder (Brookfield Ltd.). Figure 4.11 indicates the main parts of the R/S-CPS Rheometer, vane spindle installed for vane method and the Peltier thermo regulator.

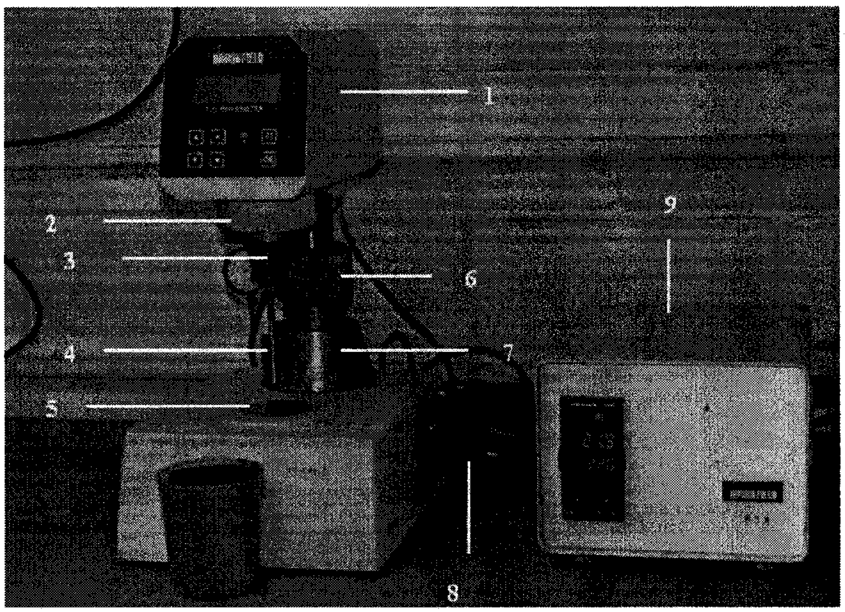

1. Measuring head of rheometer
2. Cooling flange
3. Measuring element coupling
4. Six-bladed vane spindle
5. Bottom measuring plate
6. Nonius (fine adjustment)
7. Stand
8. Height adjusting lever
9. Peltier thermo regulator

Figure 4.11. The R/S-CPS Brookfield Rheometer and Peltier thermo regulator.

The electronic unit and measuring drive have been put together in one casing. There is an interface, centronics, for connecting the rheometer directly to a printer when there is no computer available and there is another interface, RS232, for computer connection. These two interfaces are located at the backside of the measuring head. The rheometer can be connected to a computer with a special data transmission cable and the computer serial port (e.g. "COM1"). However, the rheometer can be controlled by a computer in connection with the software "Rheo 2000" which has been developed for this purpose. There is a temperature sensor for measuring the temperature under the bottom measuring plate and its connecting cable must be inserted into the socket "Pt100" at the backside of the rheometer. The technical and mechanical features of the rheometer are shown in Table 4.7.

Table 4.7. Technical features of R/S-CPS Brookfield Rheometer (Brookfield Ltd.).

Parameter	Scale	Minimum	Maximum
Torque	mNm	0.05	50
Speed	min^{-1}	0.7	800
Temperature	°C	0	150
Shear rate	s^{-1}	0	4,800
Shear stress	Pa	0	16,000
Viscosity	Pas	0.009	10,000

2. Vane Dimension and Adjustment

In this study, a custom-made, 20 mm diameter, six-bladed stainless steel vane with a height to diameter ratio of 2 was used (see Figure 4.12). A beaker, 80 mm diameter-80 mm height, was used to hold the mixture. In this case, the vane must be immersed into the mixture in such a way that the diameter of the sample around the vane is at least 40 mm; the distance between bottom of the cup and the lower edge of the vane is at least 10 mm; and, the distance between upper level of the mixture in the cup and the upper edge of the vane is 20 mm. Once the vane is immersed, a short period (e.g. 30 sec) should be allowed for the paste to stabilize from the insertion action of the vane. Gentle tapping can help restore the paste structure around the inserted vane.

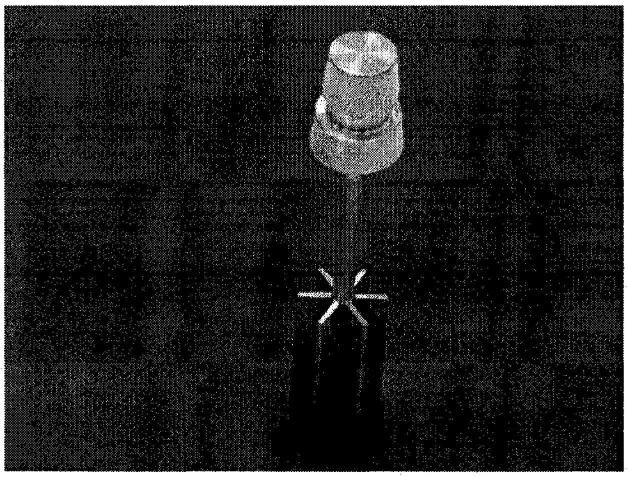

Figure 4.12. Custom made six-bladed stainless steel vane.

3. Computer System and Software

In this study a computer was used to represent the measuring results graphically. It was also possible to transfer the data from different files and sources to an excel sheet to provide the results in a graph or table. The minimum requirements for a computer, which is very basic computer, to use the Rheo 2000 software can be articulated as follows:

- CPU 486 DX2 66 MHz
- 8 MB RAM
- 10 MB free hard disk capacity
- VGA graphic card.

In this study, Version 2.7 of the software "Rheo 2000" was employed for the data acquisition system. Figure 4.13 shows the start up menu of the software which includes three options, the Block-editor, the Sequence-editor and the Measure/Analysis.

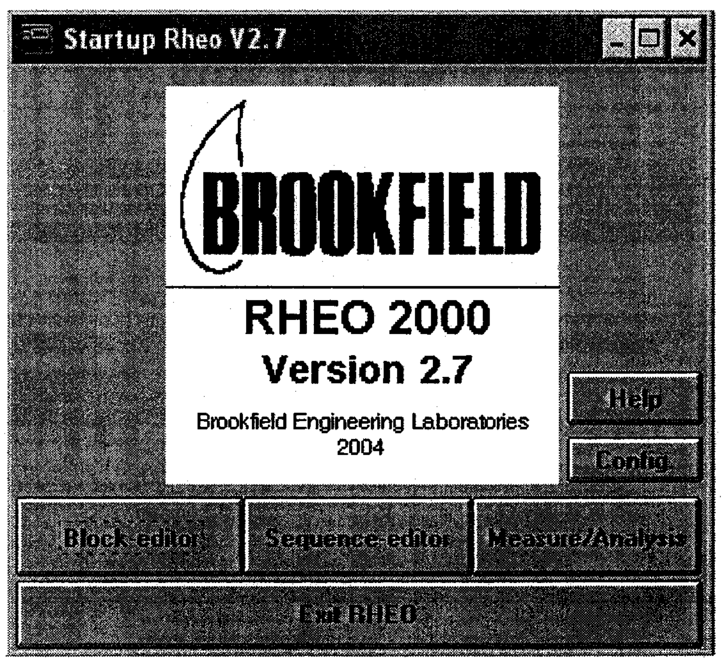

Figure 4.13: Start up menu of the software Rheo 2000.

4.5.2. Rheometery Test Procedure

In this study, after turning on the rheometer, the remote option from the main menu of the rheometer is selected for controlling the rheometer by software. At the same time, the Measure/Analysis option is actuated after starting up the software. The communication between computer and rheometer can be monitored from the Measure/Analysis box. Before placing the cup on the bottom plate of the rheometer and adjusting the height of the vane by the rheometer lever, a rheological program file should be loaded by pressing the "Load a program file" key button from the Measure/Analysis box. Now, the computer would be ready to send the command of "start" to the rheometer (Figure 4.14). The software procedures for creating a program file, and the modes in which the rheological properties of materials are measured are described in the following.

4.5.3. Controlled Shear Rate Mode

In this mode, the software is programmed to run at a fixed rotational speed (in this study 0.3 rpm for LaRonde tailings) for 120 seconds. The torque is measured during the run and the maximum torque is picked from the torque-time curve to calculate the yield stress.

1. **Yield Stress Calculation**

The yield stress of each mixture was calculated according to Equation 3.15. In this study, the relationship between yield stress and maximum torque can be considered as follows:

$H = 0.04$ m

$D_v = 0.02$ m

From Equation 3.15: $T_m = \frac{\pi D_v^3}{2}\left(\frac{H}{D_v} + \frac{1}{3}\right)\tau_y$ then:

$$\tau_y(\mathrm{Pa}) = T_m / (2.93\mathrm{E}-5) \qquad \text{(Equation 4.3)}$$

The torque values in the rheometer are presented in the form of M [%o] that corresponded to unit per thousand of ca 50 mNm. Therefore, Equation 4-3 can be changed to:

$$\tau_y(\mathrm{Pa}) = 1.706096 \times M_m \qquad \text{(Equation 4.4)}$$

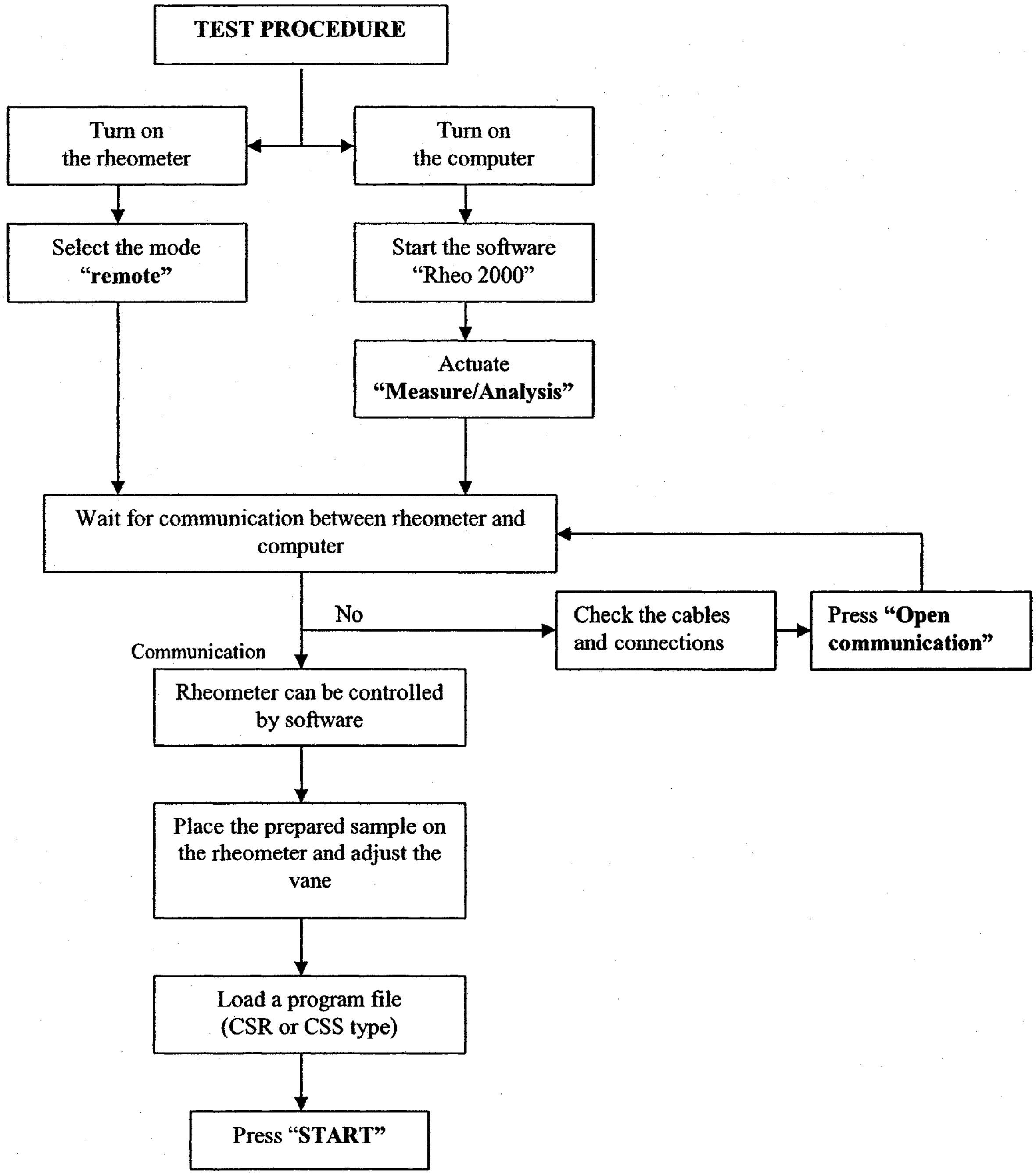

Figure 4.14: Test procedure for rheometery experiments using data acquisition software.

2. **Software Programming**

The first step to control the rheometer in the CSR mode is to create a block file. The block-editor option can be chosen from the start up menu for this purpose. After determining the values of parameters, a block file can be created by pressing the save block key. Figure 4.15 shows detail of the values chosen in this study.

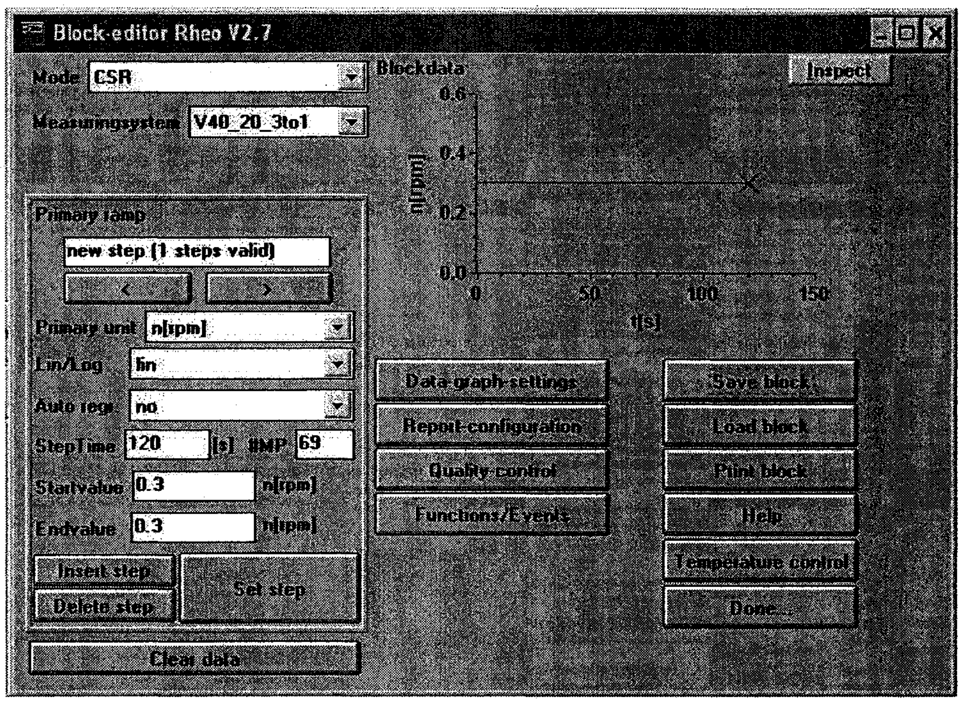

Figure 4.15. Creating a block file.

This file is then loaded from the "load program-file" in the Measure/Analysis option. The Measure/Analysis box also shows the situation of connections between computer and the rheometer (Figure 4.16). After loading the program file successfully, the rheometer begins working by pressing the "start" key.

3. **Rotational Speed**

As mentioned before, the rotational speed (n) of 0.3 rmp was considered in this study. It is very important to use a reliable rotational speed for measuring the maximum torque. The fact is that the maximum torque mostly increases with an increase in rotational speed.

In order to understand which rotational speed is more reliable, a series of experiments must be done on the mixtures. LaRonde mixtures with five different water contents and Louvicourt mixtures with six different water contents were prepared for this purpose. The maximum torque value for each mixture was measured in six different rotational speeds.

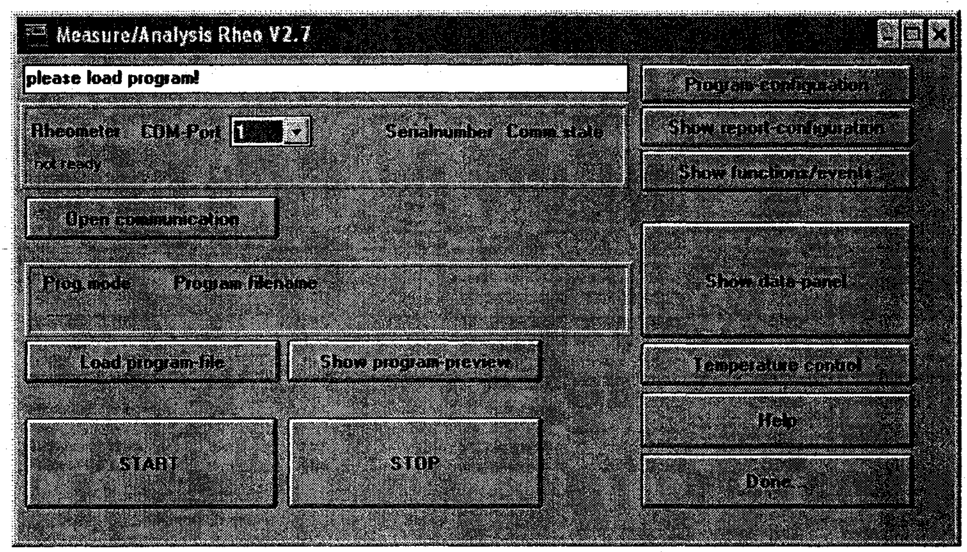

Figure 4.16. Measure/Analysis box.

Figure 4.17 only shows the maximum torque values for all the tests derived from torque-time curves. It is obvious that for each mixture three values are closer to each other. For example at the low water contents (where the maximum torque values are high) three rotational speeds of 0.3, 0.4 and 0.5 rmp are the most frequent values. The maximum torque values at 0.2, 0.3 and 0.4 rmp have approximately the same values for the mixture with high water content (more than 32%). However, the rotational speeds of 0.3 rmp and 0.4 rmp are the two most frequent in this figure. For the final rheometery experiments in this study the rotational speed of 0.3 rmp was chosen due to the existence of good correlation between the values measured in this mode and the CSS mode.

4.5.4. Controlled Shear Stress Mode

In this mode, the stress or the torque is ramped up logarithmically and yield stress is then calculated from the rheogram when the shear rate is zero. It is also possible to apply any rheological model for calculating other rheological properties. The Herschel-Bulkley model was applied in this study.

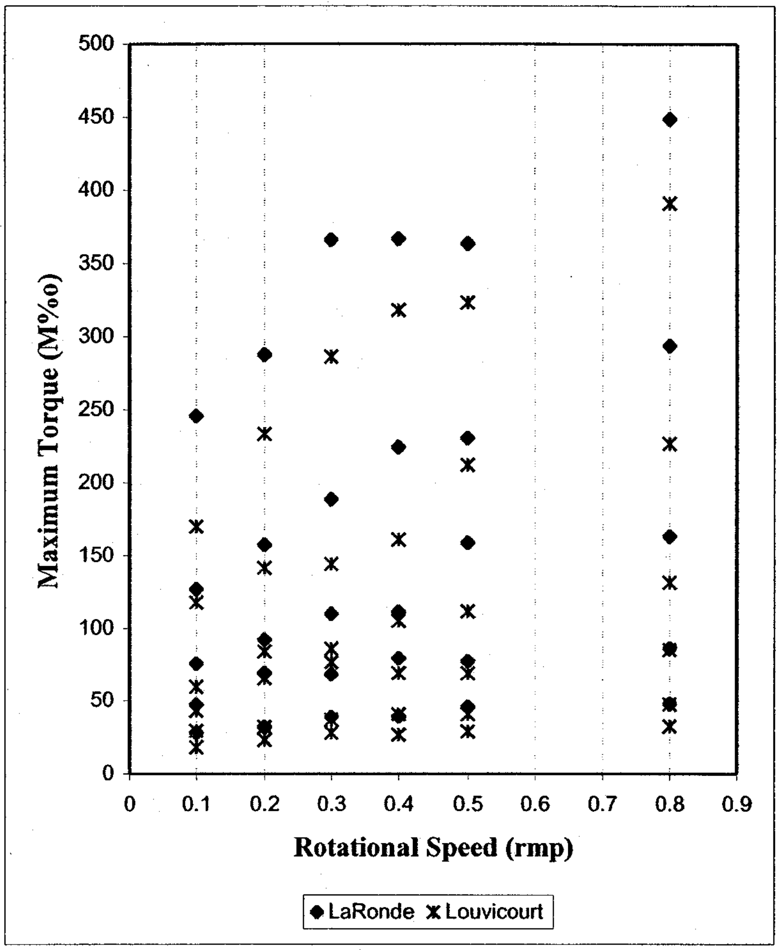

Figure 4.17. The effect of rotational speed on the maximum torque.

Figure 4.18 represents the values and parameters for creating a block file in this mode. This file is then loaded as such as a CSR file. The data can be presented as a graph on the monitor or can be transferred to an Excel sheet. The "Startvalues" for torque were changed from 1 (%o) to 100 (%o) and it depends on the yield stress of the mixtures. For the "Endvalues", the values range from 100 (%o) to 1000 (%o) to achieve the yield stress point in the slowest possible way.

If the chosen Endvalue is less than the torque it needs to initiate the flow, there is no motion and the mixture deforms plastically. When the chosen Endvalue is very higher than the yield point and the torque increases rapidly, the system underestimates the yield stress of the mixture. On the other hand, the Startvalue and the Endvalue in one-step of loading control the rate of increase of torque.

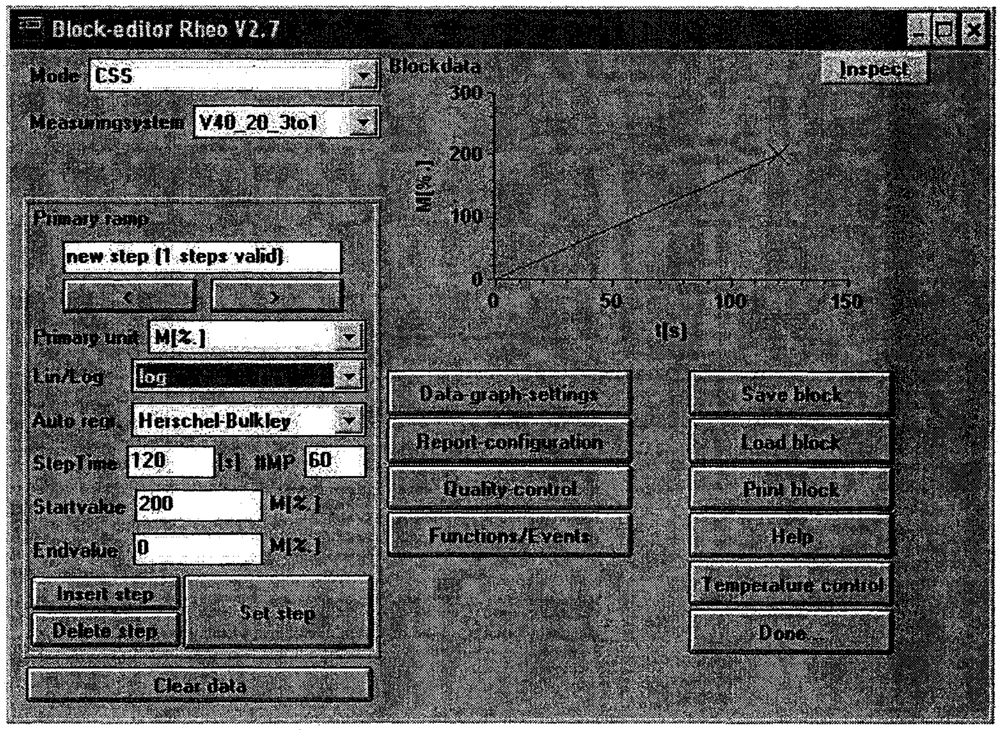

Figure 4.18. Creating a block file in the CSS mode.

CHAPTER 5
RESULTS AND DATA ANALYSIS

5.1. Classification of Results

The results of the experiments can be presented into two groups, non-cemented mixtures and cemented mixtures. The results are then interpreted for each type of mine tailings separately to estimate the reliability of the techniques employed for yield stress measurements. In addition, the results of two mine tailings are compared for determining the effect of basic properties of the mixture on the yield stress.

5.2. The Results of Non-cemented Mixtures

This group includes the results of the vane method in two modes and three methods of slump tests for both LaRonde and Louvicourt mine tailings.

5.2.1. Vane Rheometery Results of Non-cemented Mixtures

Several experiments were carried out to determine the yield stress of LaRonde and Louvicourt mine tailings at different water contents. In a controlled shear rate (CSR) mode, the torque-time curves were obtained in order to determine the maximum torque. Figures 5.1 and 5.2 show the curves at the rotational speed of 0.3 for LaRonde and Louvicourt tailings mixtures at the temperature of 20°C respectively.

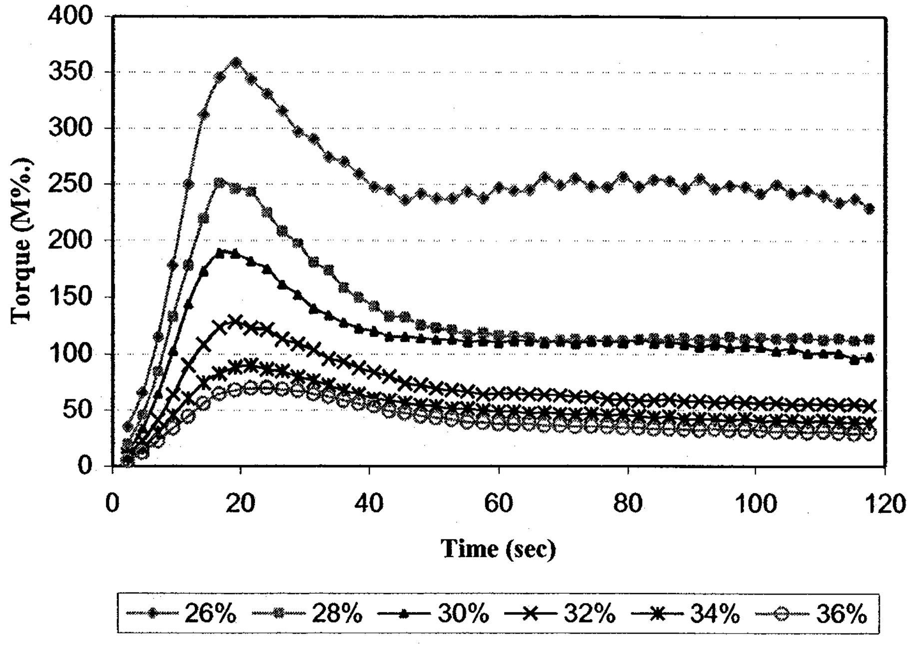

Figure 5.1. LaRonde torque-time graph for non-cemented mixtures with different water contents.

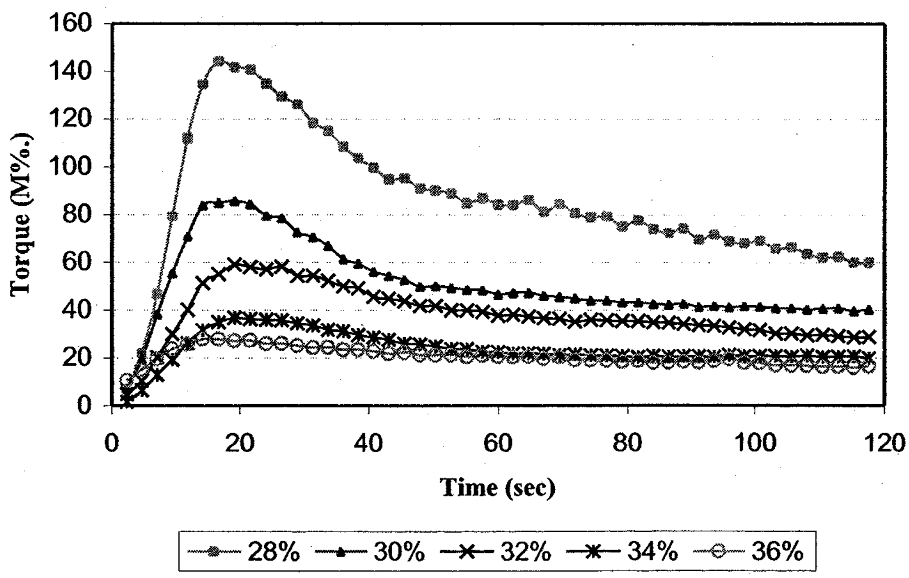

Figure 5.2. Louvicourt torque-time graph for non-cemented mixtures with different water contents.

In accordance with these figures the maximum torque values are presented in Table 5.1 for each mine tailings. The yield stress values were then calculated based on Equation 4.4.

The water contents of the tested LaRonde mixtures vary from 26% to 36%. It is noteworthy that LaRonde mine tailings have a liquid limit of 25.9%. The lowest water content mixture tested for Louvicourt mine tailings was 28% due to its liquid limit of 26.5%. According to Table 5.1 there is a significant difference between the yield stress values of LaRonde and Louvicourt mixtures at the same water content.

Table 5.1. Maximum torque and yield stress values of LaRonde and Louvicourt.

Water Content (%)	LaRonde Mine		Louvicourt Mine	
	M [%o]	Yield Stress (Pa)	M [%o]	Yield Stress (Pa)
26	358.45	611.55	-	-
28	251.06	428.33	144.1	245.85
30	188.65	321.85	85.86	146.48
32	128.09	218.53	59.03	100.71
34	89.83	153.26	36.8	62.78
36	70.27	119.88	27.89	47.58

The same mixtures were considered to determine the yield stress using the vane method in a controlled shear stress (CSS) mode. Figures 5.3 and 5.4 present the behaviour of mixtures for LaRonde and Louvicourt tailings respectively. These mixtures present "yield-pseudoplastic" behaviour at low shear rates and can be categorized as time-independent or viscoplastic fluids. At high shear rates, it seems the relationship between shear stress and shear rate is linear. The linear behaviour is particularly evident with mixtures at high water content. The yield stress values of mixtures were then calculated based on these two rheograms while Herschel-Bulkley model had been applied at the time of measurements. Table 5.2 shows the calculated values in this mode for LaRonde and Louvicourt.

Table 5.2. Yield stress values in controlled shear stress mode.

Water Content (%)	LaRonde Yield Stress (Pa)	Louvicourt Yield Stress (Pa)
26	564.611	-
28	387.754	216.929
30	319.404	142.346
32	202.499	88.792
34	153.128	62.266
36	119.223	46.63

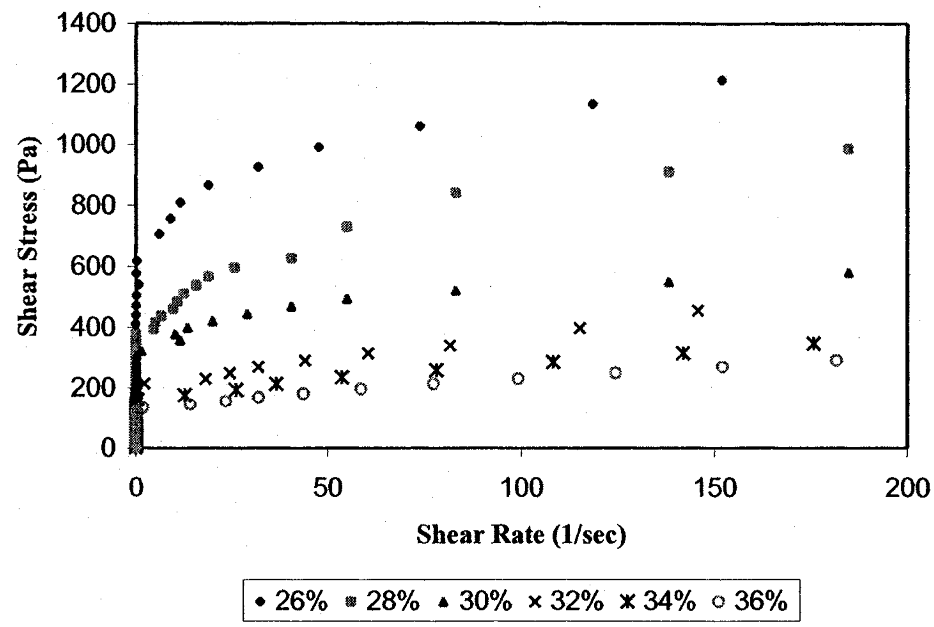

Figure 5.3. LaRonde non-cemented mixtures rheogram.

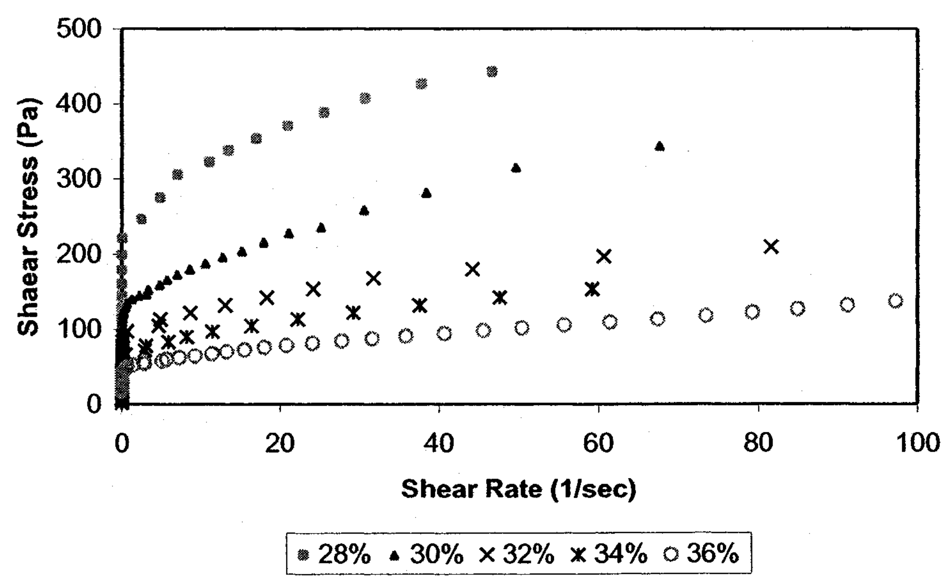

Figure 5.4. Louvicourt non-cemented mixtures rheogram.

5.2.2. The Comparison Between CSR and CSS Results

A graph of yield stress versus water content for each mine tailings was drawn to determine the correlation and relationship between the yield stress values in controlled shear rate mode and in controlled shear stress mode (Figures 5.5 and 5.6). Overall, the data obtained in different modes show an exponential feature for the range of tailings tested for each mine. The exponential equation, which defines the yield stress (τ_y) as a function of water content (w) is as follows:

$$\tau_y = ae^{b(w)}$$

The constant parameters a and b and the average relative error associated with this estimation for each series of data are shown in Table 5.3.

Table 5.3. Curve-fitting parameters and the average relative error.

Mode / Parameters	LaRonde		Louvicourt	
	CSR	CSS	CSR	CSS
a	45293	33214	75503	49117
b	-0.166	-0.1574	-0.2066	-0.1951
Average relative error (%)	2.759466	4.433646	4.972951	4.474889

According to the results and the defined equations, the correlation coefficient between the yield stress values in CSR mode and CSS is more than 0.99 for both mines. The percent of error based on the average value is then calculated as 1.09% for LaRonde and 1.54% for Louvicourt. Therefore, there is no significant difference between CSR and CSS mode in terms of yield stress measurement.

5.2.3. Standard and Cylindrical Slump Test Results

As mentioned in Chapter 4, a series of slump tests with different geometrical moulds were carried out to evaluate the accuracy of yield stress values calculated from measured slump heights.

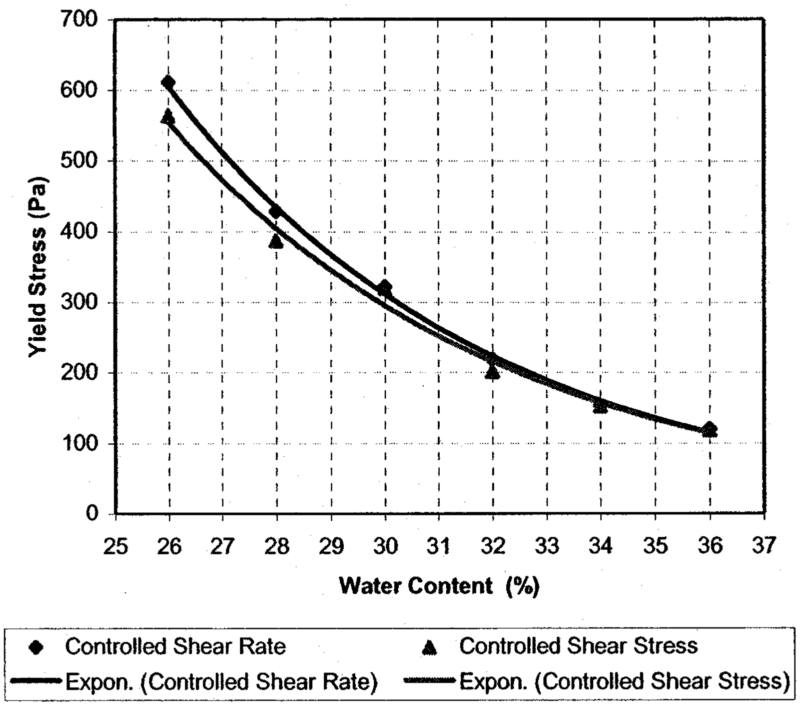

Figure 5.5. The yield stress values in CSR and CSS modes for LaRonde mine tailings.

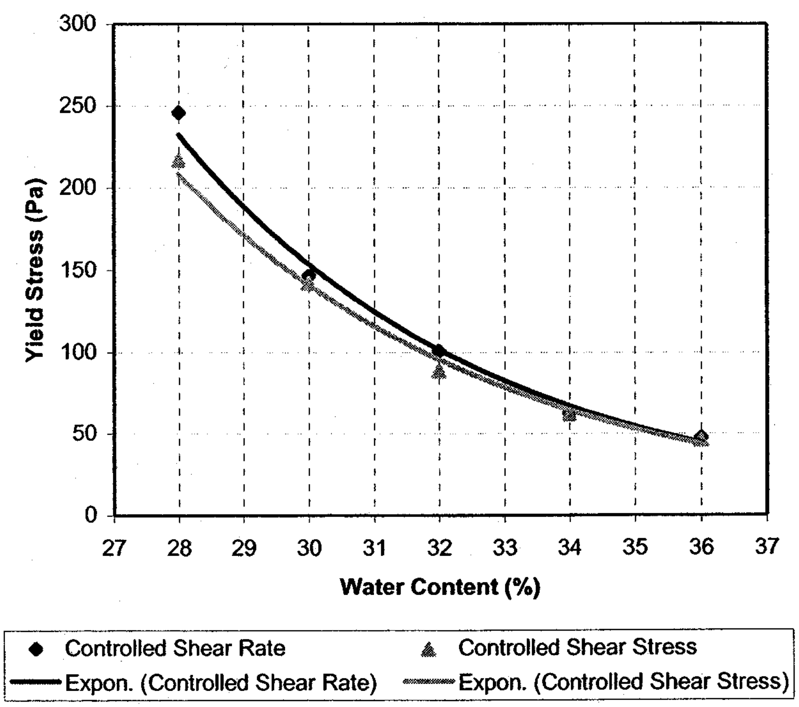

Figure 5.6. The yield stress values in CSR and CSS modes for Louvicourt mine tailings.

The slump height measured for LaRonde and Louvicourt non-cemented mixtures at different water contents using cylinders with the diameter of 150 mm and 200 mm are shown in Tables 5.4 and 5.5 as well as the calculated yield stress values from the slump height.

Table 5.4. The results of cylindrical slump tests with 150mm diameter cylinders.

Water Content (%)	**Slump (cm)**	**Dimensionless Slump**	**Dimensionless Yield Stress**	**Yield Stress (Pa)**
LaRonde				
28	7.6	0.43304	0.114638	445.388
29	7.8	0.44443	0.110815	427.1993
30	9	0.51282	0.089568	342.5942
31	10.5	0.59828	0.066601	252.7399
31.3	11.3	0.643877	0.055755	211.0792
32.6	12.3	0.701048	0.0434	162.6069
33	11.6	0.660968	0.051921	193.9074
33.2	12.4	0.706552	0.04228	157.647
34.2	13.35	0.76087	0.031855	117.817
Louvicourt				
28.2	10.4	0.592593	0.068019	254.6442
28.8	10.2	0.581197	0.070905	264.8307
29.2	10.9	0.621083	0.061062	227.711
29.6	11.3	0.643875	0.055756	207.5946
29.7	11.8	0.672365	0.049432	183.9608
29.8	11.6	0.660969	0.051921	193.1215
30.1	12.3	0.700855	0.04344	161.3688
30.9	12.8	0.729345	0.037768	139.8863
32.3	14.1	0.803419	0.024467	90.09256

The result of measured slump height using a standard conical mould is presented in Table 5.6. Equations 4.1 and 4.2 were used to calculate the yield stress values of non-cemented mixtures for each mine.

For all the methods, the calculated yield stress from slump height versus water content for each mine are shown in Figures 5.7 and 5.8.

Generally, these two figures illustrate the trend of yield stress values calculated from slump as an exponential feature due to the employed equations. The yield stress values measured with the vane method have also been presented in these figures for comparison between the data.

Table 5.5. The results of cylindrical slump tests with 200mm diameter cylinders.

Water Content (%)	Slump (cm)	Dimensionless Slump	Dimensionless Yield Stress	Yield Stress (Pa)
LaRonde				
28	10.8	0.461531	0.105235	545.1411
29	11.9	0.510736	0.090175	463.5077
29.5	12.1	0.517356	0.088255	451.8656
30.5	13.4	0.57123	0.07348	373.2701
31	15.5	0.662393	0.051607	261.1216
31.5	15.3	0.654086	0.05345	269.3748
32.4	15.2	0.649319	0.054521	272.803
33	16.1	0.685693	0.046588	231.9868
33.6	18.9	0.805899	0.024057	119.2136
34.5	18.7	0.797681	0.025424	125.0688
Louvicourt				
26.7	12.7	0.542734	0.08111	407.3276
28.2	14.8	0.632479	0.058381	291.4294
28.5	15.5	0.662393	0.051607	257.276
28.9	15.2	0.649573	0.054464	271.0881
29.3	16.1	0.688034	0.046096	229.075
29.5	17.5	0.747863	0.034249	170.0818
29.9	18	0.769231	0.03035	150.4817
30.0	17.3	0.739316	0.035857	177.7147
31.1	19	0.811966	0.023064	113.8028

Table 5.6. The results of standard slump tests.

Water Content (%)	Slump (cm)	Dimensionless Slump	Dimensionless Yield Stress	Yield Stress (Pa)
LaRonde				
28.5	13.6	0.453333	0.07679	508.0108
29	14.3	0.476667	0.071995	474.4359
29.5	17	0.56667	0.054977	360.8733
30	15.5	0.516667	0.064156	419.4802
30.5	19.5	0.65	0.041054	267.3716
31	19	0.633333	0.043709	283.5394
31.4	20.9	0.696667	0.033949	219.5245
32	20.7	0.69	0.034934	224.8167
33	21	0.7	0.033458	213.5984
33.7	23.2	0.773333	0.023288	147.8306
Louvicourt				
27.4	19	0.633333	0.04371	309.2808
28.2	21.8	0.726667	0.029628	247.6232
28.8	21.4	0.713333	0.031524	283.3777
29.1	23	0.766667	0.024165	248.3761
29.3	22.5	0.75	0.0264	168.1831
29.7	23.7	0.79	0.021135	203.0145
30.3	24.4	0.813333	0.01822	139.2136
31.2	25.4	0.846667	0.014262	90.16455

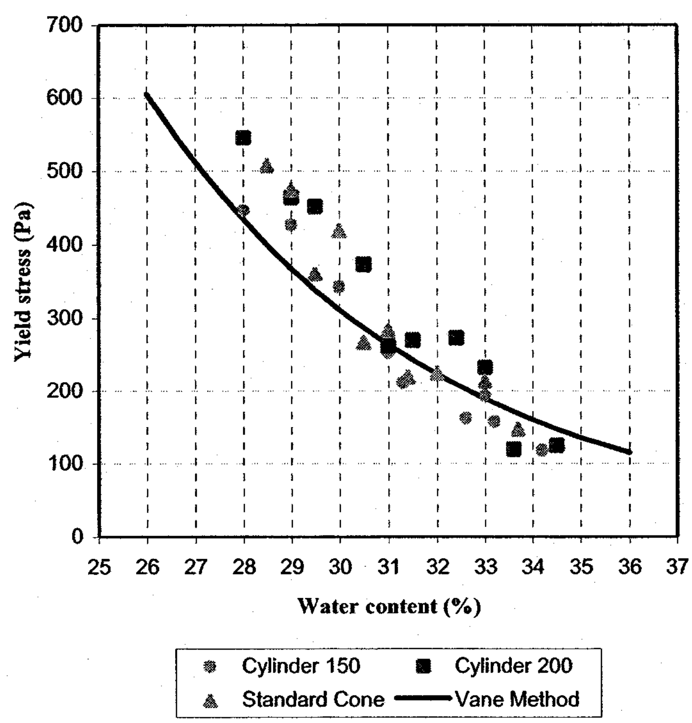

Figure 5.7. Calculated yield stress from slump height for LaRonde non-cemented mixtures.

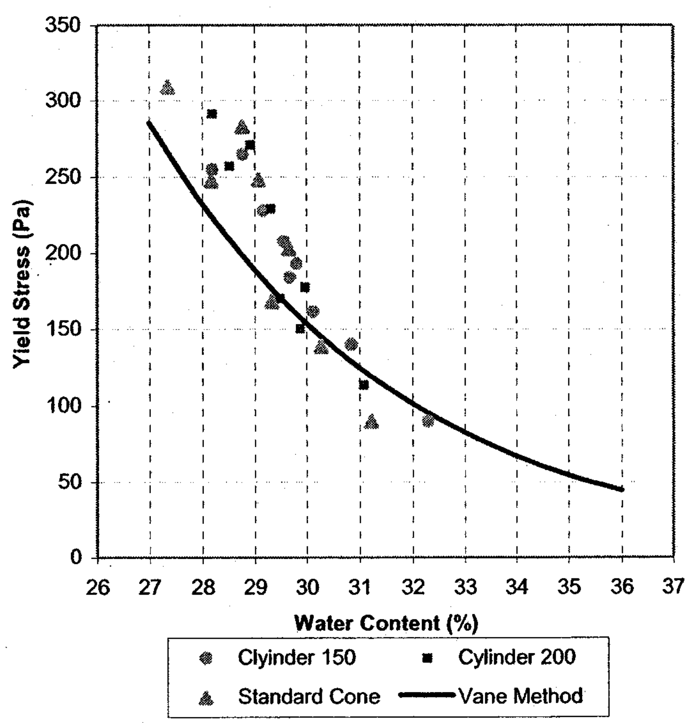

Figure 5.8. Calculated yield stress from slump height for Louvicourt non-cemented mixtures.

The range of water contents at which the mixtures have shown a typical collapse was between 28% and 35% for LaRonde samples and mostly between 28% and 32% for Louvicourt samples. On the other hand, it is impossible to measure the slump height, and consequently, to calculate the yield stress of a mixture with a water content of more than 35% for LaRonde or 32% for Louvicourt mine tailings. This impairment is due to the limitation of dimensionless slump used in calculating the yield stress. Figure 5.9 illustrates the range of dimensionless slump for LaRonde and Louvicourt mixtures at different water contents that are categorized by the type of moulds.

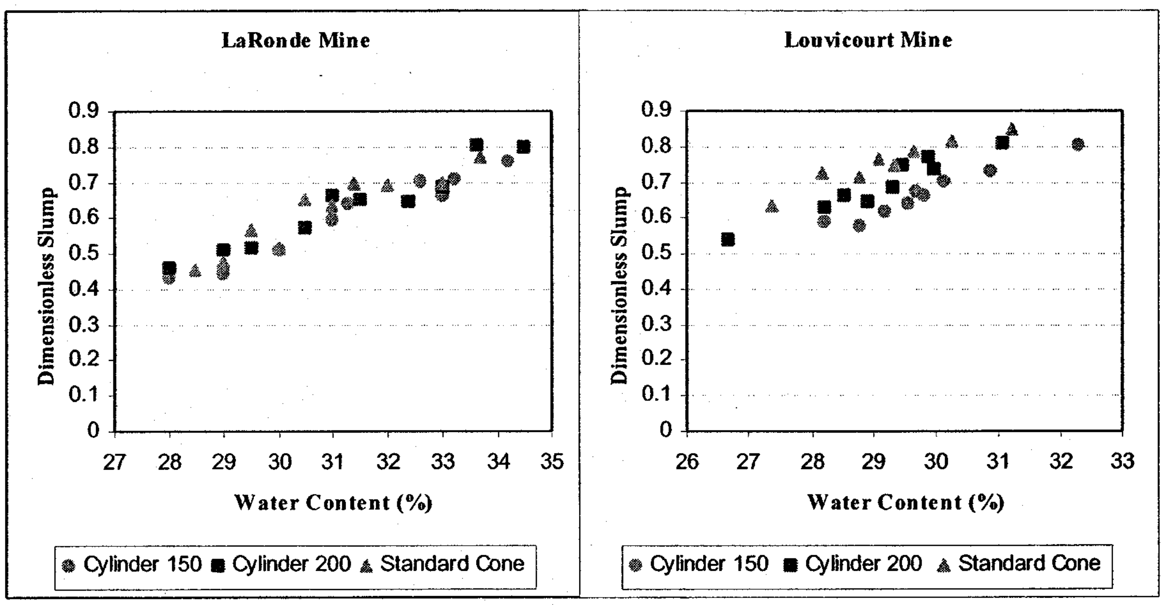

Figure 5.9. The relationship between dimensionless slump and water content of non-cemented mixtures.

The accuracy of the yield stress values calculated from slump height can then be assessed through comparison between slump values and the yield stress values obtained with the vane method. The average percent error for each slump test and the relevant correlation coefficient is shown in Table 5.7. The general equation that is used for calculating the errors is given as follows:

$$\%\text{error} = \frac{|\text{calculated} - \text{measured}|}{\text{measured}} \times 100$$

where calculated refers to slump data and measured refers to the exponential curve fitted to the vane method data.

Table 5.7. The average percent error and the correlation coefficient for slump tests.

Parameter	LaRonde			Louvicourt		
	Cylinder 150mm	Cylinder 200mm	Standard Cone	Cylinder 150mm	Cylinder 200mm	Standard Cone
Average error (%)	12.1	22.6	14.9	16.9	20.6	20.0
Correlation coefficient	0.978	0.971	0.952	0.970	0.972	0.906

5.2.4. Modified Conical Slump Test Results

As it was described in Chapter 4, a small top plate is used in this method for recording the time of slump when the material drops 10 cm from the initial state. The final slump height and the time measured for LaRonde and Louvicourt non-cemented mixtures with different water contents are shown in Table 5.8, as well as yield stress values of each mixture.

Table 5.8. The results of modified conical slump test.

LaRonde			
Water Content (%)	**Slump (cm)**	**Time (sec)**	**Yield Stress (Pa)**
26.4	14.2	0.48	1251.97
27.3	16.3	0.58	1107.67
27.2	16.8	0.68	1075.82
28.3	19.1	0.35	918.99
28.4	21	0.34	795.60
28.6	21.2	0.53	781.62
30.0	21.3	0.9	768.94
29.1	22	0.61	727.79
30.3	23.1	0.65	652.68
30.5	23.1	0.55	652.12
30.0	23.4	0.52	634.41
31.0	24.1	0.37	586.76
31.3	25	0.36	528.91
31.4	25.3	0.52	509.64
31.8	25.5	0.35	496.01
Louvicourt			
26.7	20.5	0.7	811.05
27.5	22.2	0.46	702.33
27.8	22.2	0.25	701.75
27.6	22.5	0.7	683.22
28.4	24.3	0.28	569.07
28.8	24.4	0.31	562.16
29.0	24.6	0.52	549.41
29.4	25.8	0.63	474.05
29.6	26.7	0.33	417.66

The yield stress value for each mixture has been calculated based on Equation 3.42 for this method. Figure 5.10 demonstrates the height of modified slump and standard slump versus water content for LaRonde and Louvicourt mixtures.

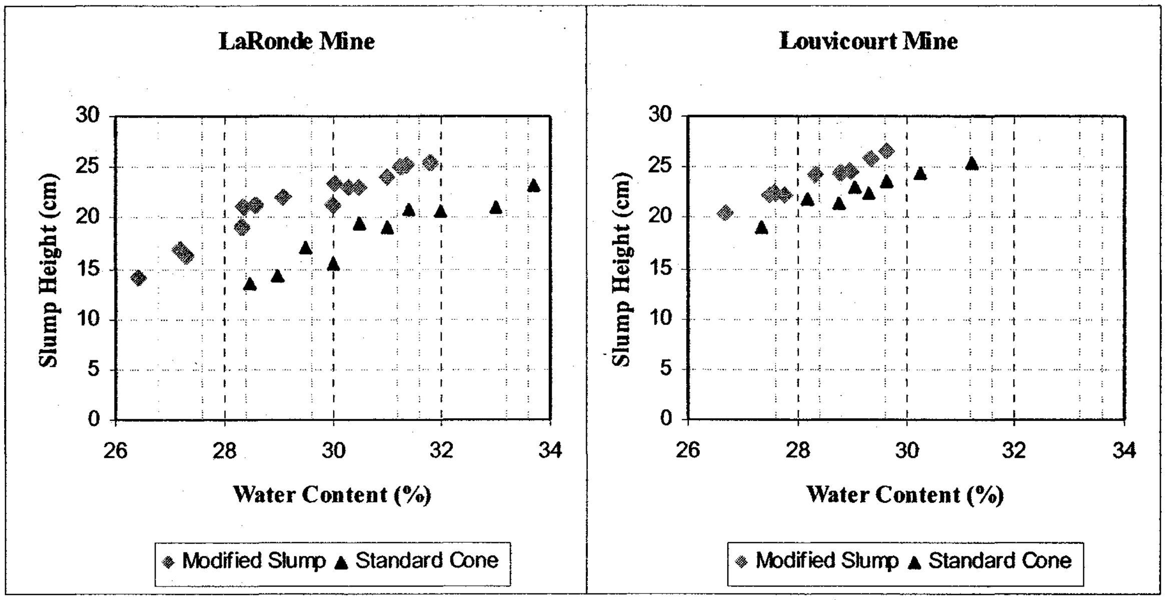

Figure 5.10. The height of modified slump and standard slump.

As seen in this figure, the final height in the modified slump test is higher than the one in the standard slump test for the same water content condition. This occurred because of the extra load of the top plate (212g) in the modified conical slump test. Consequently, there must be a difference between yield stress calculated from the slump of the modified and the standard tests. It is noteworthy to mention that the equation used for calculating the yield stress in the modified method (Equation 3.42) is different from the one used for the standard slump test. Figures 5.11 and 5.12 show the yield stresses calculated from modified slump and illustrate the huge difference between these values and the values obtained from the vane method and the standard conical slump method.

The time recorded during the experiment is used to calculate the viscosity of the mixtures. According to Table 5.8, the time values for LaRonde and Louvicourt non-cemented mixtures are less than one second duration. In this method there was no option to record the time using an automatic device. Thus, a person had a difficult task of recording the time using a stopwatch. In order to validate the reliability of the time results and before further calculation for the viscosity, the correlation between time and slump height was calculated for the mixtures with slump heights higher than 20 cm. Unfortunately, the results show a weak correlation coefficient of –0.46 for LaRonde and –0.32 for Louvicourt mixtures.

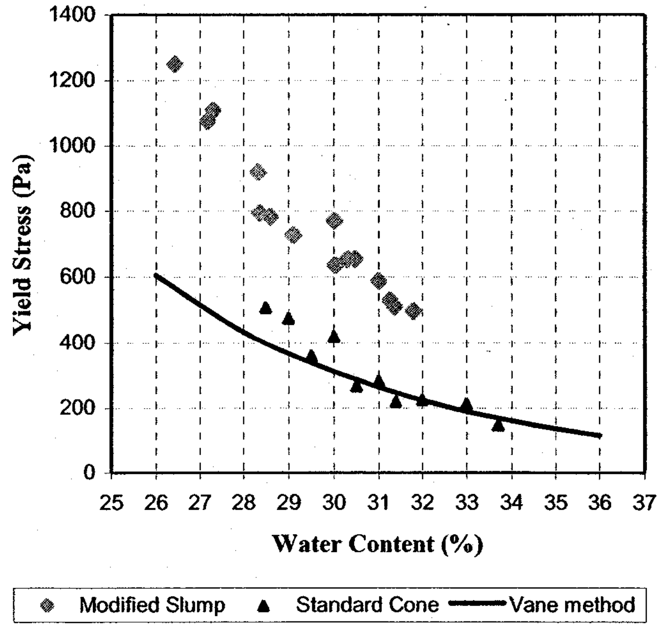

Figure 5.11. The yield stress calculated from slump of modified-conical test for LaRonde mixtures.

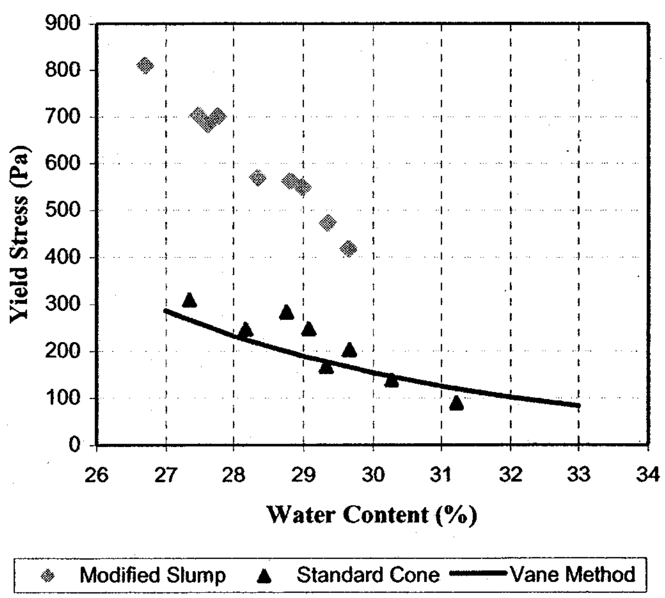

Figure 5.12. The yield stress calculated from slump of modified-conical test for Louvicourt mixtures.

The negative coefficients indicate that with an increase in slump height the time decreases, which is a necessary fact but it is not sufficient for calculating the viscosity of the mixtures with these series of data. Figure 5.13 illustrates the relationship between slump and time for both LaRonde and Louvicourt results.

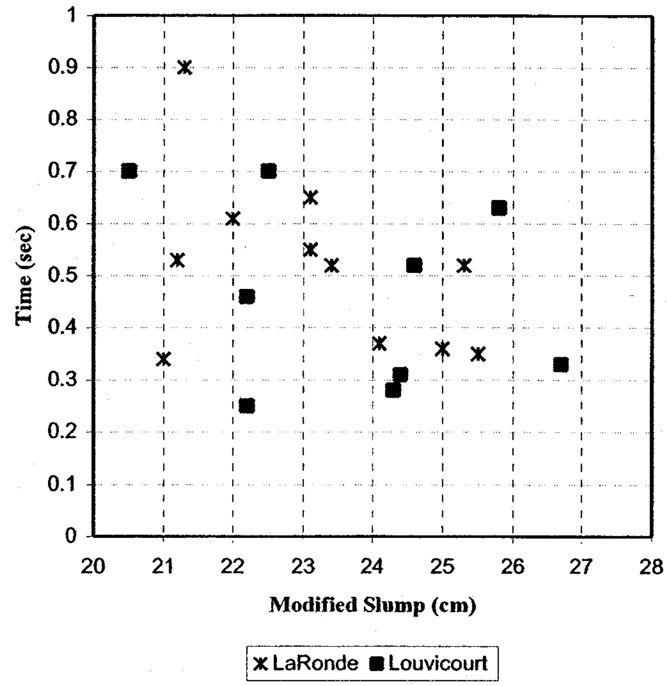

Figure 5.13. The relationship between slump and time in the modified conical slump test.

5.3. The Results of Cemented Mixtures

The measured yield stress of LaRonde and Louvicourt paste materials or cemented mixtures are presented in two groups, the vane results and the cylindrical slump test results with 150 mm diameter cylinder.

5.3.1. Vane Rheometery Results of Cemented Mixtures

In the vane method, the shear stress was applied in a controlled shear rate mode for measuring the yield stress values of cemented mixtures. Rotational speed and other parameters such as the type of vane spindle were considered as it was applied for non-cemented mixtures to draw comparison between cemented and non-cemented data.

Table 5.9 shows the obtained maximum torque and the yield stress calculated for the LaRonde and Louvicourt mixtures after 4 minutes and 12 minutes of mixing at different water contents. The water content-yield stress graphs for these series of data are presented in Figures 5.14 and 5.15.

Table 5.9. Maximum torque and yield stress values of LaRonde and Louvicourt cemented mixtures.

Water Content (%)	LaRonde Mine-Cemented Mixture				Louvicourt Mine-Cemented Mixture			
	M [%o] 4 min.	M [%o] 12 min.	Yield Stress 4min. (Pa)	Yield Stress 12min. (Pa)	M [%o] 4 min.	M [%o] 12 min.	Yield Stress 4min. (Pa)	Yield Stress 12min. (Pa)
26	580.35	590.44	990.13	1007.35	-	-	-	-
28	297.05	301.71	506.79	514.74	210.56	210.32	359.24	358.83
30	246.07	288.3	419.82	491.86	167.17	162.8	285.21	277.75
32	215.56	172.21	367.76	293.80	108.67	98.89	185.4	168.71
34	155.71	148.76	265.65	253.8	67.93	69.31	115.89	118.25
36	104.37	94.65	178.06	161.48	57.41	45.86	97.95	78.24

There is a significant increase in the measured yield stress for each type of cemented mixture in relative to the non-cemented mixtures presented in these two figures. In order to determine the percent of increase, the measured yield stress values of cemented mixtures were compared with the yield stress values of non-cemented mixtures calculated from the equations of fitted curves given in Table 5.3. The results show that the average values of the yield stress for cemented mixtures are more than 1.5 and 1.46 times the average values of mixtures without cement for LaRonde mixtures after 4 minutes and 12 minutes respectively. The Louvicourt yield stress values for cemented mixtures also indicate an increase of 1.8 times after 4 minutes of mixing and 1.7 times after 12 minutes of mixing.

The two series of yield stress values with different times of mixing for each mine paste shows a strong correlation, shown in Figure 5.16. The correlation coefficient for LaRonde mixtures is 0.988 and for Louvicourt is about 0.997. The average difference between the values measured after 4 minutes and 12 minutes of mixing time is 9.3 % for LaRonde Mine and is 7.3% for Louvicourt Mine cemented mixtures.

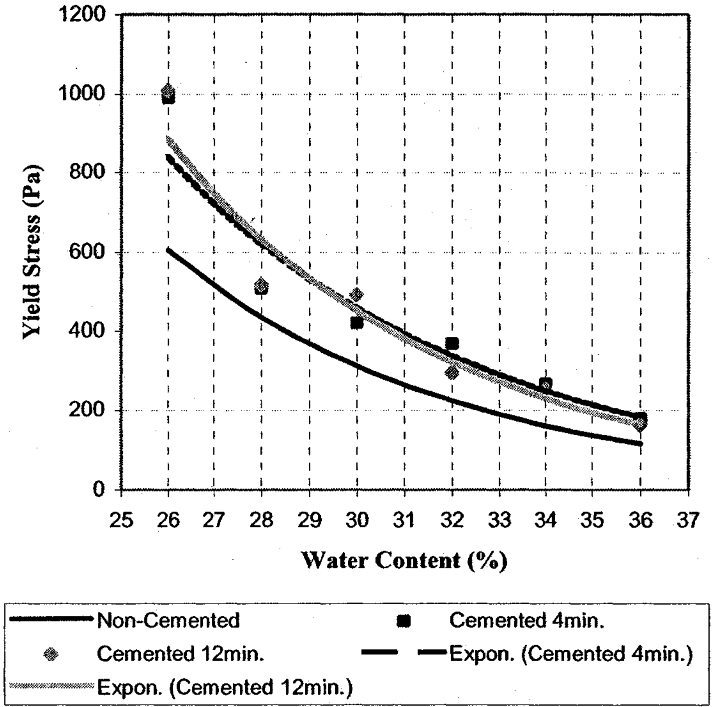

Figure 5.14. The yield stress values of LaRonde cemented mixtures after 4 minutes and 12 minutes of mixing time.

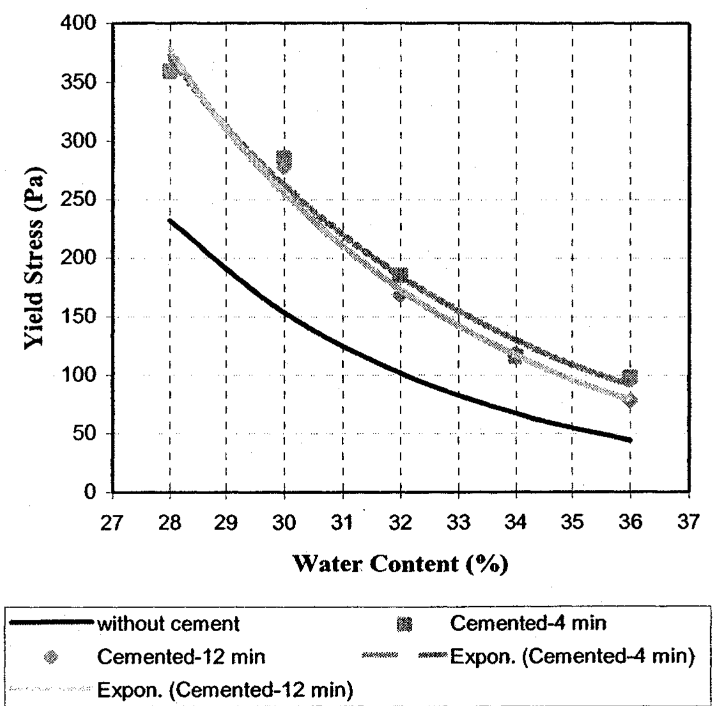

Figure 5.15. The yield stress values of Louvicourt cemented mixtures after 4 minutes and 12 minutes of mixing time.

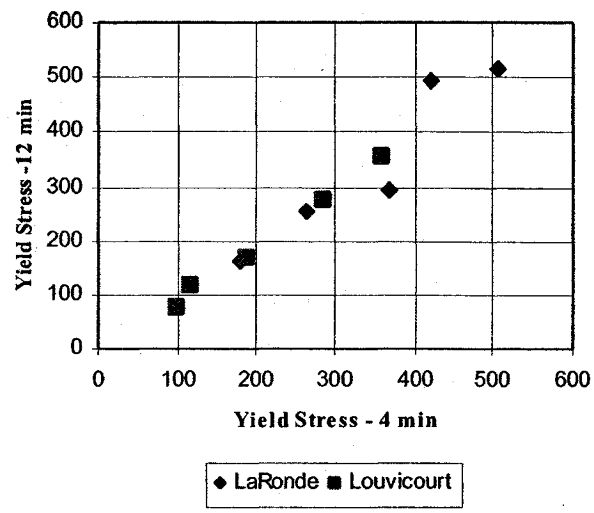

Figure 5.16. The correlation between the yield stress values measured after 4 minutes and 12 minutes for both LaRonde and Louvicourt cemented mixtures.

5.3.2. Slump Test Results of Cemented Mixtures

The cylindrical mould with a diameter of 150 mm was selected to assess the reliability of the slump test for cemented mixtures. The slump height and the related yield stress calculated from Equation 3.40 for LaRonde and Louvicourt mixtures are given in Table 5.10. The experiments were carried out after 4 minutes of mixing the material.

The cemented mixtures compared to non-cemented mixtures apparently show a decrease in the height of slump at the same water content. Figure 5.17 illustrates the difference of dimensionless slump height between cemented and non-cemented mixtures for LaRonde and Louvicourt materials. The yield stress values calculated from slump height for cemented mixtures are presented in Figures 5.18 and 5.19 and associate with the yield stress values measured with the vane rheometery for LaRonde and Louvicourt materials respectively. To compare these results with non-cemented mixture values of yield stress, the slump data of non-cemented mixtures are also shown in these two graphs. The slump test results of cemented mixtures generally underestimate the yield stress values for both LaRonde and Louvicourt materials. The average error related to these underestimations was then determined for each mine paste based on the values of yield stress measured by the vane method.

Table 5.10. The result of slump height and yield stress for non-cemented mixtures.

Water Content (%)	Slump (cm)	Dimensionless Slump	Dimensionless Yield Stress	Yield Stress (Pa)
LaRonde				
30.6	7.3	0.415954	0.12054	458.8828
30.8	7.7	0.438746	0.112712	428.4043
31.1	7.6	0.433048	0.114635	434.6794
31.4	9	0.512821	0.089568	338.8194
31.8	9.3	0.529915	0.084677	319.2973
32.2	10	0.569801	0.073853	277.596
32.3	10.2	0.581197	0.070905	266.3008
32.9	10.6	0.603989	0.065192	243.6662
33.4	10.9	0.621083	0.061062	227.3115
34.2	11.2	0.638177	0.057061	211.0433
35.4	11.6	0.660969	0.051922	190.1601
36	11.8	0.672365	0.049432	180.1472
Louvicourt				
29.8	10	0.569801	0.073853	274.7957
30.3	10.1	0.575499	0.072371	268.74
31.2	11.5	0.655271	0.053185	196.7787
31.1	11.2	0.638177	0.057061	211.204
31.6	11.7	0.666667	0.05067	187.1669
31.4	12	0.683761	0.046996	173.737
32	12.6	0.717949	0.039999	147.5099
32.6	13.1	0.746439	0.034515	126.9763
33.1	13.6	0.774929	0.029339	107.7155
34.5	13.7	0.780627	0.02834	103.4547

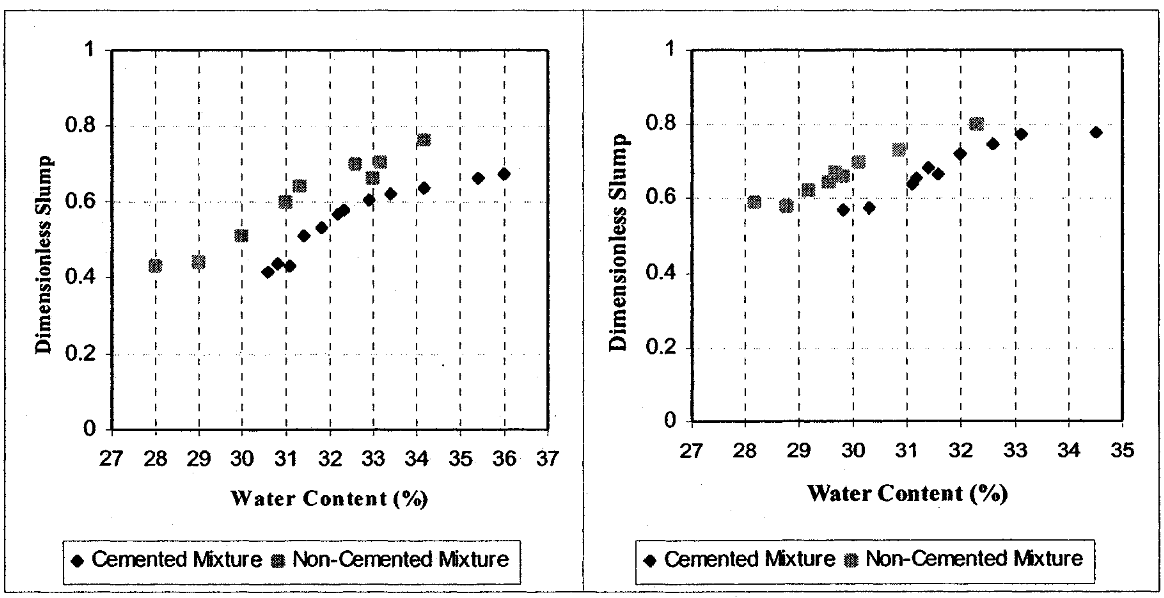

Figure 5.17. Dimensionless slump height of cemented mixtures in comparison with non-cemented mixtures for LaRonde and Louvicourt materials.

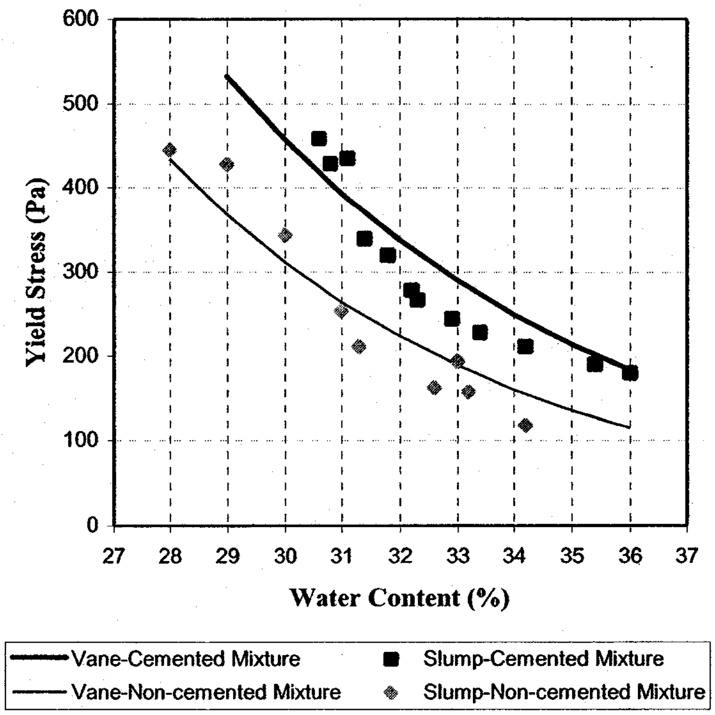

Figure 5.18. Yield stress of cemented and non-cemented mixtures calculated from slump tests and vane rheometery for LaRonde Mine materilas.

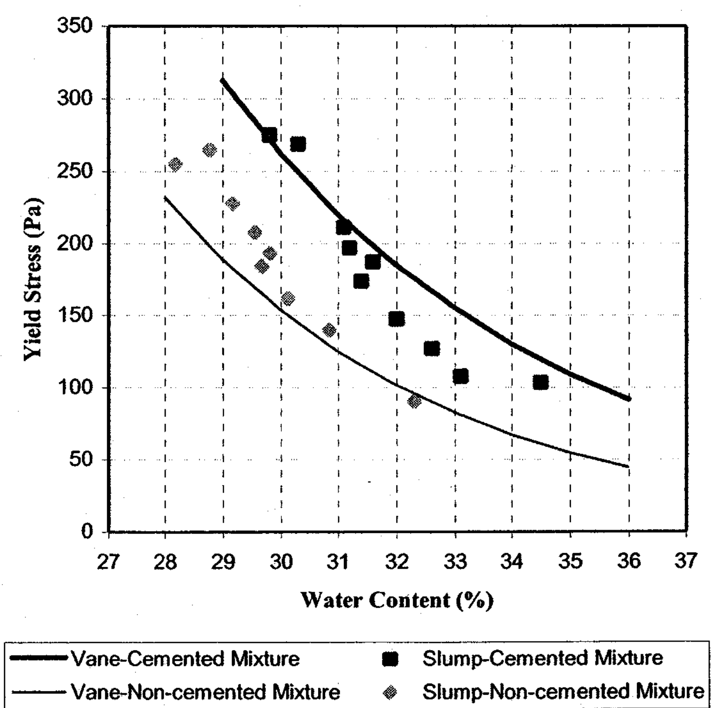

Figure 5.19. Yield stress of cemented and non-cemented mixtures calculated from slump tests and vane rheometery for Louvicourt Mine materials.

LaRonde slump data presents 10.92% error and Louvicourt slump data indicates 12.6% error.

Interestingly, the slump data for cemented mixtures shows the same trend as the slump data for non-cemented mixtures. The lowest water content of cemented mixtures in which it could be measured using slump tests showed a shift of about 2% of water content in comparison with non-cemented mixtures for both mine pastes. The same shift can be observed for the mixtures at the highest water content.

5.4. Comparison Between LaRonde and Louvicourt Results

According to the basic characterization of these two mine tailings described in Chapter 4, the chemical composition and the mineralogy of LaRonde and Louvicourt mine tailings are strikingly similar. Further similarities occur in the parameters related to these factors, such as pH and specific gravity of solids. One of the most important physical properties of mine tailings is the distribution of particle size. Referring to Table 4.6 and Figure 4.6, the difference between particle size of LaRonde and Louvicourt mine tailings is related to the percent of clay materials that are less than 2 microns. Louvicourt tailings contains 20% of clay (<2 microns), which is finer than LaRonde tailings (3% of clay).

As mentioned earlier, pH, specific gravity and particle size distribution may affect the yield stress of a mixture. In this regard, the most effective factor that causes the difference between the yield stress of LaRonde and Louvicourt paste is the size of particles.

The comparison between LaRonde and Louvicourt non-cemented mixture yield stress shows a strong correlation (0.99) between these two series of data, although the yield stress values of LaRonde material is about 2.2 times greater than the values of Louvicourt non-cemented mixtures. The correlation coefficient between LaRonde and Louvicourt cemented mixtures is also strong (0.99) while the yield stress values of LaRonde cemented mixtures are about 1.8 times the yield stress of Louvicourt cemented mixtures.

Therefore, according to the above factors and the experimental results, an increase in the percent of the fine particles in a mixture results in a decrease in yield stress. When the percent of the fine particles increases in a mixture with constant water content, the surface area of the solid parts increases. The water usually covers the surface area of the solids in a homogenous mixture. Thus, increasing the percent of the fine particles results in increasing the amount of water between particles. Clearly, the strength of the mixture is reduced due to the decrease of the strength between particles.

5.5. Discussion

Through the experience of using these two methods, vane rheometery and slump test, for obtaining the yield stress both have shown their advantages and disadvantages.

According to the results obtained for LaRonde and Louvicourt mine tailings, the vane method as a direct method of measurement shows reliable and accurate results. As mentioned in Chapter 4, one problem associated with the vane method, particularly in the controlled shear rate mode is to select a reliable rotational rate. The results used for selecting the reliable rotational rate for LaRonde and Louvicourt materials illustrate that obtaining rotational rate-maximum torque plots for a solid-liquid homogenous mixture is independent of water content. Although there are differences in the percent of clay materials (<2 microns) for both LaRonde and Louvicourt solid-liquid mixtures, the rate 0.3 (rmp) was determined as a reliable shear rate; similarly, they both contain more than 40% of fine materials (<20 microns) and exhibit almost the same basic chemical properties. It is very difficult to generalize this rate to other solid-liquid mixtures for measuring the yield stress in this mode. However, after this stage, estimating yield stress would be straightforward and simple.

In contrast, the yield stress measurements with the vane method in controlled shear stress mode are more complicated for each type of mixture. The shear stress should applied gradually until it exceeds the yield stress. The start point and end point of shear stress application as well as the rate of applied shear stress may change for each sample. This selection of parameters makes this mode challenging. However, the CSR and CSS data show a strong correlation and accurate results for each mine tailings.

In order to calculate the yield stress of cemented mixtures in this study, the vane method in controlled shear rate mode with the same rate of rotation was preferred due to its simplicity.

Sometimes it seems that using equipment such as a rheometer is more sophisticated than the slump mould, but the laboratory procedures show that obtaining data from the slump test to calculate the yield stress is not very simple. Essentially, the slump test requires a greater amount of sample and the results depend on the skill of the examiner.

Two different moulds, conical and cylindrical shapes, were used in this study. The experience shows that the cylindrical mould is less challenging than the conical mould to use. Furthermore, the cylindrical equation is easier to calculate the yield stress from slump height. In terms of the yield stress results obtained from different geometries and dimensions, the cylindrical mould with 150 mm diameter shows the best results.

As it was discussed earlier, the following equation is valid for both cylindrical and conical methods in calculating yield stress values:

$$\tau_y = \tau'_y.\rho.g.H$$

where τ'_y is dimensionless yield stress and h is the height of the mould. Assuming the same value for yield stress for both methods at the same water content, the following compares the yield stress of the cylindrical and conical methods:

$$\tau_{ycone} = \tau'_{ycone}.\rho.g.H_{cone}$$

$$\tau_{ycylider} = \tau'_{ycylinder}.\rho.g.H_{cylinder}$$

If $\tau_{y\text{-cone}} = \tau_{y\text{-cylinder}}$ then:

$$\tau'_{cylinder} = \frac{H_{cone}}{H_{cylinder}}\tau'_{cone} \qquad \text{(Equation 5.1)}$$

As the h_{cone} and $h_{cylinder}$ are constant for each test method in this study, Equation 5.1 can be written as:

for a cylinder with 200mm diameter (aspect ratio of 1.17): $\tau'_{y\text{-cylinder}} = 1.282\ \tau'_{ycone}$

for a cylinder with 150mm diameter (aspect ratio of 1.17): $\tau'_{y\text{-cylinder}} = 1.709\ \tau'_{ycone}$.

These relationships show that the dimensionless yield stress of a cylinder with 150mm diameter is greater than for the cylinder with 200mm diameter and the standard cone. It is also possible to investigate the situation of changes in dimensionless slump and real slump height without considering the density of mixtures for these geometries and dimensions at the same yield stress. For this purpose, Equations 5.2, 4.1, 4.2 and 3.40 were used to obtain the curves shown in Figures 5.20 and 5.21. The x axis in these figures is the representative of the lowest (0) and the highest (100) actual yield stress that may be calculated with these methods.

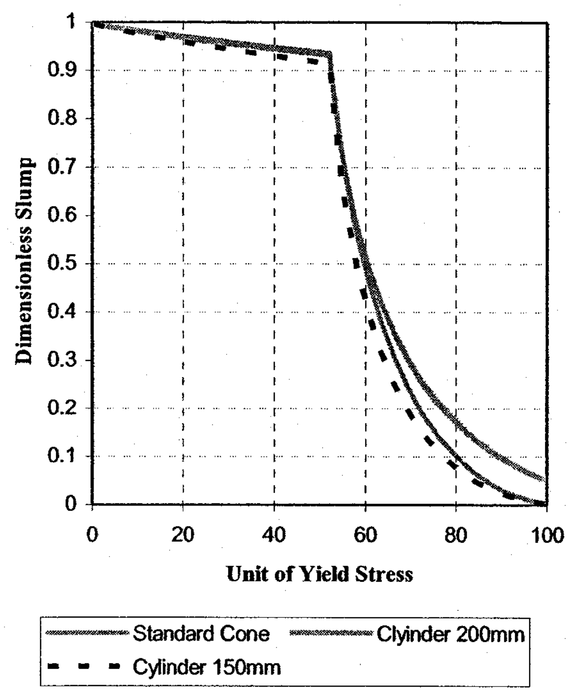

Figure 5.20. Dimensionless slump changes for cylindrical and conical moulds.

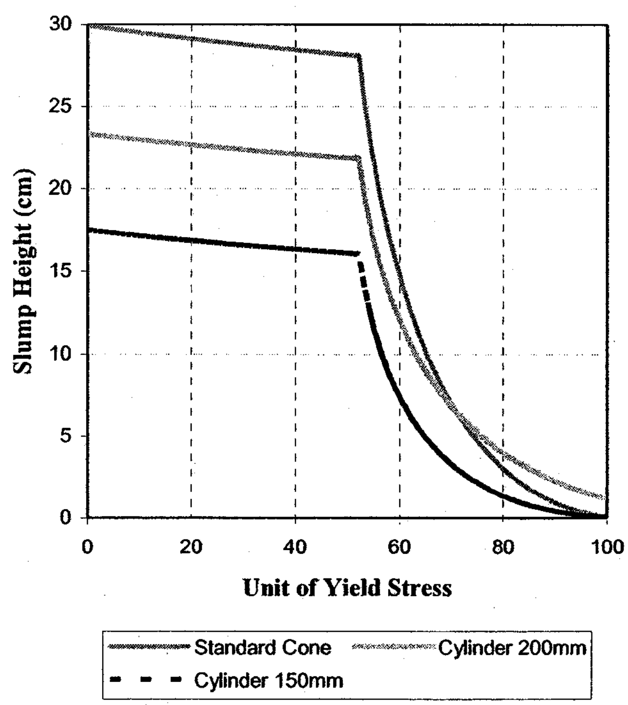

Figure 5.21. Actual slump changes for cylindrical and conical moulds.

According to Figure 5.9, the dimensionless slump heights obtained for LaRonde and Louvicourt mixtures are more than 0.4 and 0.5 respectively. Therefore, the actual yield stress is less than 60 units shown in Figure 5.20. However, values of less than 60 units in Figure 5.21 illustrate that the actual slump height of the cone mould must be greater than the slump height of the cylinders at 200mm and 150mm diameter. This comparison shows that the slump data in this study are compatible with the equations, although there are percents of error associated with the slump methods.

The modified conical slump method is the most challenging of any slump method. In this study, not only were the yield stress values overestimated, but also the time values recorded were inaccurate for calculating the plastic viscosity of the mixtures. The average yield stress values calculated with this method were 2.2 and 2.7 times the values obtained with the vane method for LaRonde and Louvicourt mixtures respectively.

The vane method in CSR mode and the cylinder with a diameter of 150mm were also employed for calculating the yield stress of cemented mixtures or paste fill materials. As was discussed before in this chapter, there was no significant difference between CSR and CSS measurements. The vane method in CSR mode was preferred due to its simplicity. The cylinder with a diameter of 150 mm was also selected because the data of this cylinder for non-cemented mixtures gave more accurate results and required use of smaller amount of sample.

Mixing time was the most important factor required to assess cemented mixtures. For this purpose, the yield stress values measured after 4 minutes and 12 minutes used the vane method. The comparison between these two mixing times indicate that the strength of material after 4 minutes and 12 minutes of mixing with cement will be similarly increased. The slump tests for cemented mixtures were carried out only after 4 minutes of mixing.

The conclusion of the thesis regarding the data obtained in this study and the recommendation for further work based on the discussion and the results will be presented in the next chapter.

CHAPTER 6
CONCLUSION AND RECOMENDATIONS

6.1. Conclusion

The rheological behaviour of two mine tailings characterized in this study was recognized as yield-pseudoplastic, although there is a significant difference between the percent of clay particles of both mine tailings. Rheological measurements were carried out while the effective parameters such as pH and temperature remained constant.

Yield stress measurements in controlled shear rate and controlled shear stress modes with the vane method show reliable results for cemented and non-cemented homogenous mixtures. The most important advantage of using the vane method is to obtain the yield stress of material directly and without any data reduction procedure. In comparison with other methods, there is no wall friction error when the material is sheared in this method.

In controlled shear rate mode, the maximum torque increases when shear rate increases and it thus results in an increase in the yield stress. Therefore, a rotational speed should be used within a range where the maximum torque shows a minimum of change. The rotational speed of 0.3 (rpm) was determined as the best rate of rotation for both types of mine tailings in this study.

To make a homogenous mixture, not only a minimum amount of fine particles (<20 microns) is required but also the size of coarse particles should be less than 1 mm. In this study, the percent of fine particles is more than 40% for each mine tailings that is suitable to make a homogenous mixture, but the amounts of clay particles (< 2 microns) influence the rheological parameters. Yield stress measurements indicate that the finer the particle size the smaller the yield stress values.

Cemented mixtures or paste materials apparently present greater values of yield stress relative to non-cemented mixtures at the same water content for each mine tailings type. The amount of cement used for making a paste form is 5% of the mixture solids weight. Cement was mixed with the solid-liquid mixture for 4 minutes and 12 minutes. Yield stress measurements show that the mixing time of 4 minutes and 12 minutes has the same effect on the yield stress of mixtures.

Slump test methods or in-situ methods for calculation of yield stress show some errors in comparison with the vane rheometery measurements. Slump test methods, as the results indicate in this study, can be used as a secondary method or as a quality control test in the field. The procedure to carry out the test is not very sophisticated; the equipment used is inexpensive and available in different geometries and dimensions. A range of yield stress values of mixtures with different water contents can be determined by slump tests, but there is a limitation of mixture flowability. Slump heights and consequently the calculated yield stresses do not present reliable values for the mixtures with low water contents. In contrast, mixtures with high water contents flow properly along the slump mould, but sometimes they may exceed the height range of the slump mould. The range of water content depends on the particle size distribution of the mixture. As the mine tailings properties are unique for each mine, it is impossible to generalize any results that are related to the basic properties of mine tailings.

The diameter of cylinders with similar aspect ratios has no effect on the calculated yield stress, although cylinders at 150 mm diameter show the less percent error in this study. Standard cone and cylinder moulds at 200 mm diameter demonstrate the same accuracy while more volume of samples are required for these two moulds relative to cylinders at 150 mm diameter. The cylinder material should be made from PVC or stainless steel.

The modified conical slump test, which is used for determining the yield stress of fresh concrete, overestimates the yield stress values for mine tailings. Even though some modification was made on the top plate, laboratory experience showed that this plate is not a proper apparatus to record the time for viscosity calculation. The idea of using this method was to compare the relationship between viscosity, slump height and time for each mine tailings.

6.2. Recommendations

Recommendations for further work can be articulated as follows:

- The effect of binders and additives such as slag and fly ash on the yield stress of material should be assessed.
- The relationship between particle size distribution and degree of saturation should be better understood to recognize their effects on yield stress.
- The equation for the modified conical slump test should be reanalyzed to estimate better values for the yield stress of materials.
- An automatic device for measuring the time in the modified conical slump test should be designed for viscosity calculation.
- The effect of chemical composition on the yield stress of material should be better understood.

REFERENCES

Annual book of ASTM standards, 1994. Designation C 136 –93, Standard test method for sieve analysis of fine and coarse aggregates. Volume 04.02 Concrete and Aggregate.

Annual book of ASTM standards, 1994. Designation D 75-87, standard practice for sampling aggregates. Volume 04.08, soil and rock; dimension stone; geosynthetics.

Annual book of ASTM standards, 1994. Designation D 854- 83, Standard test method for specific gravity of soils. Volume 04.08, soil and rock; dimension stone; geosynthetics.

Annual book of ASTM standards, 1998. Designation C 143/C 143M-97 Standard Test Method for Slump of Hydraulic-Cement Concrete, vol. 04.02, Concrete and Aggregates, ASTM, 89– 91.

Annual book of ASTM standards, 1998. Designation D 4648-87 Standard Test Method for Laboratory Miniature Vane Shear Test for Saturated Fine-Grained Clayey Soil, vol. 04.08, ASTM, 800– 805.

Bantoft E., 1959. Some measurements on pigment-plasticizer dispersions. In rheology of dispersed systems, ed.C.C. Mill, pp. 105-26, London: Pergamon.

Barens H.A. and Carnali J.O., 1990. The vane-in-cup as a novel rheometer geometry for shear thinning and thixotropic materials. Journal of rheology, 34 (6).

Barnes H.A. and Nguyen Q. D., 2001. Rotating vane rheometry - a review. Journal of non-Newtonian fluid mechanics, 98.

Benzaazoua M., Fall M. and Belem T., 2004. A contribution to understanding the hardening process of cemented pastefill. Minerals Engineering, 17(2004) 141-152.

Benzaazoua M., Belem T., Bussie`re B., 2002. Chemical factors that influence the performance of mine sulphidic paste backfill. Cement and Concrete Research, 32 (2002) 1133–1144.

Bhattacharya S. 1999. Yield stress and time-dependent rheological properties of mango pulp. Journal of Food Science, 64(6): 1029–1033.

Bingham E.C. Green H., 1920. Paint a plastic material and not a viscous liquid. The measurement of its mobility and yield value. Proc. Am. Soc. Test. Matl. 20:640-75.

Bird R. B., Gance D. and Yarusso B. J., 1983. The rheology and flow of viscoplastic materials. Review of chemical engineering. Vol. 1.

Boger D.V., 1998. Environmental rheology and the mining industry. Proceedings of the Sixth International Symposium on Mining with Backfill. The Australasian Institute of Mining and Metallurgy Publication Series, Brisbane, Australia.

Boger D.V., 2002. Paste and thickened tailings – A guide. Edited by Jewell R.J., Fourie A.B., and Lord E.R., The University of western Australia. ISBN: 174052 070 X.

Brackebusch F. and Shillabeer J., 1998. Use of Paste for Tailings Disposal. Mine fill '98, Sixth International Symposium on Mining with Backfill. Brisbane, Australia.

Brackebusch F., 2002. Design of paste tailings disposal system. Proceedings 34th Annual Meeting of the Canadian Mineral Processors. Ottawa, Canada.

Brookfield viscometers Ltd, 1998. Operating manual for R/S-CPS rheometer, version 1.20 E. Harlow, Essex U.K.

Carreau P.J., 1968. PhD dissertation. Department of Chemical Engineering. University of Wisconsin, Madison.

Casson N., 1959. A flow equation for pigmented oil suspension of the printing ink type. Mill C.C., Rheology of dispersed systems. Pergamon Press, New York. Pg. 84-104.

Cayouette J., 2002. Optimization of the paste backfill plant at Louvicourt mine. Proceedings 34th Annual Meeting of the Canadian Mineral Processors. Ottawa, Canada.

Chandler J.L., 1986. The stacking and solar drying process for disposal of bauxite tailings in Jamaica. Proceedings of the International Conference on Bauxite Tailings, Kingston, Jamaica. Jamaica Bauxite Institute.

Christensen G., 1991. Modeling the flow of fresh concrete: the slump test. PhD thesis, Princeton University.

Cincilla W A, Landriault D A and Verburg Rens, 1997. Application of paste technology to surface disposal of mineral wastes. Tailings and Mine Waste'97. Belkema, Rotterdam. ISBN 90 5410 857 6.

Clayton S., Grice T. G. and Boger D. V., 2003. Analysis of the slump test for on-site yield stress measurement of mineral suspensions. International Journal of Mineral processing, 70 (2003) 2-21.

Cokelet G.R., Merrill E.W., 1963. The rheology of human blood-measurement near and at zero shear rate. Trans. Soc. Rheol. 7: 303-17.

Cooke R. and Paterson A., 1996. The design of slurry pipeline system. A short course presented at the Breakwater Lodge Victoria and Alfred Waterfront, Cape Town, South Africa. Paterson and Cooke consulting Engineers.

Cooke R., 2001. Paste Reticulation System: Myths and Misconceptions. Minefill 2001: proceedings of the 7th international Symposium on mining with Backfill.

Cross M.M., 1965.Rheology of non-Newtonian fluids: a new flow equation for pseudo-plastic systems. J. Colloid Sci. 20, Pages 417-437.

Crowder J. J., Grabinsky M. W. F. and Klein K.A., 2002. Proceeding of the 55th Canadian geotechnical conference. Niagara Falls, Ontario, Canada.

Davis S.S., 1971. Viscoelastic properties of pharmaceutical semisolids III. Non-destructive oscillatory testing. J. Pharm. Sci. 60: 1351-55.

De Souza, E., De Gagne, D. and Archibald, J. F., 2001. Minefill Applications, Practices and Trends in Canadian Mines. Minefill 2001: proceedings of the 7th international Symposium on mining with Backfill.

Evan I.D., 1992. Letter to the editor: On the nature of the yield stress. Journal of Rheology, 36(7).

Ferraris C. F. and De Larrard F., 1998. Modified slump test to measure rheological parameters of fresh concrete. Cement Concrete and Aggregates Vol.20, No. 2.

Ferraris C.F., 1996. Measurement of rheological properties of high performance concrete: state of the art report, NISTIR 5869, National Institute of Standards and Technology, July, 33 p.

Gawu S.K.Y. and Fourie A.B., 2004. Assessment of the modified slump test as a measure of the yield stress of high-density thickened tailings. Canadian Geotechnical Journal, 41.

Grabinsky M.W., Theriault J. and welch D., 2002. An overview of paste and thickened tailings disposal on surface.

Govier G.W. and Aziz K., 1972. The flow of complex mixtures in pipes. Van Nostrand Reinhold. New York.

Hassani F. and Archibald J., 1998. Mine Backfill, CIM electronic book.

Herschel W.H. and Bulkley R., 1926. Measurement as consistency as applied to rubber-benzene solutions. Proc. Am. Soc. Test. Matls. 26: 621-33.

Hibbeler R.C., 1997. Mechanics of Materials, 3rd ed. Prentice-Hall, Upper Saddle River, NJ, pp. 530–536.

Hobson G.D., 1940. J. Inst. Pet. Technol., 26, 533.

Hu C., De Larrad F. and Gjerv O. E., 1995. Rheological testing and modeling of fresh high performance concrete. Materials and Structures, Vol. 28.

James A. E., Williams D. J. A. and Williams P. R., 1987. Direct measurement of static yield properties of cohesive suspensions. Rheology Acta, Vol. 26.

Jewell R.J., Fourie A.B., and Lord E.R., 2002. Paste and thickened tailings – A guide. The University of western Australia. ISBN: 174052 070 X.

Jillavenkatesa A., Dapkunas S. J. and Lum L. H., 2001. Particle size characterization. National Institute of standards and Technology, special publication 960-1, U.S. department of commerce, Washington.

Keentok M. 1982. The measurement of yield stress of liquids. Rheologica Acta, 21: 325–332.

Komatsu H., Mitsui T. and Onogi S., 1973. Non-linear viscoelastic properties of semi-solid emulsions. Trans. Soc. Rheol. 17: 351-64.

Krieger J.M., 1990. The role of instrument inertia in controlled stress rheometers. Journal of Rheology, 34: 471-83.

Kuganathan K., 2001. A method to design optimum paste-fill mixes through flow cone and mini slump cone testing. Minefill 2001: Proceedings of the 7th International Symposium on Mining with Backfill.

Landriault D.A. and Lidkea W.L., 1993. Paste fill and high density slurry backfill. Innovative Mine Design for the 21st Century, Bawden and Archibald (eds), Balkema, Rotterdam, ISBN 90 54103256.

Landriault D.A., 1995. Paste backfill mix design for Canadian underground hard rock mining, in: F.P. Hassani, P. Mottahed. Proceedings of the 97th Annual General Meeting of the CIM Rock Mechanics and Strata Control Session, Halifax, Nova Scotia.

Landriault D.A., Tenbergen R., 1995. The present state of paste fill in Canadian underground mining. Proceedings of the 97th Annual Meeting of the CIM Rock Mechanics and Strata Control Session, Halifax, Nova Scotia.

Lazarus J. H. and Slatter P. T., 1986. Comparative rheological characterization using a balanced beam tube viscometer and rotary viscometer. Proceedings of the 10th international conference on the hydraulic transport of solids in pipes, BHRA.

Li, M. and Moerman, A., 2002. Perspectives on the scientific and engineering principles underlying flow of mineral pastes. Proceedings 34th Annual Meeting of the Canadian Mineral Processors. Ottawa, Canada.

Liddell P. V. and Boger D. V., 1994. Influence of processing on the rheology of the titanium dioxide pigment suspensions. Ind. Eng. Chem. Res. 1994, 33,2437-2442.

Liddell P. V. and Boger D. V., 1996. Yield stress measurements with the vane. Journal of Non-Newtonian Fluid Mechanics, 63.

Lin S.F. and Brodkey R.S. 1985. Rheological properties of slurry fuels. Journal of Rheology. 29: 147-75.

Magnin A. and Piau J.M., 1990. Cone and plate rheometery of yield stress of fluids, study of an aqueous gel. Journal of Non-Newtonian Fluid Mechanics, 36: 85-108.

Murata J., 1984. Flow and deformation of fresh concrete. Mate´riaux et Constructions (Paris) 17, 117– 129.

Nagase Y. and Okada K., 1986. Hydrogenous behaviour after yielding of solid suspensions. Journal of Rheology, 30: 112-42.

Naylor J., Farmery R. A. and Tenbergen R. A., 1997. Paste backfill at Macassa Mine with flash paste production in a PPSM. Canadian Mineral Processors Conference, Ottawa, Ontario.

Newman Philip, 1992. The Preparation and transportation of paste backfill. Master's thesis, McGill University.

Nguyen Q. D. and Boger D. V., 1983. Yield stress measurement for concentrated suspensions. Journal of Rheology, 27(4).

Nguyen Q. D. and Boger D. V., 1985. Direct yield stress measurement with the vane method. Journal of Rheology, 29(3).

Nguyen Q. D. and Boger D. V., 1992. Measuring the flow properties of yield stress fluids. Annual Review of Fluid Mechanics, 24.

Ouellet J., Bidwell T. J. and Servant S., 1998. Physical and Mechanical Characterization of Paste Backfill by Laboratory and In-situ Testing. AusIMM '98 –The Mining Cycle. MtIsa.

Papenhuijzen J.M.P., 1972. The role of particle interactions in the rheology of dispersed systems. Rheology Acta, 11: 73-88.

Pashias N., Boger D. V., Summers K. J. and Glenister D. J., 1996. A fifty-cent rheometer for management of environmentally sensitive ore tailings. Mineral Processing External Meeting Review, Vol. 20.

Pashias N., Boger D.V., Summers J., and Glenister, D.J. 1996. A fifty-cent rheometer for yield stress measurements. Journal of Rheology, 40(6): 1179–1189.

Paterson A., 2002. Is slump a valid measure of the rheological properties of high concentration paste slurries? BHR Group 2002 Hydrotransport 15.

Pryce-Jones J., 1952. Studies in thixotropy. Kolloid-Z, 129: 96-122.

Rajani B. and Morgenstern N., 1991. On the yield stress of geotechnical materials from the slump test. Canadian Geotechnical Journal, 28, 457–462.

Ritcey G. M., 1989. Tailings Management (Elsevier, Amsterdam).

Robinsky E.I., 2000. Sustainable development in disposal of tailings. Tailings and Mine Waste'00. Balkema, Rotterdam, ISBN 90 5809 1260.

Roux le K., Bawden W.F., and Garbinsky M.W.F., 2002. Assessing the interaction between hydration rate and fill rate for a cemented paste backfill (CPB). Proceeding of the 55th Canadian Geotechnical and 3rd Joint IAH-GNC Groundwater Specialty Conferences, Niagara Falls, Ontario, Canada.

Russell J. L., 1936. Proc. R. Soc. London Ser. A, 154, 550.

Schowalter W.R. and Christensen, G., 1998. Toward a rationalization of the slump test for fresh concrete: comparisons of calculations and experiments. Journal of Rheology 42 (4), 865–870.

Slatter P. T., 1994. Transitional and turbulent flow of non-Newtonian slurries in pipes. Ph.D Thesis. University of Cape Town, South Africa.

Slatter P. T., 1997. The rheological characterization of sludges. Water Science Technology, 36 (11) 9.18.

Slatter P. T. and Wasp E.J., 2002. The Bingham Plastic rheological model: friend or foe? BHR Group 2002 Hydrotransport 15.

Slatter P. T., 2004. The Measurement And Role Of Rheology In Paste Pipelining. International Seminar on Paste and Thickened Tailings. Paste and Thickened Tailings Paste 2004.

Slottee J. S., 2004. Update on the application of paste thickeners for tailings disposal - mine paste backfill. International Seminar on Paste and Thickened Tailings Paste and Thickened Tailings. 31 March. 2 April 2004, Cape Town, South Africa.

Sofra F., and Boger D.V. 2000. Exploiting the rheology of mine tailings for dry disposal. *In* Tailings and Mine Waste '00: Proceedings of the 7th International Conference, Fort Collins, Colo., 23–26 Jan. 2000. A.A. Balkema, Rotterdam, The Netherlands. pp.69–180.

Sofra F., and Boger D.V. 2001. Slope prediction for thickened tailings and pastes. *In* Tailings and Mine Waste '01: Proceedings of the 8th International Conference, Fort Collins, Colo., 15–18 Jan. 2001. A.A. Balkema, Rotterdam, The Netherlands.pp. 75–83.

Steffe J.F., 1992. Yield stress: phenomena and measurement. In Advances in Food Engineering. Edited by R.P. Singh and A.Wirakartakusumah. CRC Press, Boca Raton, Fla. pp. 363–376.
Steffe J.F., 1996. Rheological methods in food process engineering. ISBN: 09632036-1-4. Freeman Press. USA.

Tanigawa Y., Mori H. and Watanabe K., 1991. Analytical and experimental studies on casting of fresh concrete into wall form. Transcription of the Japan Concrete Society, Vol. 13.

Tanigawa Y. and Mori H., 1989. Analytical study on deformation of fresh concrete. Journal of Engineering Mechanics, Vol. 115, No. 3, March.

Tenbergen R A, 2000. Paste dewatering techniques and paste plant circuit design. Tailings and Mine Waste'00. Balkema. ISBN 90 5809 126 0.

Uhlherr P.H.T., Guo J., Fang T.N., and Tiu C. 2002. Static measurement of yield stress using a cylindrical penetrometer. Korea–Australia Rheology Journal, 14(1): 17–23.University of the West Indies, pp. 101– 105.

Utracki L. A., 1988. The rheology of two phase flows. Rheological Measurement. London: Elsevier.

Van den Temple M., 1971. Structure of multi-phase systems: In elasticity, plasticity and structure of matter, ed. R. Houwink H. K., de Decker. Cambridge University Press.

Van Dijk H. 2001. Pumping of high concentration tailings. Mining Environmental Management, 9(5): 21–23.

Van Wazer J.R. 1963. Viscosity and flow measurement. Interscience publishers, New York.

Verkerk C.G. and Marcus R.D., 1988. The pumping characteristics and rheology of paste fills. Backfill in South African Mines. Johannesburg, SAIMM, pp. 221-233.

Vickery J.D. and Boldt C.M.K., 1989. Total tailings backfill properties and pumping. Innovations in Mining Backfill Technology, Hassani et al. (eds), Balkema, Rotterdam. ISBN 906191 985.

Wildemuth C.R. and Williams M.C., 1985. A new interpretation of viscosity and yield stress in dense slurries: coal and other irregular particles. Rheology Acta, 24: 75-91.

Yan J. and James A.E., 1997. The yield surface of viscoelastic and plastic fluids in a vane viscometer. Journal of Non-Newtonian Fluid Mechanics, (70) 237-253.

Yoshimura A. and Prud'homme R., 1987. A comparison of techniques for measuring yield stresses. Journal of Rheology, 31(8).